



# **Design and Implementation of Anti-collision Algorithms for Dense RFID Systems**

**Der Technischen Fakultät der Universität Erlangen-Nürnberg**

**zur Erlangung des Grades**

**DOKTOR-INGENIEUR**

**vorgelegt von**

**Hazem Abdelaal Ahmed Elsaid Ibrahim**

**Supervisor**

**Prof. Dr.-Ing. Albert Heuberger**

October 1, 2017

## Abstract

Radio Frequency Identification (RFID) is a rapidly emerging technology that wirelessly transmits the identity of transponders (tags) attached to an object or a person. The RFID technology took more attention since the adoption of the EPCglobal Class 1 Gen 2 standard in 2005. It has replaced other automatic identification systems like barcodes in some applications, e.g. logistics. In such applications, the identification time is very critical performance parameter. Currently, developments are underway in various areas of RFID to decrease the total identification time for a massive number of tags. The present thesis focuses on passive Ultra High Frequency (UHF) RFID, whose transmission on the Medium Access Control (MAC) layer is scheduled by Framed Slotted Aloha (FSA). Conventional FSA regards only the reply of a single tag as a successful slot. Empty and collided slots are considered as losses. Therefore, the reading efficiency is limited due to empty and collided slots. Modern physical layer systems have the capability of converting part of the collided slots into successful slots. This is called Collision Recovery. Moreover, modern RFID readers can identify the type of slot, e.g., successful, collided, or empty. In addition, the readers are able to terminate a slot earlier upon recognizing that it is empty. The performance of such systems depends strongly on two main parameters: First, the precise estimation of the number of tags in the reading area. Second, the optimization of the FSA frame length.

In this thesis, a novel tag estimation method is introduced, taking into consideration the collision recovery capability of modern RFID systems. The proposed method provides the advantage of giving a novel closed form solution for the tag population estimator, which considers the collision recovery probability of the used system. Simulation results indicate that the proposed solution is more accurate when compared to state-of-the-art.

Apart from that, closed form solutions for the optimum FSA frame length for different scenarios are calculated. The first scenario is the Time-Aware Framed Slotted ALOHA. It considers the differences in slots durations without collision recovery capability. The second scenario is the Time-Aware with constant collision recovery coefficients system. This proposal provides a novel closed form equation for the frame length considering the different slot durations and the collision recovery capability with equal coefficients. Moreover, a

new calculation method of the collision recovery probability per frame is presented. In the third scenario, the multiple collision recovery coefficients system is introduced. There, the differences in the collision recovery probability coefficients are examined with equal slots durations. In this regard, the values of the collision recovery coefficients are extracted from the physical layer parameters. Finally, a Time-aware and Multiple collision recovery system is suggested, taking into account the multiple collision recovery probability coefficients in addition to the different slot durations. For each scenario, timing comparisons are presented in the latter simulation results show the reading time reduction using the proposed frame length compared to other the state-of-the-art algorithms.

This thesis focuses on the EPCglobal C1 G2 standard. Therefore, the tags cannot be modified, and all the improvements are done only on the reader side. However, due to the limitation of the EPCglobal C1 G2, there is still a room of improvement between the proposed solutions and the theoretical lower bound of the identification time. Therefore, compatible improvements of the EPCglobal C1 G2 standard are proposed. This proposal includes compatible modifications in the UHF RFID tags/readers, to be capable of acknowledging more than a sole tag per slot. Finally, the obtained results demonstrate that the proposed system optimizations lead to identify tags in significantly shorter time, which is crucial for time-sensitive applications.

# Contents

<b>1</b>	<b>Introduction</b>	<b>1</b>
1.1	Motivation . . . . .	1
1.2	Thesis Contribution . . . . .	3
1.3	Document Outline . . . . .	5
<b>2</b>	<b>Introduction to RFID</b>	<b>7</b>
2.1	Historical Development of RFID . . . . .	7
2.2	System Components . . . . .	8
2.3	Frequency Bands . . . . .	11
2.4	RFID Communication Standards . . . . .	12
2.5	Collision Problems . . . . .	13
<b>3</b>	<b>RFID Anti-collision Protocols</b>	<b>17</b>
3.1	PHY-Layer Anti-collision Protocols . . . . .	17
3.2	MAC-Layer Anti-collision Protocols . . . . .	19
3.3	DFSA with EPCglobal C1G2 . . . . .	28
3.4	Cross Layer Anti-Collision Protocol . . . . .	30
<b>4</b>	<b>Estimation of the Tag Population</b>	<b>35</b>
4.1	State-of-the-Art Estimation Algorithms . . . . .	35
4.2	Novel Collision Recovery Aware Tag Estimation . . . . .	42
<b>5</b>	<b>Frame Length Optimization</b>	<b>55</b>
5.1	Time Aware System . . . . .	56
5.2	Time and Collision Recovery System . . . . .	65
5.3	Multiple Collision Recovery System . . . . .	71
5.4	Time and Multiple Collision Recovery System . . . . .	80

5.5	Comparison of the Proposed Algorithms . . . . .	86
<b>6</b>	<b>Proposed Improvements of EPCglobal C1 G2</b>	<b>91</b>
6.1	EPCglobal C1 G2 Reading Process . . . . .	92
6.2	Proposed System Description . . . . .	93
6.3	Performance Analysis . . . . .	98
6.4	Measurement and Simulation Results . . . . .	101
<b>7</b>	<b>Conclusions and Future Work</b>	<b>105</b>
7.1	Conclusions . . . . .	105
7.2	Open Issues and Future Work . . . . .	106
	<b>Bibliography</b>	<b>117</b>

# Chapter 1

## Introduction

Radio Frequency Identification (RFID) is a technology that uses communication through radio waves to transfer data between a reader and electronic tags attached to an object, either to be identified or tracked. The RFID technology has benefits with respect to (wrt.) other identification technologies [1], such as no line-of-sight connection, fully automotive identification process, robustness, identification speed, bidirectional communication, reliability in different environment conditions, bunch detection and secured communication. Thus, RFID became particularly the optimum solution for several applications where other identification technologies such as bar-codes are unsuitable, for example, inventory tracking, supply chain management, automated manufacturing, etc [2–4]. Due to the crucial significance of the RFID system in different real-world applications, RFID systems have received large attention from both, research groups and industry. Recently, many work has been published on the area of RFID systems either in hardware and software design, or in protocols and applications, etc [5–7]. In this chapter, the research motivation will be presented. In addition, the thesis contributions and outline will be highlighted.

### 1.1 Motivation

During the past few years, the number of applications that use RFID has increased, and their number will potentially further grow in the near future. One of its main applications is logistics, where, for example, many tags (transponders) may be closely placed on pallets. Thus, in such systems, we have a single

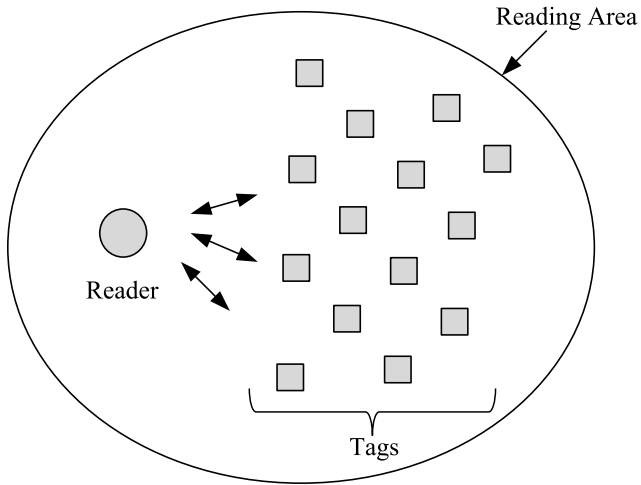


Figure 1.1: Dense RFID network with single RFID reader

RFID reader responsible to identify a bunch of tags in the reading area as shown in figure 1.1. This naturally requires fast RFID readers (interrogators), in order not to slow down the delivery process of the actual goods. According to [8–10], the EPCglobal C1 G2 [11] is the most commonly used RFID standards in logistics. It is based on Time Division Multiple Access (TDMA), which leads to a certain probability of tag-collisions on the communications channel. Owing to their low price and simple design, tags can neither sense the channel nor communicate with the others. Hence, the readers are responsible for coordinating the network, and avoiding collisions using anti-collision algorithms.

According to the previously published RFID work, Frame Slotted ALOHA (FSA) [12, 13] is the most widely used Medium Access Control (MAC) anti-collision protocol for RFID systems due to its simplicity and robustness. In FSA, the communication timing between the reader and the tags is divided into TDMA frames, each frame includes a specific number of slots. The frame length is a function of the existing number of tags in the reading area. During the reading process, each active tag randomly assigns itself to one of the available slots in a frame. Therefore, each slot can take one of the three different states: 1) Successful Slot: Only one tag chooses this slot, is fully identified, and then deactivated by the reader. 2) Collided Slot: Multiple tags reply, resulting in a collision. The collided tags normally remain in their active state and retry their transmission in the next frame. 3) Empty Slot: No tag responds and the

slot remains unused. Therefore, the reading efficiency is limited by the effect of two main parameters:

1. The accuracy of FSA frame length: If the frame length is higher than the optimum value, many empty slots in this frame will be present, which reduces the reading efficiency. If the frame length is lower than the optimum value, this will result many collided slots, which again reduces the reading efficiency. Thereby, choosing the optimum value in FSA frame length is the most crucial optimization parameter in such application.
2. The robustness of the number of tags estimation: The optimum FSA frame length strongly depends on the actual number of tags in the reading area. However, in real-world applications, the number of tags of the reading area is unknown. Therefore, the more precise the number of tags estimation, the better reading efficiency achieved.

Recent research groups have focused upon using the PHY (Physical) Layer properties, in the so-called Collision Recovery phenomena, to convert part of the collided slots into successful slots [14, 15]. This decreases the losses which result from collisions. Moreover, modern RFID readers have the ability to identify the type of the slot (successful, collided, or empty). Thus, the RFID readers are able to terminate the slot earlier as soon as they recognize the absence of a tag reply [16, 17], which eliminates the effect of the empty slots.

According to the previous discussion, the number of tags estimation algorithm and the optimum FSA frame length strongly depend on the PHY-layer properties of the used system.

## 1.2 Thesis Contribution

This thesis aims to improve the performance of existing UHF RFID systems, mainly by minimizing the total identification delay. The accomplished work focused on optimizing the FSA frame length and the number of tags estimation algorithm for dense RFID networks, taking into consideration the MAC/PHY-layer parameters. All modifications are on the reader side, as the improved system has to follow the EPCglobal C1 G2 standard [11]. Moreover, results

are compared to the theoretical lower limit for this standard. Finally, compatible upgrades of the EPCglobal C1 G2 standard are proposed, thus granting additional improvements for the overall performance. The main contributions of this thesis can be summarized as follows:

1. A novel number of tags estimation method was developed, taking into consideration the collision recovery capability of the system. The main advantage of the proposed method is that it provides a novel closed-form solution for the tag population estimator, which considers the collision recovery probability of the used system. Simulation results indicate that the proposed solution is more precise compared to the methods presented in the literature. Timing comparisons presented in the simulation results show the reduced identification delay of the proposed estimation method compared to other proposals.
2. A closed-form solution for the optimum frame length for FSA was provided by optimizing the Time-Aware Framed Slotted ALOHA reading efficiency, which considers the differences in the slot durations. Simulations indicate that the proposed solution gives the most accurate results with respect to the exact solution.
3. Another closed-form solution for the optimum frame length for FSA was settled by optimizing the Time and constant collision recovery coefficients aware reading efficiency. The proposed solution gives a novel closed form equation for the frame length considering the different slot durations and the collision recovery capability with equal coefficients. Moreover, a new method was introduced to calculate the capture probability per frame. Simulations indicate that the proposed solution gives accurate results for all relevant parameter configurations without any need for multi-dimensional look-up tables.
4. A novel closed-form solution for the optimal FSA frame length was established, which considers the differences in the collision recovery probabilities. The values of the collision recovery coefficients are extracted from the physical layer parameters. Timing comparisons are presented in

simulation results to show the mean reduction in reading time using the proposed frame length compared to other proposals.

5. Further, a new closed-form solution for the optimal Frame Slotted ALOHA (FSA) frame length was created. The novel solution considers the multiple collision recovery probability coefficients, and the different slot durations. Timing comparisons are presented in the simulation results to show the reading time reduction using the proposed frame length compared to other the state-of-the-art algorithms.
6. Finally, compatible improvements of the EPCglobal C1 G2 standard are proposed. They require some compatible modifications in the UHF RFID tags/readers, to be capable of acknowledging more than a single tag per slot.

### 1.3 Document Outline

A brief outline of this document is presented as follows. Chapter 2 introduces the historical background and literature survey of RFID systems. Chapter 3 presents collision problem in the RFID systems and the existing anti-collision algorithms. Moreover, the concept of proposed cross-layer anti-collision algorithm will be defined. Chapter 4 reports the most commonly used number of tags estimation algorithms in the RFID system. Afterwards, the proposed collision recovery aware maximum likelihood estimation algorithm is discussed. In this part, a closed-form solution for the estimated number of tags in the reading area is suggested taking into consideration the collision recovery capability of the used system. Chapter 5 shows different case studies for FSA frame optimization. Each case depends on the PHY-layer parameters. Hence, in every case, a closed-form solution for the optimum FSA frame length is an analytically derived function of the estimated number of tags and the PHY-layer parameters. Chapter 6 provides compatible improvements of the EPCglobal C1 G2 standard. In this system, such modifications to tags/readers, can acknowledge more than single tag per slot. Finally, chapter 7 concludes this document by highlighting the main issues addressed in this thesis and outlining some of the future research aspects.



# **Chapter 2**

## **Introduction to RFID**

This chapter provides an overview of the historical development of RFID. In addition, it describes the basic principles and the major technical aspects related to the RFID technology and its standardization. At the end, it will present the major issues in dense networks.

This chapter is organized as follows: Section 1 gives an overview about the historical development of the RFID. Section 2 presents the main components of the system. In section 3, I show the operating frequency bands in the RFID. Afterwards, I will present the classification of the RFID standards in section 4. Finally, the RFID collision problem will be described in section 5.

### **2.1 Historical Development of RFID**

In the year 1935, the first notion of RFID system was invented by a Scottish physicist called Robert Alexander for detecting aircraft [18]. Next, in 1950, the British government developed the first prototype of the RFID system, which is known as Identification Friend or Foe (IFF) system [19]. This system was designed for aeronautical applications. Between the 1950s and 1960s, there was a big development in the RFID systems for different applications, e.g. the application of the microwave [20] and radio transmission systems that modulate passive responders [18]. In the 1970s, RFID was intensively applied to logistics, transportation, vehicle tracking, livestock tracking as well as industrial automation. The first US patent in this field was published in 1973 for the invention of an active RFID tag with re-writable memory [19]. Nowadays, the

low power ultra high frequency (UHF-RFID) system research has gained certain importance. In 2008, the US Department of Defense have announced that they plan to use electronic product code (EPC) [1] technology to track goods in their supply chain. In Europe, RFID was intended to improve industrial applications and to enable short-range systems for animal control [20]. In Japan, RFID was used for contact-less payments in transportation systems [18].

## 2.2 System Components

As shown in figure 2.1, conventional RFID systems consist of three main components: 1) RFID tags or transponders which are attached to the object requested to be identified or tracked. 2) RFID reader and antennas which control data transmission and the whole identification process. 3) Processing device commonly called Middle-ware. It is always a software processing device. All the external processing depending on the application is done on this device using the EPC code which is identified by the reader from the tag. In the following sections, each component will be described in further details.

### 2.2.1 Tags

The tag is the device, which is attached to the object. It stores information and might be incorporated to sensors. This information includes their unique EPC, which is a standardized identification code. When tags are within the reading range of the reader, they receive a command from the reader asking them about their EPC. They reply with their identification data to the reader, which processes the information according to the current application. Generally, RFID tags are categorized into the following categories:

**Passive tags** Passive tags are the most commonly used tags in tracking and supply chain markets [21, 22]. They are extremely simple and inexpensive devices (less than 0.10 €). Passive tags do not contain any power source so they derive all of the required energy for their operation from the signals emitted by the reader. This energy activates the circuit of the tags. Then, they send a reply signal that includes their information. The maximum communication

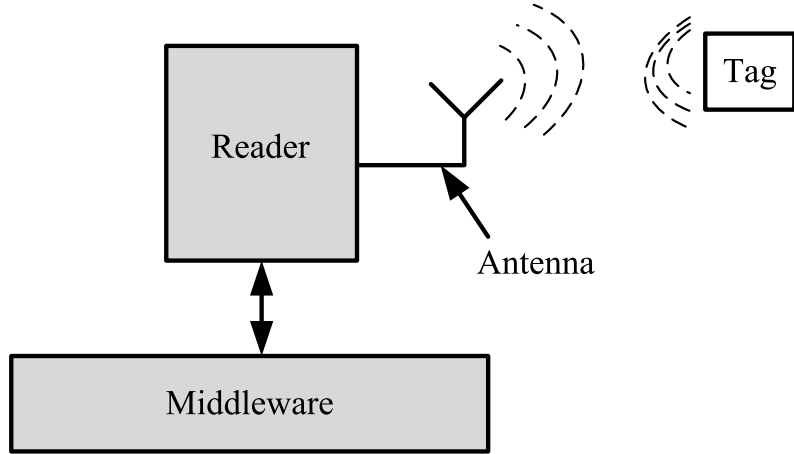


Figure 2.1: Main UHF RFID system components with single reader and back-scatter UHF tag

range is up to a few meters.

**Active tags** Active tags are the second commonly used type of tags. They have a fully autonomous power source [23,24]. These devices are more expensive than passive ones (starting from 10 €) because they incorporate circuits with a microprocessor and a memory to read, write, rewrite or erase data from an external device. However, there are several advantages of active tags compared to the passive ones. Among them are the following: 1) Active tags support long reading distance, i.e. more than 100 meters. 2) In addition, they also support immunity to the interference especially in harsh environment e.g. environments with high amounts of metals, such as shipping containers. 3) Owing to their power supply property, they are easily connected with sensors, thus, monitoring the environment depending on the application e.g. food or drug shipments.

**Semi-passive tags** In semi-passive tags, batteries are used on board to power the controller or the chip and may contain additional devices such as sensors [25,26]. The signals, which are generated by the reader are only used to activate tags in coverage. Then, the tag's reply is generated using the energy emitted from the internal batteries. Semi-passive tags can communicate over longer distance than the normal passive tags. Moreover, the circuitry activation of the semi-passive tags is faster than in passive tags.

### 2.2.2 Readers

The RFID reader is the most important element in an RFID system [23]. It is responsible to access the tag information. The reader decodes the received data from the tags then sends this information to the middle-ware. The reader performance depends strongly on two factors: First, the decoder architecture. Second, the antenna design.

**Decoder architecture** Readers can be classified according to the type of tags as follow:

**Readers dealing with active tags** In active RFID systems, since active tags are able to initiate the communication between them, any active tag can act as a reader. However, when active tags act as a reader, they must be connected to a computer or a network (via a wired or wireless link) to send the received data from its network [22].

**Readers dealing with passive tags** They have to meet the following key requirement: Their transmission power must be sufficient to feed the surrounding passive tags [13]. These tags obtain energy from the transmitted signal using back-scattering technique. Back-scattering technique is the reflection of the reader's carrier wave where it modulates the signal which includes the tag's data. Then, the reader detects the tag's response, processes the signal and reads the information sent by the tag.

**Antennas** Antenna designs are strongly dependent on the operating frequency [27]. In case of low range applications, such as LF (125 kHz) or HF (13.56 MHz) range, antennas are embedded in the readers. However, in case of UHF applications, antennas have to be external. Moreover, polarization of the used antenna is one of the most critical issues. Antenna polarization affects directly the RFID system performance. In RFID systems, there are two types of antenna polarization:

**Linearly polarized antennas** Using these antennas, the electrical field component of the transmitted signal is propagated in a plane, and tags have

to be also orientated in the same direction of the transmitted signal [28]. For optimum receiving efficiency, this technique requires linearly polarized tags.

**Circularly polarized antennas** Using these antennas, the electromagnetic waves are transmitted in circularly polarized patterns. This type of polarization is used when the orientation of tags with respect to the reader can not be controlled. Using circularly polarized antennas, a communication with both, linearly and circularly, tags can be established. However, circularly polarized antennas have a shorter reading range compared to the linearly polarized ones [29, 30].

### 2.2.3 Middle-ware

In some applications, the tag identifier is used as an input for a database to get an information related to this object e.g. shipment orders, expiring date, etc. This kind of processing is done in a set of software tools called middle-ware. The EPCglobal standards [11] define specifications for the middle-ware of RFID systems. Meanwhile, RFID systems are still an evolving technology. Thus, RFID middle-ware should be flexible enough so that it could be adapted to the future changes with minimal efforts.

## 2.3 Frequency Bands

The most important differentiation criteria for RFID systems are the operating frequency of the reader. Selecting the most adequate frequency is a function of the following properties:

- Technical properties of the application e.g. The RFID channel contains metals or not.
- Cost of the system.
- Behavior of the electromagnetic waves at these different frequencies.

First RFID systems started with Low Frequency (LF) band RFID systems [31]. After few years, the RFID systems have operated in High Frequency (HF)

Table 2.1: Frequency Bands for RFID Systems [32]

Frequency Band	Range	Common Frequencies
Low Frequency (LF)	0.5 m	125 kHz, 134.2 kHz
High Frequency (HF)	1 – 3 m	13.56 MHz
Ultra High Frequency (UHF)	10 m	866 MHz Europe 915 MHz USA
Microwave ( $\mu$ W)	> 10 m	2.45 GHz, 3.0 GHz

band [32]. Using only these two band made a big limitation on the RFID applications. Thus, Recent years, the number of RFID systems operating in the Ultra High Frequency (UHF) range have increased because of the dramatic decrease in its component's price [33]. Thus, it is expected to see the RFID microwave band more available and affordable in the market. The availability of all bands with affordable costs will give the RFID users more facilities to take easier decision in which band they need to build up their applications.

Table 2.1 presents the most common frequencies for each band as well as the maximum allowed distance for each band. It is necessary to note that Table 2.1 does not present the only possible operating frequencies. It presents only the most commonly used frequencies in each band. Thus, it is possible to find systems, operating at different frequencies, within each frequency band. This thesis focused upon the UHF frequency band, because it is suitable for the passive dense RFID applications.

## 2.4 RFID Communication Standards

There are different standards of the communication between the RFID reader and the corresponding tags. Although the EPCglobal C1G2 standard is the most extended and adopted for passive dense RFID networks, yet, there are further other standards. Table 2.2 shows the most common RFID standards with a short description for each one. This thesis discusses the Generation 2, Class 1 standard, because it is the most suitable standard for dense RFID network, as the cost of the system is ideal for such applications.

Table 2.2: RFID standards classification [11]

Standards Classification	Description
Generation 1, Class 0	Read only passive tags Unique EPC programmed in the factory
Generation 1, Class 0+	Identical to the normal Generation 1, Class 0 tags Tags can be programmed by users
Generation 1, Class 1	Similar to Generation 1, Class 0 or 0+ tags Identified by readers from different companies
Generation 2, Class 1	Faster data rates than Generation 1 tags Rewritable memories
Generation 2, Class 2	Similar to Generation 2, Class 1 tags More noise immunity
Generation 2, Class 3	Semi-passive or battery assisted tags
Generation 2, Class 4	Active tags
Generation 2, Class 5	Active tags Capability to power on other tags

## 2.5 Collision Problems

In RFID systems, both readers and tags communicate using the same frequency. Thus, simultaneous transmission could happen that leads to collisions. Collisions destroy the identification number EPC of the tag and may also interfere control commands of the readers. Thereby, the collision problem is the main source of delays in the identification process. There are two types of collisions: reader collisions and tag collisions. The following sections describe in details both types and how each of them affects the performance of the system.

### 2.5.1 Readers Collisions

There are two main types of readers collisions or interference in RFID systems: multiple readers to tag collision and reader to reader collision.

**Multiple Readers to Tag Collisions:** Multiple readers-to-tag collisions occurs when one tag is simultaneously located in an overlapped area between two neighbor reading areas [34, 35], and both readers communicate simultaneously with the shared tag as shown in figure 2.2. In this situation, the tag will not be able to determine such communication, due to the interference between the two

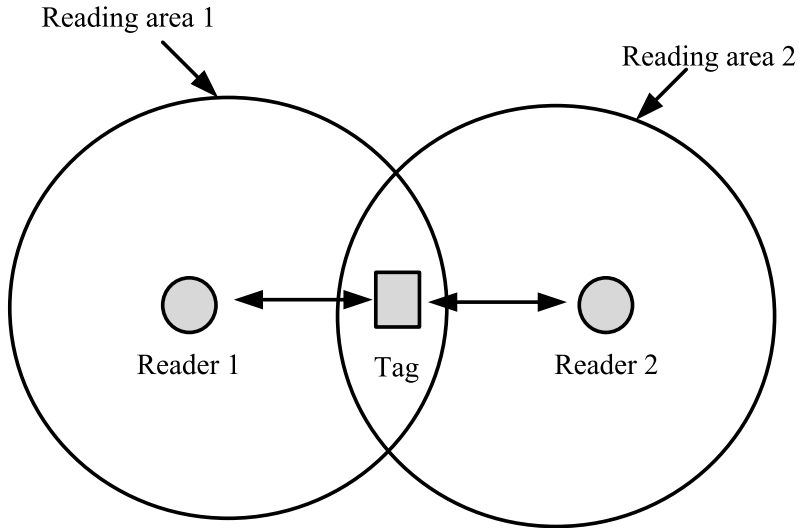


Figure 2.2: Multiple readers to a single tag collision

readers commands. Therefore, the tag will not respond to any readers. Finally, this slot would be an empty one leading to losses in the total identification time.

**Reader to Reader Collisions:** Reader-to-reader collisions, or interference, occurs when the signal generated by a reader acts as a jamming signal for a neighbor reader as shown in figure 2.3. This signal might prevent the second reader from communicating with its tags in its reading area [36, 37]. Such interference can occur even if there is no overlapping area between the reading areas. This interference affects the total identification time of the interfered system.

### 2.5.2 Tag Collisions

This type of collision is the most common type of collision in dense RFID systems [38–41]. In such systems, we have a single RFID reader and multiple tags as shown in figure 2.4. The main objective is to identify all tags in the reading area in the minimum possible time. However, in dense networks, the number of tag collisions increases, which decreases the reading efficiency, and hence increases the reading time. Different research groups are currently associated with how efficiently develop an anti-collision protocol for such systems.

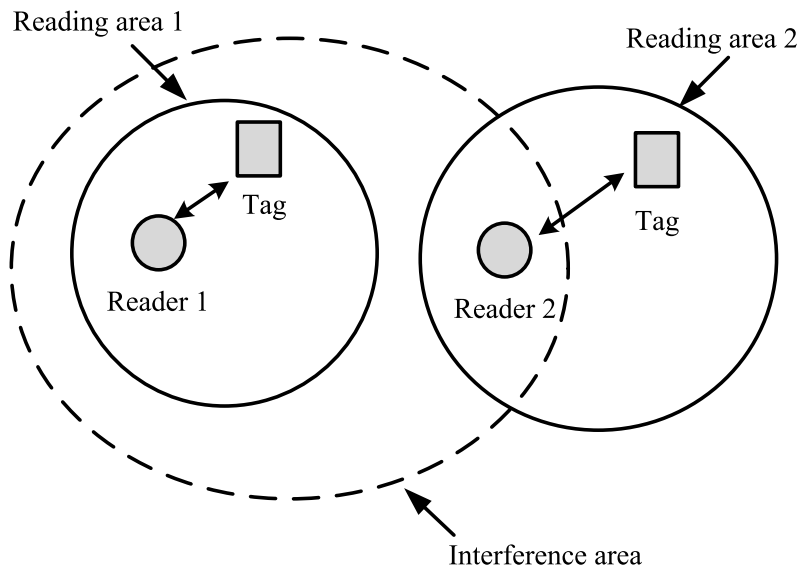


Figure 2.3: Multiple readers interference

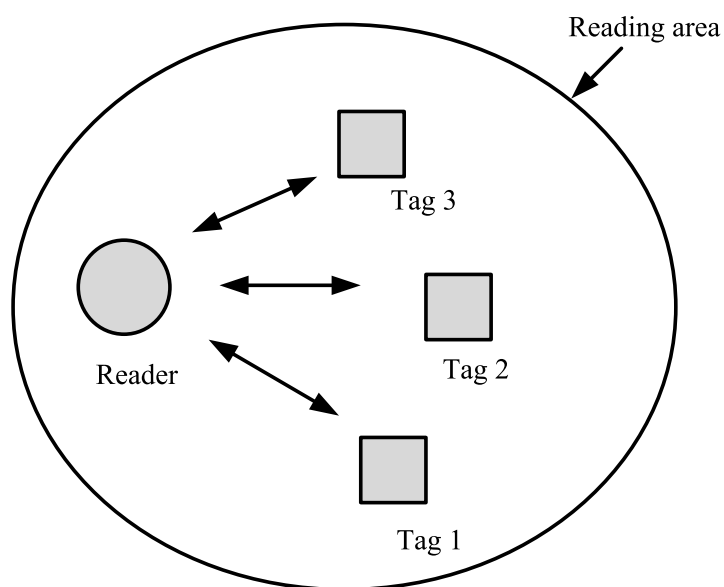


Figure 2.4: Multiple tags to a single reader collision

Table 2.3: RFID standards classification [11]

Standards Classification	Description
Generation 1, Class 0	Read only passive tags Unique EPC programmed in the factory
Generation 1, Class 0+	Identical to the normal Generation 1, Class 0 tags Tags can be programmed by users
Generation 1, Class 1	Similar to Generation 1, Class 0 or 0+ tags Identified by readers from different companies
Generation 2, Class 1	Faster data rates than Generation 1 tags Rewritable memories
Generation 2, Class 2	Similar to Generation 2, Class 1 tags More noise immunity
Generation 2, Class 3	Semi-passive or battery assisted tags
Generation 2, Class 4	Active tags
Generation 2, Class 5	Active tags Capability to power on other tags

Anti-collision protocols can be classified into two main types: Physical layer protocols and MAC layers protocols. In this thesis, I am focusing on the applications which include only a single RFID reader and dense RFID tag populations. The main motivation of this thesis is to minimize the total identification time for a dense and passive RFID networks. Therefore, in this thesis, there are different proposals to solve the tag collision problem by enhancing the existing anti-collision protocols taking into consideration the physical layer parameters. Moreover, the applications of the dense RFID networks are following the EPC-global C1 G2 standards [11]. Thus, the proposed improvements in this thesis are done only on the reader side. Finally, chapter 6 will propose slight modifications in the standard to have further improvements and, at last, compare the results against each other.

# Chapter 3

## RFID Anti-collision Protocols

This chapter presents the most common anti-collisions algorithms for passive RFID systems, either by using the physical layer or the MAC layer. More emphasis will be upon the anti-collision algorithms which are compatible with the EPCglobal C1 G2 standard, as this is the focus of this thesis.

This chapter is organized as follows: section 1 gives an overview about the physical layer anti-collision algorithms. In section 2, different MAC-layer anti-collision algorithms are presented, thus clarifying the main differences between them. Afterwards, a brief description for the EPCglobal C1 G2 reading process will be presented in section 3. Section 4 will give an introduction about the collision recovery and the slots duration in modern RFID readers and the effect of these parameters in MAC-layer anti-collision algorithm, which will be focused on, in the remaining part of this thesis.

### 3.1 PHY-Layer Anti-collision Protocols

Different physical layer anti-collision protocols have been developed to separate colliding signals on the physical layer. Figure 3.1 shows the most common physical layer anti-collision protocols, which are: FDMA, SDMA, CDMA and TDMA. These algorithms will be briefly discussed in the following paragraphs:

**Frequency Division Multiple Access (FDMA):** In this protocol, the frequency band is divided into different sub-frequency bands and tags are distributed among them [42]. However, this technique adds complexity to the

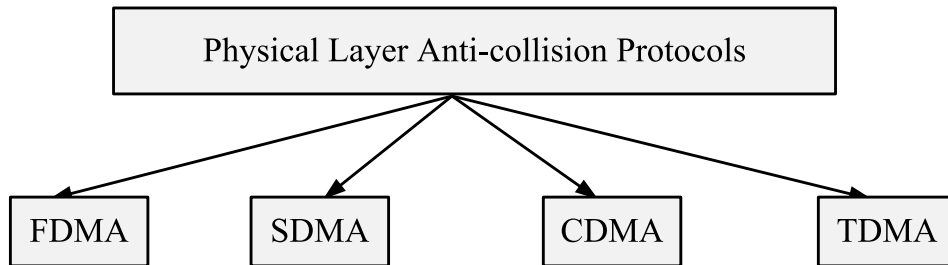


Figure 3.1: Common existing PHY-Layer anti-collision protocols

system. Readers should be able to decode different frequencies at the same time. Moreover, tags should be able to select its desirable sub-channel, which is incompatible with EPCglobal C1 G2. Only active tags can do such functionality.

**Space Division Multiple Access (SDMA):** This technique makes use of spreading tags over the reading area. It provides a high increase in the reading efficiency [43]. The main drawback is the cost of implementing the RFID reader with multiple antennas. Moreover, in dense applications, the distances between the tags is very small to be distributed on the reading area.

**Code Division Multiple Access (CDMA):** This protocol uses spread-spectrum modulation techniques to transmit the data over the entire spectrum [44]. CDMA is the ideal procedure for many applications, e.g. navigation systems. However in case of RFID systems, it is not compatible with EPCglobal C1 G2, as the cost of the tags will be dramatically increased. Thereby, it is not a sufficient protocol within the scope of this thesis.

**Time Division Multiple Access (TDMA):** In this protocol, a single frequency band is divided to time slots and is assigned to tags. One of the most important features of this technique is that each tag must be synchronized to the time slots and send its information at the beginning of the selected slot [45]. This technique can be directly applied to passive RFID systems. In such systems, the simplicity of tags transfers the complexity to the readers, where the reader has to control the time synchronization. However, in active RFID systems, synchronization can be either centralized or distributed to the tags.

In UHF passive dense RFID system, both TDMA and SDMA are the most commonly used PHY-layer anti-collision protocols. In these systems, there is only a single reader versus a large number of tags. Thus, there is no problem to increase the complexity of the reader. However, the tags should be as cheap and simple as possible.

## 3.2 MAC-Layer Anti-collision Protocols

Unfortunately, the physical layer anti-collision proposals are not cost effective for the market challenges of the passive RFID technologies. Therefore, collision solutions are commonly implemented at the MAC-layer. This section will discuss the most common MAC-layer anti-collision protocols.

Figure 3.2 presents the main classification of the most common MAC-layer anti-collision protocols. According to figure 3.2, MAC-layer anti-collision protocols is classified into two main categories: deterministic protocols and probabilistic protocols. Deterministic protocols are used in systems with known number of tags to be identified in the reading area. These types of protocols are mainly based on tree algorithms for the identification processes. Probabilistic protocols are used in systems with an unknown number of tags. Probabilistic protocols are mainly based on ALOHA algorithm.

The following sections will discuss in details the most commonly used anti-collision algorithms either deterministic or probabilistic based algorithm.

### 3.2.1 Deterministic Anti-collision Protocols

These protocols are commonly named tree-based anti-collision protocols. Using these algorithms, the reader aims to identify a set of tags in the coverage area in subsequent time slots [46]. Each time slot contains a query command, transmitted from the reader, and the response of tags in the reading area. If there is more than one tag reply in one slot, a collision occurs and the reader tries to split the tags into two subgroups. The reader repeats the splitting procedure until it receives a single tag reply. Tree based anti-collision protocols can be classified into two groups:

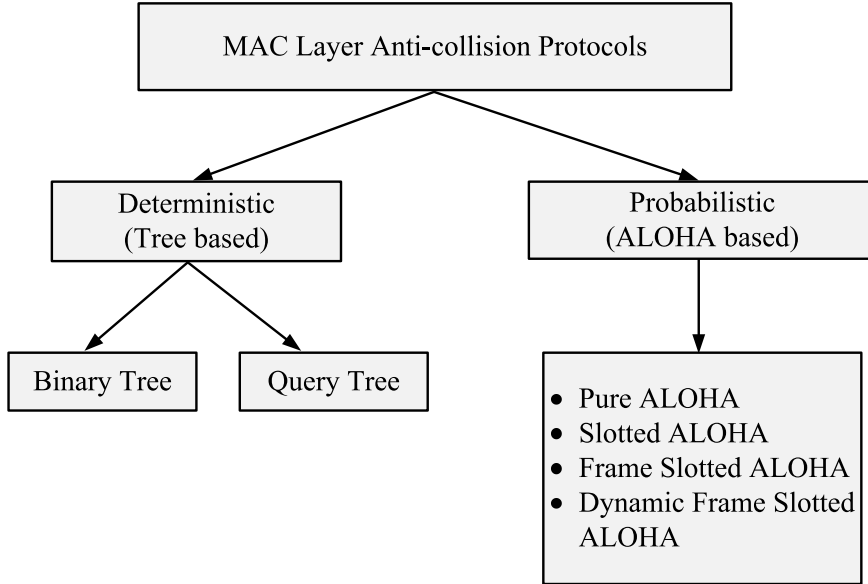


Figure 3.2: Common existing MAC-Layer anti-collision protocols

### Binary tree

The binary tree algorithm [47] is commonly used in tree-based anti-collision protocols. Using this algorithm, if a collision occurs in a time slot, each collided tag selects randomly '0' or '1'. Thus, the colliding tags will be separated into two subgroups. Tags, which have selected '0' always transmit their IDs to the reader first. If a collision re-occurs, collided tags are splitted again by selecting '0' or '1'. Tags, which have selected '1' have to wait until all other tags which have selected '0' are successfully identified by the reader. This procedure continues recursively until the subset is reduced to one tag, that is identified without collisions.

Figure 3.3 shows an example of the binary tree algorithm resolving the collision of four tags in a reading area. Thus, we have a collided time slot at the beginning. At time slot 2, each collided tag has to choose '0' or '1' randomly. In our example, tags 1 and 2 have selected '0'. However, tags 3 and 4 have selected '1'. According to binary tree algorithm, tags 3 and 4 have to wait until tags 1 and 2 are successfully identified. Therefore, time slot 2 is a collided slot due to the collision between tags 1 and 2. Due to collision, both tags 1 and 2 have to choose either '0' or '1'. In this example, both tags 1 and 2 have selected '1'. This resulted and empty slot in time slot 3 and collided

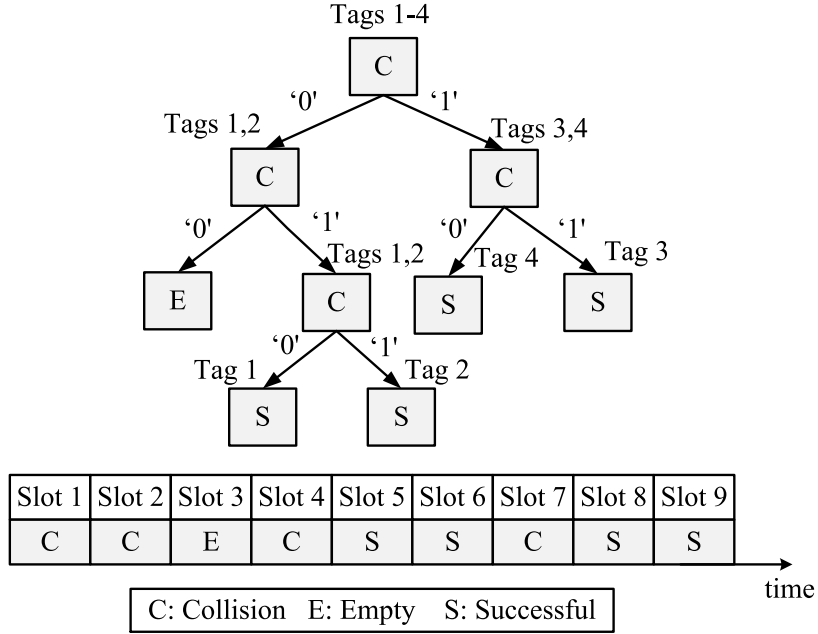


Figure 3.3: Binary tree anti-collision algorithm example

slot in time slot 4. Afterwards, tag 1 has selected '0' and tag 2 has selected '1'. This random selection made them separated and results in two successive successful slots in time slots 5 and 6. At this moment, tags 3 and 4 started their identification process. The reader repeats the previous process until identifying all tags in the reading area.

### Query tree

Another category from tree algorithm is the query tree algorithm [48]. It is also commonly used in tree-based anti-collision algorithm. Using this algorithm, the broadcast is a query signal asking the tags for a reply. If there is a collision, it starts splitting the collided tags into two groups by sending a new query signal with a single bit 0 or 1 randomly. Tags in the reading area receive this signal and match this bit with their ID. If this bit matches their ID, they transmit their ID. If a collision happened again, the reader adds another random bit 0 or 1 to its next query signal. This process is repeated until the reader receives a successful single tag reply.

Figure 3.4 presents an example for the query tree algorithm resolving the collision of 4 tags in a reading area. At time slot 1, the reader broadcasts a query

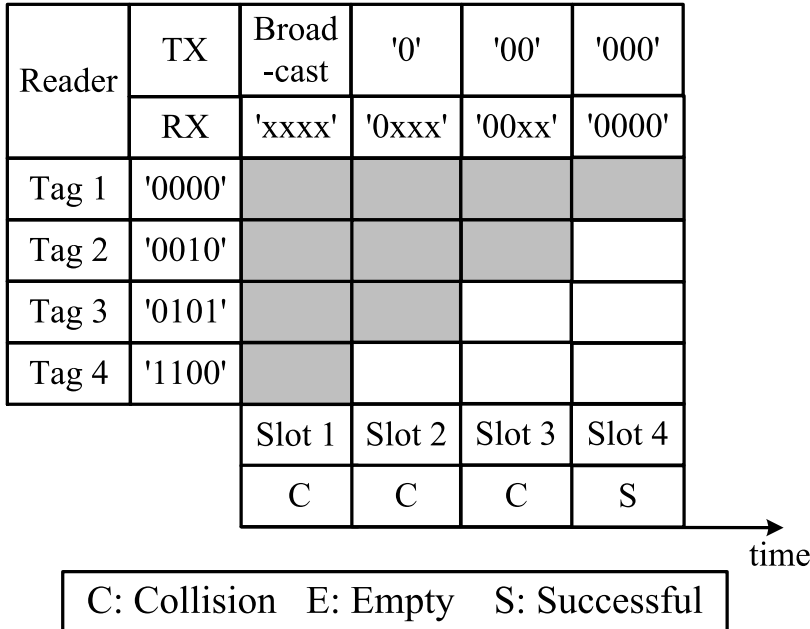


Figure 3.4: Query tree anti-collision algorithm example

signal asking them for a reply. A collision between the four tags is happening. The reader sends a '0' in a new query signal at time slot 2. However, there are three tags sharing this bit, so a new collision between the three tags is happening. Thereby, the reader has sent a '00' in its next query signal in time slot 3. At this time, there is a collision between two tags, leading the reader to send '000' in time slot 4. At last, the reader has received a single successful reply from tag 1. This process is repeated until the reader identify all the tags in the reading area.

### 3.2.2 Probabilistic Anti-collision Protocols

The main problem of using tree-based protocols is that these protocols are not efficient in dense networks (large number of tags), due to the increase in identification time [49]. Therefore, in dense network, ALOHA anti-collision protocols are more suitable. ALOHA anti-collision protocols are the most commonly used in UHF active and passive RFID. In these protocols, the readers do not know exactly the number of tags in the reading area to be identified. ALOHA anti-collision protocols are classified into the following four groups:

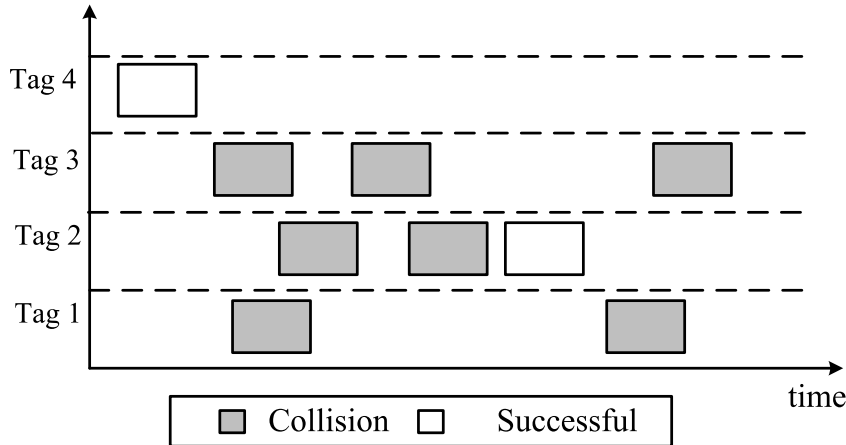


Figure 3.5: Example of pure ALOHA protocol

### Basic ALOHA

The first one is the widely known basic ALOHA [50] anti-collision protocol. Basic ALOHA is the simplest anti-collision protocol for passive read-only-memory RFID tags. This protocol works as follows: The reader sends a query signal to power on tags. Then, tags send their ID randomly in time. The reader can only recognize the single tag reply case, without any ability to handle the collision. According to [50], the maximum reading efficiency is 18.4 %. Figure 3.5 shows an example of basic ALOHA for a single reader identifying four tags.

### Slotted ALOHA

The second ALOHA anti-collision protocol is the slotted ALOHA (SA) protocol [51]. As shown in figure 3.6, slotted ALOHA is based on basic ALOHA. However, the time is divided into slots. In this protocol, the reader broadcasts a query signal which includes the beginning of each slot. Each tag chooses randomly if it will transmit in this slot or wait for a coming slot. The main advantage of this technique compared to basic ALOHA is: In slotted ALOHA, tag replies are completely synchronized. Therefore, collided slots are completely timing overlapping tags. However, in the basic ALOHA protocol, the partial timing overlapping exists. Thus, the maximum reading efficiency using slotted ALOHA is 36.8 % [51].

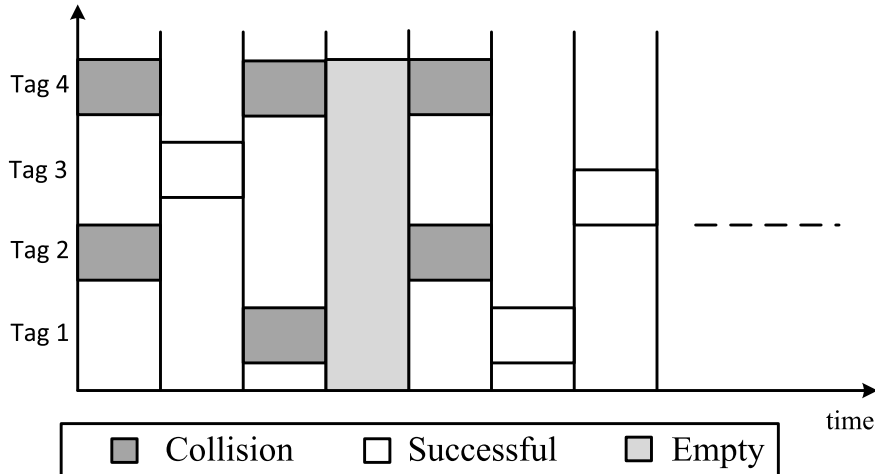


Figure 3.6: Example of slotted ALOHA

### Framed Slotted ALOHA (FSA)

The third group is Framed Slotted ALOHA (FSA) [49]. The FSA anti-collision protocol uses a fixed frame length. Thus, the frame length is fixed during the complete tag identification process. At the beginning of each frame, the reader broadcasts a query signal to all tags. This signal includes the frame size. Each tag has to choose random number between 0 and  $L - 1$ , where  $L$  is the frame length. If a collision happened, the colliding tags have to wait for the next frame.

Figure 3.7 presents an example for the identification process of four tags using FSA. In this example, the frame length is selected to four slots. According to figure 3.7, tag 4 transmits in the first slot alone. Thus, it is a successful slot. In the second slot, no tag has replied. So, it is an empty slot. In the third slot, tags 2 and 3 have replied together, which results in a collided slot. According to the FSA rules, tags 3 and 4 are not allowed to resubmit their IDs again during the same frame. Thus in slot 4, tag 1 only is allowed to reply to have another successful slot. In the next frame, the same procedure is repeated until all tags are identified.

### Dynamic Frame Slotted ALOHA (DFSA)

The final type of ALOHA anti-collision protocols is Dynamic Framed Slotted ALOHA (DFSA) [52]. Using this algorithm, the number of slots per frame is

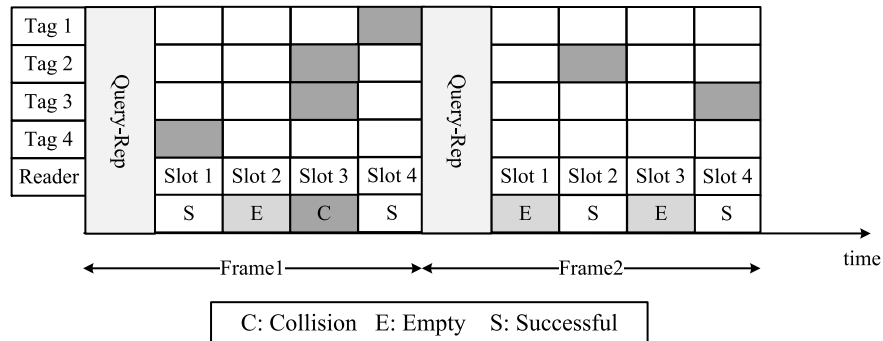


Figure 3.7: Example for Frame Slotted ALOHA

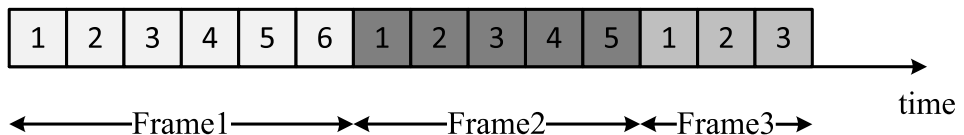


Figure 3.8: Slots of Dynamic Frame Slotted ALOHA

variable as shown in figure 3.8. According to the previously published RFID work, DFSA [53] is the most widely used anti-collision protocol for RFID systems owing to its simplicity and robustness. In DFSA, the reading process is divided into successive frames, in which each frame includes a specific number of slots. During the reading process, each active tag randomly assigns itself to one of the available slots in the frame. Therefore, each slot can take one of the following three variable states: 1) Successful Slot: One tag only chooses this slot, is fully identified, and then is deactivated by the reader within the successive frames. 2) Collided Slot: Multiple tags reply, resulting in a collision. The collided tags normally remain in their active state and retry their transmission in the next frame. 3) Empty Slot: No tag responds and the slot remains unused.

Increasing the reading speed can directly be translated into the maximization of the number of successful slots wrt. the number of idle or collided slots. Based on the Random Access Theory [54], for a given number of  $n$  tags, the expected number of empty  $E$ , successful  $S$ , and collided  $C$  slots in each frame with a length of  $L$  slots can be expressed by the following equations:

$$E = L \left(1 - \frac{1}{L}\right)^n, S = n \left(1 - \frac{1}{L}\right)^{n-1}, C = L - E - S \quad (3.1)$$

The conventional definition of the expected reading efficiency  $\eta_{conv}$  is given by the ratio between the expected number of successful slots  $S$  in a frame and the frame length  $L$  [55]:

$$\eta_{conv} = \frac{S}{L} \quad (3.2)$$

Based on (3.1) and (3.2), this results in the conventional definition of the efficiency:

$$\eta_{conv} = \frac{n}{L} \left(1 - \frac{1}{L}\right)^{n-1} \quad (3.3)$$

Figure 3.9 shows the FSA reading efficiency  $\eta_{conv}$  for a constant frame length  $L = 64$  and different numbers of tags. The main goal of optimizing the DFSA algorithm is finding the optimal frame length  $L$ , which maximizes the reading efficiency  $\eta_{conv}$ . Based on (3.3), the reading efficiency  $\eta_{conv}$  is maximized when:

$$L_{opt} = n \quad (3.4)$$

In practical applications, the number of tags  $n$  in the interrogation region is unknown. Furthermore, the number of tags may even vary, e.g. when the tags are mounted on moving goods, and because successfully read tags get inactive in the following frames. Therefore, such applications employ DFSA [56]. First, DFSA has to estimate the number of tags in the interrogation area, and then has to calculate the optimal frame size  $L$  for the next reading frame. Figure 3.10 presents a summary for DFSA. As shown in the chart, the reader starts with an initial frame length. Then, it broadcasts this frame length to the tags in the reading area. Afterwards, it performs a normal FSA. At the end of the frame, the reader checks if there are any successful or collided slots. If yes, the reader estimates the remaining number of tags in the reading area, and then optimizes the next frame length and starts again normal FSA. If not, the reading cycle will be terminated.

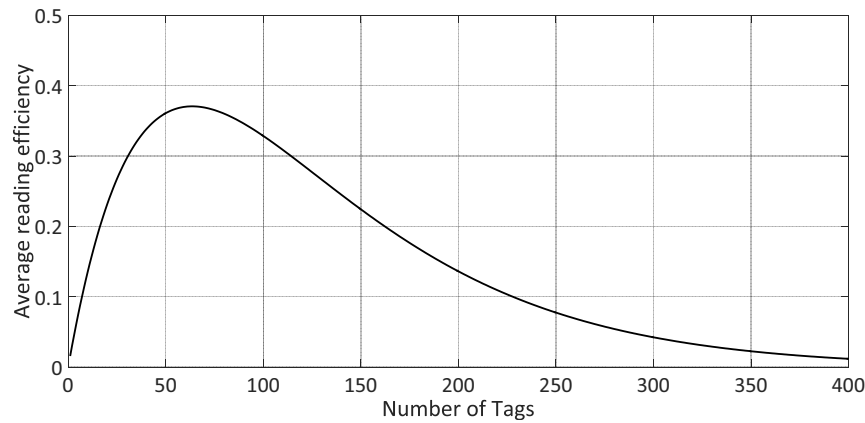


Figure 3.9: Frame Slotted ALOHA Reading efficiency, maximum reached for  $L = n = 64$  tags of  $\eta_{conv} = 0.36$

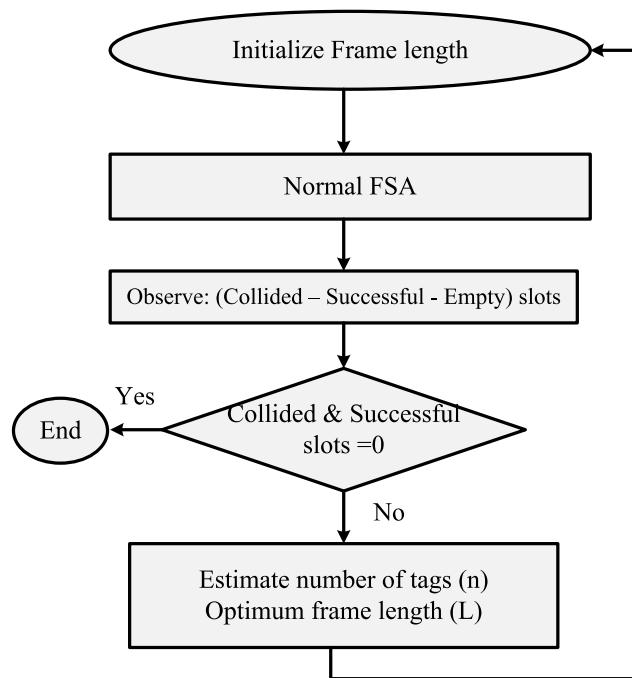


Figure 3.10: Flow chart of Dynamic Framed Slotted ALOHA (DFSA)

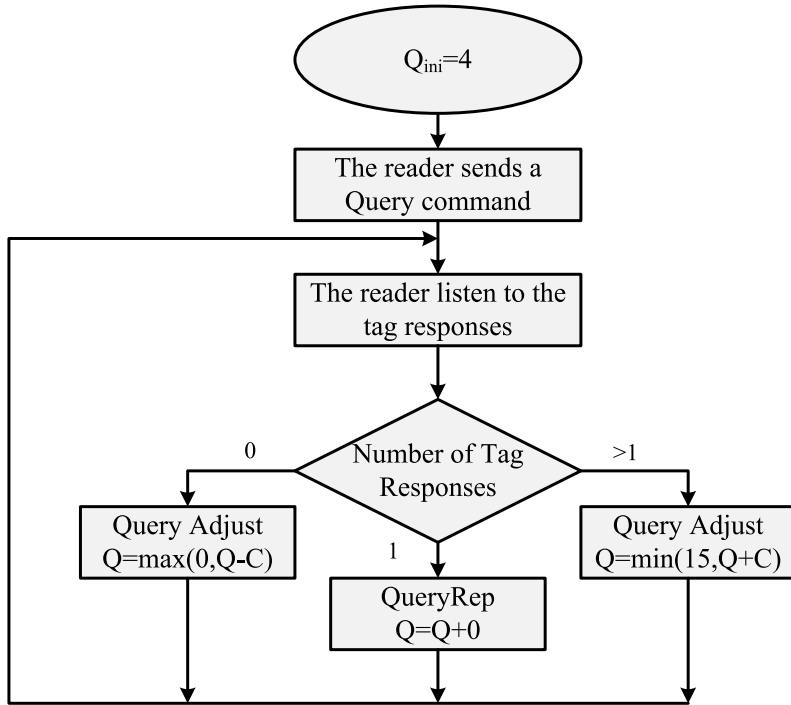


Figure 3.11: Conventional variable frame length procedure EPCglobal C1 G2 [11]

### 3.3 DFSA with EPCglobal C1G2

In this section, a brief introduction about DFSA with EPCglobal C1 G2 [11] will be given. The reading process consists of multiple inventory rounds. Each inventory round has a different frame length. Figure 3.11 shows an example for the frame length adaptation in EPCglobal C1 G2. According to figure 3.11, the initial frame length is  $2^{Q_{ini}}$ , where  $Q_{ini} = 4$ . Then each slot is checked. If there is no tag reply, the frame length should be decreased. If it is a collided slot, the frame length is increased. Finally, if the slot is a successful slot, the frame length will remain as it is.

Figure 3.12 shows an example for timing diagram of different inventory rounds between a single RFID reader and different tag reply situations. The reader starts with a query command. In this command, the reader broadcast the current frame length for all the tags in the reading area. Each tag has to choose a random slot between 0 and  $2^Q - 1$ .

Figure 3.12a shows the case of single tag reply. In this case, the tag replies

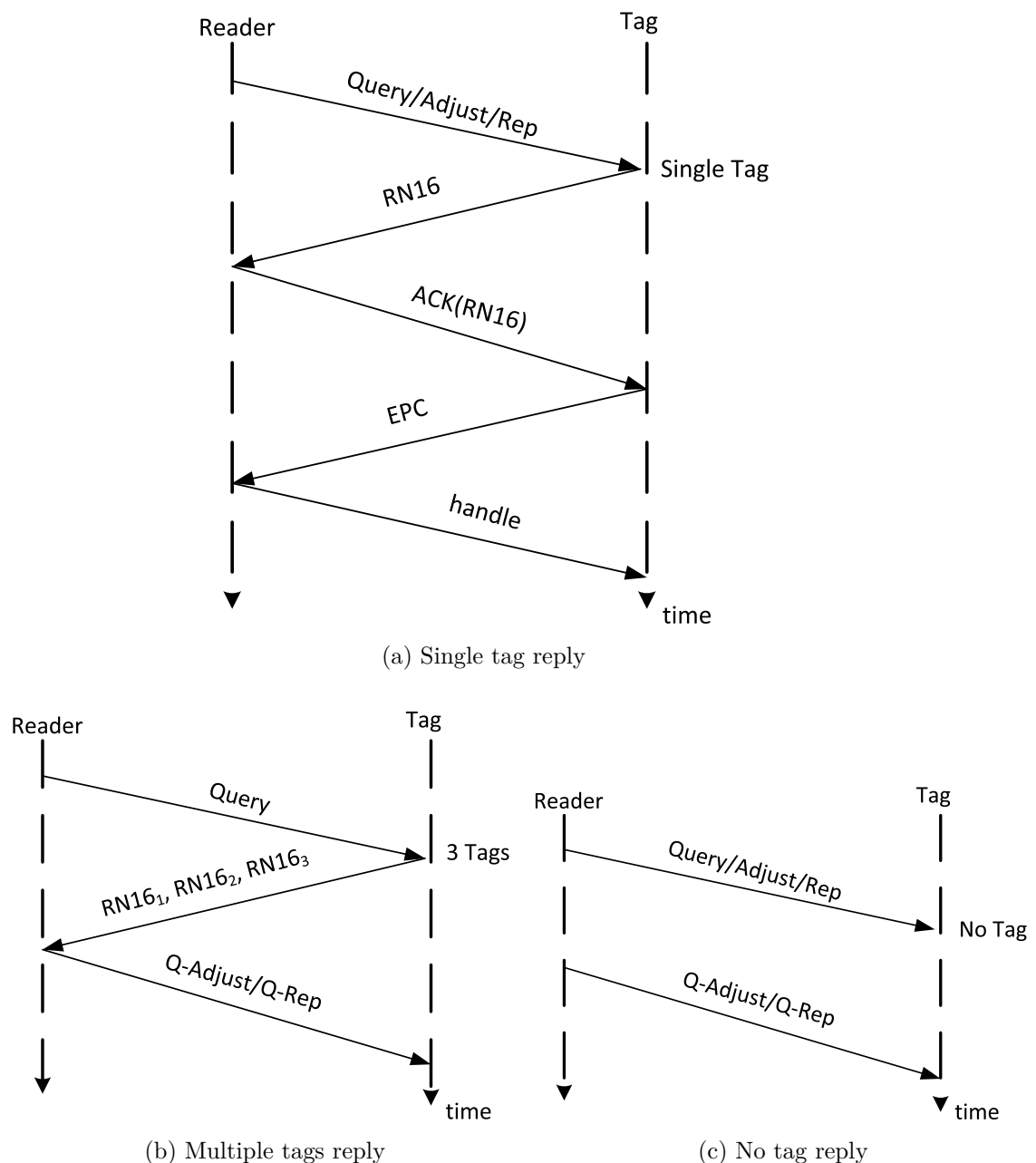


Figure 3.12: Example of an inventory between reader and different tag reply situations [11]

with its Random Number 16 (RN16), which is a 16 bits random number. When the reader receives this RN16 it will acknowledge this tag with an ACK command including this RN16. As soon as the tag receives a valid Acknowledgment (ACK) with its RN16, it will reply with its unique Electronic Product Code (EPC). Finally, the reader will send a handle command to the tag to mute it until the end of the complete reading process. In figure 3.12b, the reader starts broadcasting a query command for tags in the reading area. In the proposed example, three tags select this slot. Therefore, the reader receives simultaneously three different RN16s. In this case, the conventional RFID reader will not be able to decode any of these RN16s. The tags will wait for the next frame to be identified. Afterwards, the reader broadcasts a query-rep command to inform all the remaining tags that the next slot will start. Figure 3.12c shows the behavior of an empty slot in EPCglobal C1 G2. The reader starts with a query command, and waits for a tag reply during a certain time out period. If there is no tag reply during this time, it would terminate the the slot by sending a new query-rep command.

## 3.4 Cross Layer Anti-Collision Protocol

Recently, RFID receivers have been developed to be able to convert a part of collided slots into successful slots. Moreover, new RFID readers can even identify the type of the slots and terminate the empty and collided slots earlier. In this section, a brief discussion about these two parameters will be presented. Afterwards, a motivation to reconfigure the MAC layer to make use of the PHY-layer parameters is presented.

### 3.4.1 Collision Recovery in UHF RFID

Collision recovery in RFID systems is the capability of the reader to convert a part of the collided slots into successful slots. According to EPCglobal C1 G2, the reader can only acknowledge one single tag per slot. According to [57], the collision recovery capability of the RFID system depends on different factors: The capabilities of the receiver e.g. number of antennas, the distance between the collided tags, and the type of the channel.

Recently, some research groups (e.g. [58]) have concentrated on collision recovery using the spatial diversity of the received signal. They have proposed the following reading efficiency equation:

$$\eta = P(1) + \alpha \cdot \sum_{i=2}^n P(i), \quad (3.5)$$

where  $\sum_{i=2}^n P(i)$  is the probability of collision,  $\alpha$  is the average collision resolving probability coefficient. In this efficiency equation, the RFID reader can convert  $\alpha$  part of the collided slots into successful slots. The authors have assumed unlimited and equal collision resolving probabilities coefficients. For example, the probability to resolve two collided tags is identical to the probability to resolve ten collided tags, which is a strong simplification. Another research groups [59–62] considered the limited capability of a RFID reader to resolve collisions. They have proposed a limited reading efficiency expressed as:

$$\eta = \sum_{i=1}^M P(i), \quad (3.6)$$

where  $P(i) = \binom{n}{i} \left(\frac{1}{L}\right)^i \left(1 - \frac{1}{L}\right)^{n-i}$ , and  $M$  represents the number of collided tags that the reader is capable to recover. The authors assumed that the probability to recover one tag from  $i$  collided tags equals to 100%, independently of the actual  $i$ .

According to (3.5) and (3.6), the reading efficiency strongly depends on the capability of the physical layer to resolve the collision. Thus, in this thesis, the effect of the collision recovery capability on the MAC layer optimization will be addressed in more details.

### 3.4.2 Slots Durations in EPCglobal C1 G2

Conventional RFID systems cannot identify the type of the slots in FSA [56]. Therefore, such systems consider that the slot duration of FSA is constant, neglecting the type of the slot. Modern RFID readers can quickly identify the type of a slot (i.e. idle, successful, or collided). Hence, the durations of the different slot types are not identical, which reduces the overall reading time. Figure 3.13 shows two frames, each one with a frame length of  $L = 6$  slots. The first frame in (a) presents the conventional view of the frame with equal slots

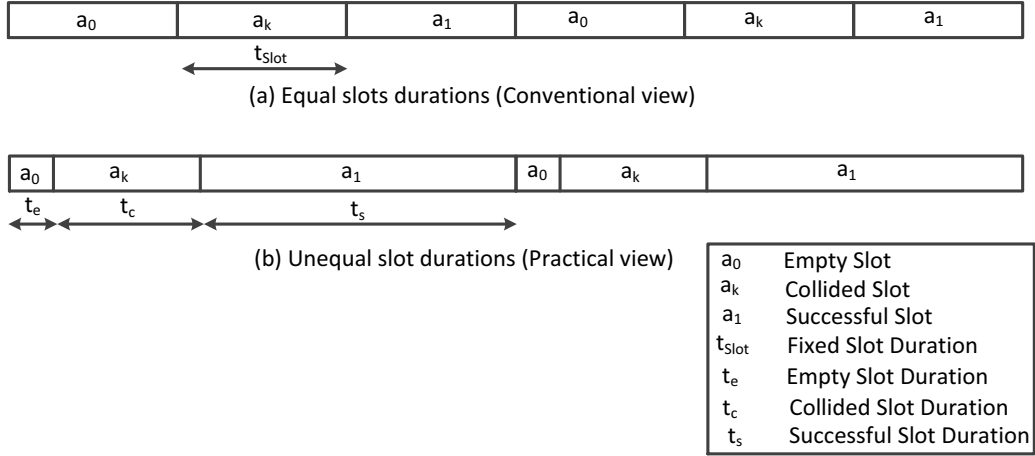


Figure 3.13: Equal and unequal views of slots in Frame Slotted ALOHA with frame length  $L = 6$ .

durations  $t_{Slot}$  for all slot types. The second frame in (b) presents the behavior of the real RFID slots behavior. Here, the slot duration depends on the slot type.

Figure 3.14 shows an example of a real measurements for slots durations using the Universal Software Radio Peripheral SDR receiver (USRP B210) [63]. In these measurements, we used a sampling frequency of  $f_s = 8$  MHz, because the total RFID bandwidth in the European system is 4 MHz, the tags data rate is 160 kbps. For the given parameters and as shown in figure 3.14, the collided slot duration is  $\simeq 1200 \mu\text{sec}$ , and the empty slot duration is  $\simeq 200 \mu\text{sec}$ .

According to the above discussion, the reading efficiency equation will be affected by the differences in slots duration, hence, the MAC layer optimization. In this thesis, the differences in slot duration length will be addressed in more details in the MAC layer optimization.

Summarizing, the main lack in the previous RFID research is that the MAC layer is optimized independently on the PHY layer layer. However, the PHY-layer properties affect the optimization parameters of the MAC layer, e.g. the number of tags estimation and the optimum frame length. In this thesis, I will concentrate on optimizing the DFSA anti-collision protocol. In the proposed algorithm, the physical layer parameters will be taken into consideration, which are presented on the physical collision recovery capability of the RFID reader and the differences in slot durations.

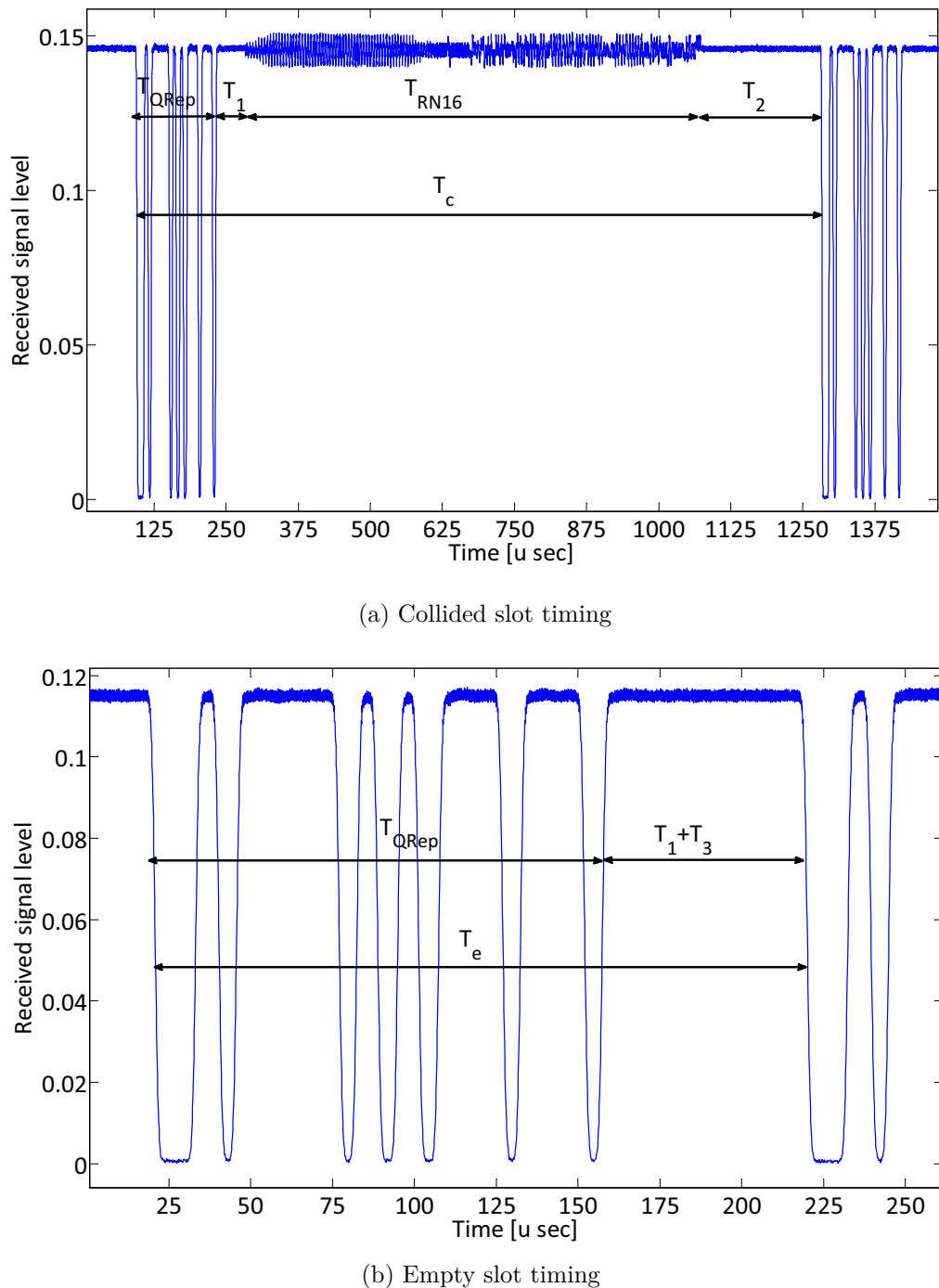


Figure 3.14: Slots durations measurements,  $f_s = 8\text{ MHz}$ , tag Backscatter Link Frequency  $BLF = 160\text{ kbps}$



# Chapter 4

## Estimation of the Tag Population

In this chapter, the most common estimation algorithms following the EPC-global C1 G2 standard [11] are presented. Afterwards, a novel number of tags estimation method called “Collision Recovery Aware Tag Estimation” will be introduced. The proposed method takes into consideration the collision recovery probability from the physical layer.

This chapter is organized as follows: section 1 shows the conventional number of tags estimation algorithms with performance analysis comparisons between them. Section 2 presents the novel collision recovery aware number of tags estimation method. Using this algorithm, a closed form solution for the estimated number of tags will be presented. The proposed solution gives a direct relation between the estimated number of tags and the frame length, successful and collided number of slots and the physical layer collision recovery probability.

### 4.1 State-of-the-Art Estimation Algorithms

The performance of the FSA algorithm strongly depends on the accuracy of the number of tags estimation and the frame size. For fast identification of RFID tags, an estimation of the number of RFID tags with the highest possible accuracy is the key issue for Framed-Slotted ALOHA based protocol. The

number of tags estimation function calculates the number of tags based on feedback from the previous frame, which includes the number of slots filled with empty, successful and collided slots. This information is then used by the function to obtain the number of tag estimate, and hence the optimal frame size  $L$  for a given round. According to the literature [53], the most common estimation algorithms are classified into four groups: heuristic Q-slot family, indirect heuristics Q-frame family, error minimization estimation, and Maximum Likelihood (ML) estimation.

#### 4.1.1 Heuristics Q-slot Family

The EPCglobal C1 G2 standard [11] proposes an alternative frame length adaptation mechanism without any prior tag estimation. Using this mechanism, the initial frame length is fixed  $Q_{ini} = 4$ . Then, the frame length is adjusted slot by slot according to the slot type: empty, successful, or collided. The performance of this scheme strongly depends on the value of the variable  $C$ , where  $C \in (0.1, 0.5)$ . Since the value of  $C$  is not clearly defined in the standard, there are different proposals optimizing the value of  $C$ . c.f. Figure 3.11 shows the flow diagram of the heuristics Q-slot family.

**$Q^{+-}$ Algorithm** This algorithm was proposed by [64]. Using this algorithm, the query command is transmitted only if the reader has to calculate a new value of  $Q$ . Otherwise, the reader transmits the QueryRep command, because the Query command length is 22 bits and the QueryRep command length is only 4 bits. Moreover, The variable  $C$  is replaced by two variables:  $C_e$  and  $C_c$ .

$C_e$  is used when an empty slot is detected by the reader, whereas,  $C_c$  is used when a collided slot is detected by the reader. The values of  $C_e$  and  $C_c$  are calculated numerically regardless the number of tags in the reading area.

**Optimum-C Algorithm:** This algorithm was proposed by [65], where the optimum value of  $C$  is calculated numerically versus the previous value of  $Q$ . This is done by simulating a passive RFID system for the complete range of  $Q \in [0, \dots, 15]$  for each  $Q$  and  $C \in [0.1, \dots, 0.5]$  with step size 0.1. At last, the best combination is the one which gives the minimum identification delay.

**Slot Count Selection (SCS) Algorithm:** This algorithm was proposed by [66], in which the variable  $C$  is replaced by two variables  $C_1$  and  $C_2$  like using the  $Q^{+-}$  approach [64]. However,  $C_1$  and  $C_2$  for the SCS algorithm are calculated slot by slot as a function of other parameters. These parameters depend primarily on the Reader-to-Tags (R-T) and Tags-to-Reader (T-R) data rates. According to [66], the system performance will be improved if the values of  $C_2$  and  $C_1$  are set to be  $C_2 \in [0.1, 1]$  and  $C_1 = 0.1$ , respectively. The authors neglected the effect of the modulation and the encoding scheme. According to [67,68], the correct value of (T-R) data rate strongly depends on the modulation and the encoding scheme.

According to [69], the heuristics Q-slot family is an, almost optimum anti-collision algorithm for small RFID networks, which have number of tags less than 50 tags. However, in dense network, the performance of such algorithms is degraded.

#### 4.1.2 Indirect Heuristics Q-frame Family

In dense RFID networks, the indirect heuristics Q-frame family gives better performance [69]. In this family, the proposed algorithms first calculate the estimated number of tags in the reading area  $\hat{n}$ . Then, it adjusts the optimum frame length  $L$  that maximizes the reading efficiency. The estimation process is based on information from the previous frame.

**Lower Bound:** This method was proposed by [56], taking a very trivial assumption for the lower bound of the number of tags in the reading area  $\hat{n}$ . It is not related to any theoretical lower bound. Additionally, it claims that each collided slot involves two collided tags. Therefore, it is presented as:

$$\hat{n}_i = S_i + 2 \cdot C_i \quad (4.1)$$

where  $i$  presents the frame index,  $S_i$ , and  $C_i$  are successively present the number of successful and collided slots in frame  $i$ .

**Schoute Algorithm:** The Schoute algorithm [52] is based on the hypothesis that the frame length is equivalent to the number of unidentified tags  $L = \hat{n}$

since this is a direct way to optimize the system throughput. Schouste's method also supposes that the number of unidentified tags  $\hat{n}$  could be infinite. Let  $P_c$  be the probability that a slot is a collision slot and  $P_s$  be the probability that a slot is a success slot. Then, the estimated collision rate  $C_{rate}$  is expressed as follows:

$$C_{rate} = \frac{P_c}{1 - P_s} \quad (4.2)$$

For dense RFID networks,  $\hat{n}$  is a large number, the rate  $C_{rate}$  can be thus calculated as follows:

$$C_{rate} = \lim_{n \rightarrow \infty} \frac{P_c}{1 - P_s} \cong 0.418 \quad (4.3)$$

More details are discussed in [70].

Thus, the average number of tags involved in a collision slot  $C_{tag}$  is then computed as follows:

$$C_{tag} = \frac{1}{C_{rate}} \cong 2.39 \quad (4.4)$$

Therefore, Schouste's method estimates the number of estimated tags  $\hat{n}$  as follows:

$$\hat{n}_i = S + 2.39 \cdot C_i \quad (4.5)$$

However, the supposed conditions in this method are too strict that some deviations would be generated if the real situation differs much from the strict conditions.

**C-Ratio:** The authors of the C-Ratio estimation method [71] proposed a binomial distribution for the number of tags. They assume the tags select a slot with probability of success  $P = \frac{1}{L}$ , where  $L$  is the frame length. The collision ratio is defined as the ratio between number of collided slots  $C_i$  and the frame length  $L_i$ , where  $i$  is the frame index. Therefore, the C-Ratio can be expressed as:

$$C_{ratio} \triangleq \frac{C_i}{L_i} = 1 - \left(1 - \frac{1}{L_i}\right)^{n_i} - \left(1 + \frac{n_i}{L_i - 1}\right) \quad (4.6)$$

The optimum value of  $\hat{n}_i$  is obtained by searching for all possible values of  $n$  that makes the right hand side of (4.6) gives the closest value of C-Ratio, under

the condition that  $n_i \geq 2 \cdot C_i$ .

In [72], the authors used the same concept as the C-Ratio. However, they presume independent binomial distributions of the tags in each slot. Thus, the modified C-Ratio is expressed as:

$$\frac{C_i}{L_i} = \sum_{j=2}^{n_i} \binom{n_i}{j} \left(\frac{1}{L_i}\right)^j \left(1 - \frac{1}{L_i}\right)^{n_i-1} \quad (4.7)$$

To simplify the searching process, this estimator suggests applying an upper bound to estimate the number of tags.

#### 4.1.3 Error Minimization Estimation

Vogt proposes an estimation algorithm based on the minimum squared error (MSE) estimation [54]. It minimizes the distance between the observed empty  $E$ , successful  $S$ , collided  $C$  slots and their expected values  $E_{exp}$ ,  $S_{exp}$ ,  $C_{exp}$  for a given frame length  $L$ . It is presented as:

$$\varepsilon_{conv}(L, S, C, E) = \min_n \{|E_{exp} - E| + |S_{exp} - S| + |C_{exp} - C|\} \quad (4.8)$$

where

$$E_{exp} = L_i \left(1 + \frac{1}{L_i}\right)^n, S_{exp} = n \left(1 + \frac{1}{L_i}\right)^{n-1}, C_{exp} = L_i - E_{exp} - S_{exp} \quad (4.9)$$

However, this method requires numerical searching to find the optimum value of the number of tags  $\hat{n}$ . Moreover, the author assumed that tags are identically distributed over slots, which is generally not a valid assumption.

#### 4.1.4 Maximum Likelihood (ML) Tag Estimation

The main concept of ML number of tags estimation is to compute the conditional probability of an observed events assuming that this conditional probability is function of the number of tags  $n$ . Subsequently, the  $\hat{n}$  is the estimated number of tags which maximizes this conditional probability. In [73], the author proposes a ML number of tags estimation by finding the optimum  $\hat{n}$  that gives exact  $E$  empty slots,  $S$  successful slots, and  $C$  collided slots, if there are  $L$  slots.

In addition, he uses a multi-nomial distribution with  $L$  repeated independent trials. Each trial has one of three possibilities:  $P_e$  empty,  $P_s$  successful, or  $P_c$  collision, where  $P_e$ ,  $P_s$ , and  $P_c$  follow binomial distribution [56] and can be presented as:

$$P_e = \left(1 + \frac{1}{L}\right)^n, P_s = \frac{n}{L} \left(1 + \frac{1}{L}\right)^{n-1}, P_c = 1 - P_e - P_s \quad (4.10)$$

The probability that in  $L$  trials given  $E$  empty slots  $S$  successful slots, and  $C$  collided slots occur is:

$$P(\hat{n}|L, S, C, E) = \frac{L!}{E!S!C!} P_e^E P_s^S P_c^C, \quad (4.11)$$

This probability is the general term of the multi-nomial expansion of  $(P_e + P_s + P_c)^L$ . Therefore, for a read cycle with frame length  $L$ , a posterior probability for the number of tags  $n$  when  $E$  empty slots,  $S$  successful slots, and  $C$  collided slots are observed, is calculated as shown in (4.11).

#### 4.1.5 Performance Comparison for Existing Estimation Protocols

According to literature [74–76], the most common comparison estimation performance metric is called relative estimation error  $\epsilon$  versus the normalized number of tags  $n/L$ . It presents the absolute difference between the actual number of tags and the estimated one divided by the actual number of tags in the reading area. Accordingly, it is defined as:

$$\epsilon = \left| \frac{\hat{n} - n}{n} \right| \times 100 \% \quad (4.12)$$

Figure 4.1 shows the comparison of the most common number of tags estimation algorithms used in the passive UHF RFID systems. The comparison metric is the average relative estimation error  $\epsilon$ , which is calculated using Monte-Carlo simulations with 1000 iterations. According to figure 4.1, the simplest estimation algorithm presented is the lower bound Schoultz algorithm [52]. It gives accurate result only when FSA frame length is equal to the number of tags  $L = n$ . ML [73] estimation method is the most accurate estimation algorithm

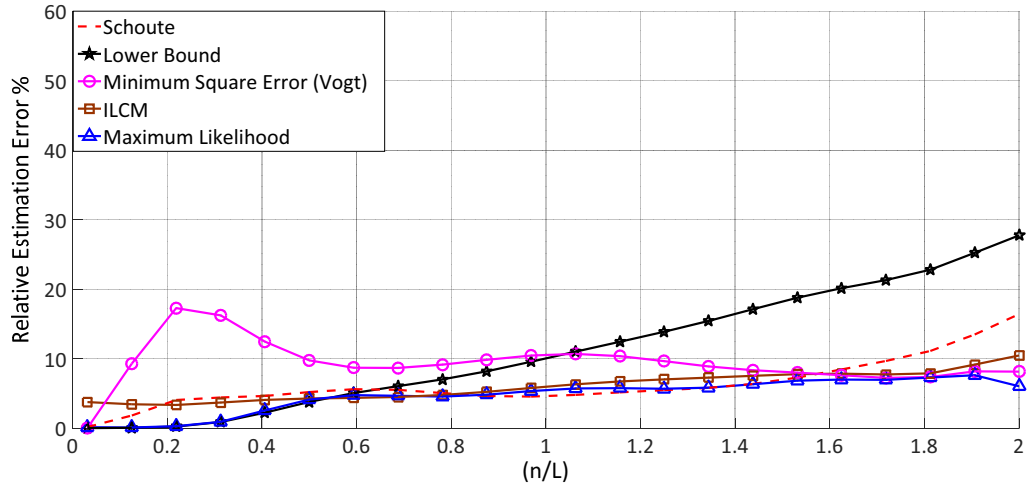


Figure 4.1: Relative estimation error  $\epsilon$  vs. normalized number of tags  $n/L$  for the common state-of the-art estimation algorithms

along the different values of  $L$  and  $n$ . It gives the minimum relative estimation error even in dense RFID networks, which is the main focus of the proposed work. However, according to [76], the complexity of the ML algorithm is much higher than the other estimation algorithm, because it searches for the value  $n$  that maximizes the estimation probability. This disadvantage makes ML estimation not a practical solution for dense RFID networks.

Figure 4.2 displays another comparison metric, which is the mean identification time required to identify  $n$  number of tags. The comparison is between the average identification time using FSA algorithm with the most common existing number of tags estimation protocols. According to figure 4.2, the Maximum Likelihood (ML) estimator [73] achieves the closest approach to the perfect estimation algorithm. However, the numerical searching complexity of the ML estimator [73] might lead to numerical instability problems for simple low-end devices as described in [53]. This leads us to search for a method compromising between the accuracy of the protocol and the stability of its implementation for dense RFID networks. Moreover, all these methods do not take into consideration the collision recovery capabilities effect of the modern RFID physical layer.

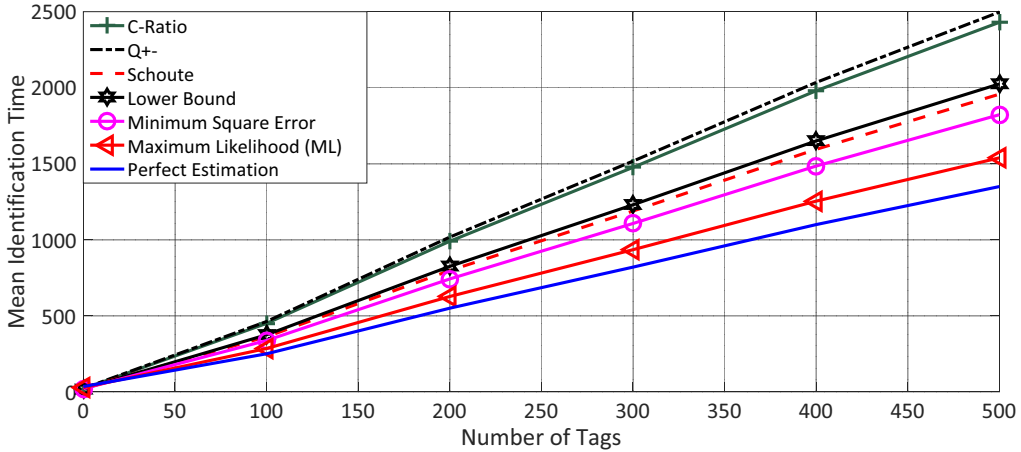


Figure 4.2: Mean identification time using FSA for simulated common state-of-the-art estimation algorithms versus the number of tags in the reading area.

## 4.2 Novel Collision Recovery Aware Tag Estimation

The previously mentioned literature proposed various estimation methods. Accordingly, the ML estimation method is the most precise. However, it possesses two main disadvantages: 1) It is implemented using numerical methods, which needs many calculations and iterations to find the optimum estimated value. 2) It neglects the physical layer effect, which is an inaccurate assumption. Modern systems are capable of converting part of collided slots into successful slots e.g. [60, 61]. In such systems, the number of collided and successful slots delivered to the MAC layer are inaccurate information about the real number of tags at the reading area. Therefore, it is important to take into consideration the collision recovery capability. Li [58] used the estimation approach of [54], hence, considering the collision recovery probability. However, this method leads to multi-dimensional searching, which needs a lot of iterations and complex calculations.

In this section, a novel closed-form solution for the estimated number of tags  $\hat{n}$  is proposed taking into account the collision recovery probability of the system. Then, calculating the collision recovery probability from the physical layer parameters will be demonstrated. The proposed solution gives a direct and linear relation between the estimated number of tags  $\hat{n}$  and the frame length

$L$ , successful and collided number of slots  $S$ ,  $C$ , and the collision recovery probability  $\alpha$ .

### 4.2.1 System Model Under Collision Recovery Probability

In this section, a novel number of tags estimation method is given. The proposed method is based on the classical ML estimation presented in [73]. According to the aforementioned method, the optimum value of  $\hat{n}$  which maximizes the conditional probability of the observing vector  $v = \langle C, S, E \rangle$  is used, given that  $n$  tags transmit at a frame length  $L$ :

$$P(\hat{n}|L, S, C, E) = \frac{L!}{E!S!C!} P_e^E P_s^S P_c^C, \quad (4.13)$$

where  $C$ ,  $S$ ,  $E$  are the number of collided, successful, and empty slots per a frame length  $L$ , successively, and  $P_e$ ,  $P_s$ ,  $P_c$  are the probabilities of empty, successful and collided transmissions per slot, respectively. Owing to the fact that modern RFID readers have a collision recovery capability, thereby, the physical layer converts part of collided slots into successful slots based on the following relation:

$$E = E_b, S = S_b + \alpha \cdot C_b, C = C_b - \alpha \cdot C_b, \quad (4.14)$$

where  $C_b$ ,  $S_b$ ,  $E_b$  are successively the expected number of collided, successful, and empty slots before the collision recovery of the system, and  $C$ ,  $S$ ,  $E$  are respectively the expected number of collided, successful, and empty slots after collision recovery of the system, where  $\alpha$  is a variable indicates the collision recovery capability of the physical layer. The calculation of the collision recovery probability will be discussed in details in the following sections. Figure 4.3 clarifies the flow diagram of the proposed system. In this system, the physical layer gives the MAC layer information about its collision recovery capability.

In the MAC layer, only the values of  $C$ ,  $S$ ,  $E$  are known after the PHY-layer collision recovery. In this stage, there is no information about these values before the collision recovery. Thus, the conventional estimation systems, including the classical ML number of tags estimation in (4.13) use the values of  $C$ ,  $S$ ,

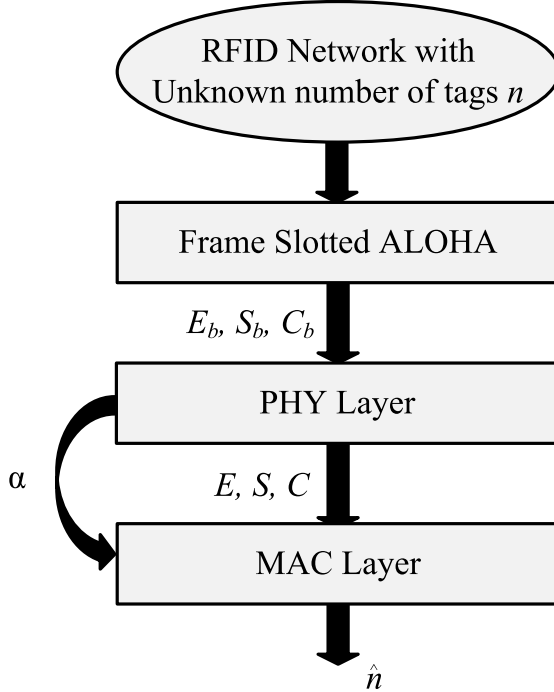


Figure 4.3: Physical layer collision recovery capability

$E$  after collision recovery in their calculations. However, these values are not accurate indicators for the actual number of tags in the reading area. In the proposed solution, the value of the current average collision recovery probability  $\alpha$  is estimated, as it will be shown in details in the following section. Finally, the expected corresponding values of  $C_b$ ,  $S_b$ ,  $E_b$  are calculated as:

$$E_b = E, C_b = \left\lfloor \frac{C}{1 - \alpha} \right\rfloor, S_b = S - \left\lceil \frac{\alpha}{1 - \alpha} \right\rceil C \quad (4.15)$$

Under the condition:

$$L = E_b + S_b + C_b \quad (4.16)$$

Thus,  $C_{b(max)} = L - E_b$  and  $S_{b(min)} = 0$ . Therefore, the proposed collision recovery aware ML conditional probability can be formalized as:

$$P(\hat{n}|L, S, C, E, \alpha) = \frac{L!}{E_b! S_b! C_b!} P_e^{E_b} P_s^{S_b} P_c^{C_b} \quad (4.17)$$

According to [77, 78], for those situations in which  $n$  is large and  $\frac{1}{L}$  is very small, the Poisson distribution can be used to approximate the binomial dis-

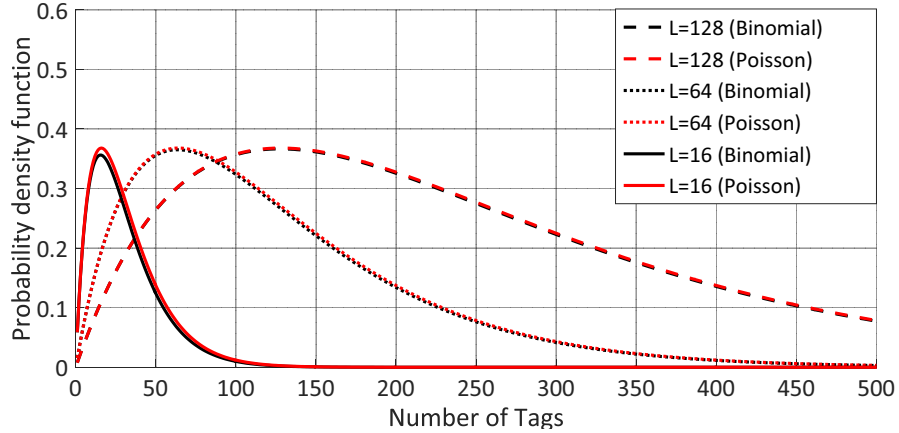


Figure 4.4: Binomial distribution and its Poisson approximation for probability of success using different frame lengths

tribution. Figure 4.4 shows the success probability using Binomial distribution and its Poisson approximation versus the number of tags with different frame lengths. According to figure 4.4, the larger the number of tags  $n$  and the longer the frame length  $L$ , the better is the approximation. Based on figure 4.4, this approximation is valid under conditions  $n \geq 10$  and  $L \geq 16$ .

This thesis focuses on dense RFID networks. So, the use of the suggested approximation in [53] for the tag probability of transmission per slot, which is considered as independent Poisson random variables with unknown mean  $\gamma = \frac{\hat{n}}{L}$ , is applicable. Thus, the probability functions can be presented as follow:

$$P_e = e^{-\gamma}, P_s = \gamma \cdot e^{-\gamma}, P_c = 1 - e^{-\gamma} - \gamma \cdot e^{-\gamma} \quad (4.18)$$

After substituting by (4.18) in (4.17) the proposed conditional probability is:

$$P(\hat{n}|L, S, C, E, \alpha) = \left( \frac{L!}{E_b!S_b!C_b!} \right) \gamma^{S_b} \cdot e^{-\gamma \cdot L} \cdot (e^{-\gamma} - 1 - \gamma)^{C_b} \quad (4.19)$$

The term of  $\frac{L!}{E_b!S_b!C_b!}$  is not a function of the number of tags. It is only an offset and can be normalized. Thus, the proposed normalized conditional probability is:

$$P(\hat{n}|L, S, C, E, \alpha) = \gamma^{S_b} \cdot e^{-\gamma \cdot L} \cdot (e^{-\gamma} - 1 - \gamma)^{C_b} \quad (4.20)$$

Equation (4.20) gives a conditional probability for the estimated number of

tags for a given number of successful, collided, empty slots and collision recovery probability. The computation of (4.20) can be done by numerical searching to obtain the optimum value of  $\hat{n}$  which maximizes (4.20). Hence, the calculation of (4.20) leads to multi-dimensional lookup table, which leads to time consuming, especially in case of dense network containing large number of tags  $n$ .

#### 4.2.2 Derivation of the Proposed Closed Form Solution

This section will propose a closed form solution for the collision recovery aware estimation. This is achieved by differentiating (4.20) with respect to  $\gamma$  and equate the results to zero. After differentiating, the equation can be simplified as:

$$e^{-\gamma} \left( 1 + \frac{\gamma(\gamma \cdot L - S_b)}{(\gamma \cdot L - S_b - \gamma \cdot C_b)} \right) - 1 = 0 \quad (4.21)$$

The analysis of (4.21) indicates that the relevant values for  $\gamma$  are in the region close to one [79]. Hence, we can develop a Taylor series for  $e^{-\gamma}$  around one which leads to:

$$e^{-\gamma} \simeq 1 - \gamma + \frac{1}{2}\gamma^2 - \frac{1}{6}\gamma^3. \quad (4.22)$$

After substituting (4.21) and some additional simplifications, the final equation is a fourth order polynomial:

$$\underbrace{\frac{1}{120}(L - C_b)\gamma^4}_{(a)} + \underbrace{\frac{1}{24}\left(L - C_b - \frac{S_b}{5}\right)\gamma^3}_{(b)} + \underbrace{\frac{1}{6}\left(L - C_b - \frac{S_b}{4}\right)\gamma^2}_{(c)} + \underbrace{\frac{1}{2}\left(L - C_b - \frac{S_b}{3}\right)\gamma}_{(d)} - \underbrace{\left(C_b + \frac{S_b}{2}\right)}_{(e)} = 0 \quad (4.23)$$

Equation (4.23) has four roots [80]:

$$\begin{aligned}\gamma_{1,2} &= -\frac{b}{4a} - S \pm 0.5 \sqrt{\underbrace{-4S^2 - 2P + \frac{q}{S}}_X} \\ \gamma_{3,4} &= -\frac{b}{4a} + S \pm 0.5 \sqrt{\underbrace{-4S^2 - 2P - \frac{q}{S}}_Y},\end{aligned}\quad (4.24)$$

where  $P = \frac{8ac-3b^2}{8a^2}$ ,  $q = \frac{b^3-4abc+8a^2d}{8a^3}$

$$\text{and, } S = 0.5 \sqrt{-\frac{2}{3}P + \frac{1}{3a} \left( Q + \frac{\Delta_0}{Q} \right)}, \quad Q = \sqrt[3]{\frac{\Delta_1 + \sqrt{\Delta_1^2 - 4\Delta_0^3}}{2}}.$$

$$\text{with, } \Delta_0 = c^2 - 3bd + 12ae, \quad \Delta_1 = 2c^3 - 9bcd + 27ad^2 - 72ace$$

According to equation (4.16), the signs of the polynomial coefficients are constant and have the following signs:  $a > 0$ ,  $b > 0$ ,  $c > 0$ ,  $d > 0$ , and  $e < 0$ .

Using Descartes' rules of sign [80], the number of real positive solutions of a polynomial can be counted. Assuming that the polynomial in (4.23) is  $P(\gamma)$ , and let  $\nu$  be the number of variations in the sign of the coefficients  $a, b, c, d, e$ , so  $\nu = 1$ . Let  $n_p$  be the number of real positive solutions. According to Descartes' rules of sign [80]:

- $n_p \leq \nu$  which means that  $n_p = 0$  or  $1$ .
- $\nu - n_p$  must be an even integer. Therefore,  $n_p = 1$ .

Hence, there is only one valid real positive solution for the equation. Hereby, the valid solution will be identified. There are two possibilities for the solutions:

1. One positive real solution and the remaining three solutions are negative. In this case, all solutions are real and we just need to identify the root having the largest values from the four solutions. According to (4.24), the value of the square roots  $\sqrt{X}$  and  $\sqrt{Y}$  are positive reals, because we do not have complex solutions. This means,  $\gamma_1 > \gamma_2$  and also  $\gamma_3 > \gamma_4$ . So, the solution will be either  $\gamma_1$  or  $\gamma_3$ . Moreover, the value of  $S$  should be also positive real, and  $q$  has always negative real value. so  $\gamma_3 > \gamma_1$  which means in this case that our solution is  $\gamma_3$ .

2. Two complex solutions, one real positive solution, and one negative solution. In this case, we have either  $\gamma_{1,2}$  or  $\gamma_{3,4}$  real solutions.  $S$  should be

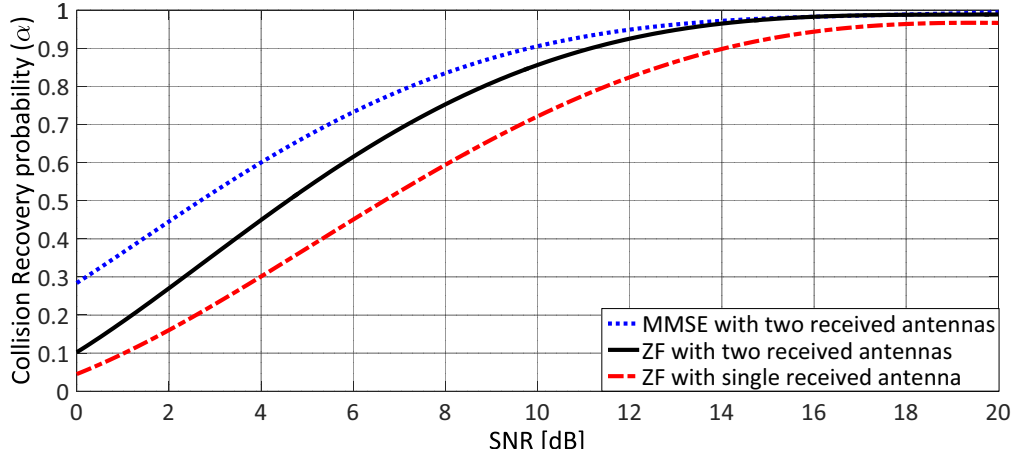


Figure 4.5: Collision recovery probability versus the signal to noise ratio

positive real number, and the complex value comes only from the square roots  $\sqrt{X}$  and  $\sqrt{Y}$ . Moreover,  $q$  has always negative real value. Therefore, in (4.24) the value of  $X < Y$ . So  $\gamma_{1,2}$  must be the complex roots, and as mentioned before that  $\gamma_3 > \gamma_4$ , so  $\gamma_4$  is the negative root and  $\gamma_3$  is the positive real root.

Based on the above discussion, the proposed closed form solution for the collision recovery aware tag estimation is:

$$\hat{n} = \left( -\frac{b}{4a} + S + 0.5\sqrt{-4S^2 - 2P - \frac{q}{S}} \right) \cdot L \quad (4.25)$$

Equation (4.25) gives a direct and linear relation between the estimated number of tags  $\hat{n}$  and the current frame length  $L$ , and gives an alternative solution to the numerical searching with (4.20). Thus, using (4.25), neither look-up tables nor searching, which reduces the complexity and the processing time of the estimation algorithm, is needed.

### 4.2.3 Collision Recovery Probability Calculation

The collision recovery capability is the ability of the reader to actively convert collided slots into successful slots. This capability does not only exist in the modern RFID readers but also in the simple readers, when the tags are well separated. Thus, the received signal power of the near tag will be much stronger than the received signal power from the far tag. Therefore, this ability is a function of two main parameters: First, the characterization of the RFID

reader e.g. (receiver type, number of antennas, etc.). Second, the function of the current Signal-to-Noise Ratio (SNR). Therefore, it extends the capture probability, which is mainly an effect of the channel, resulting in a significantly higher probability to recover collided slots.

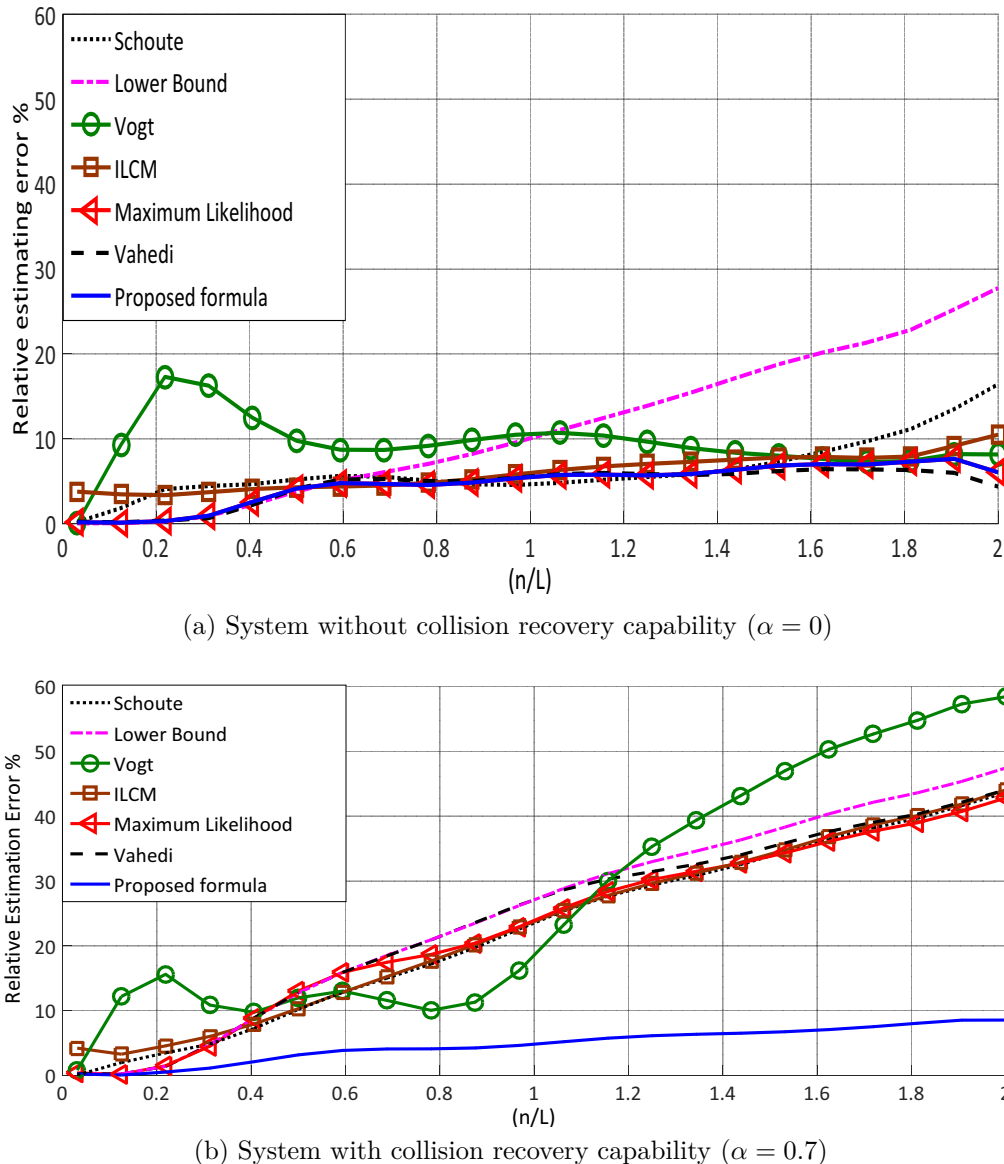
Figure 4.5 shows three receivers proposed by [81]. These three receivers are: 1) the Minimum Mean-Square Error (MMSE) receiver, 2) the Zero Forcing(ZF) receiver with two receiver antennas, and 3) the ZF receiver with a single receiver antenna. The authors of [81] presented Bit Error Rate (BER) curves for the different receiver types as a function of the SNR. Thus, the BER can be mapped to a Packet Error Rate (PER) by means of simulations using the same methodology presented in [79]. Afterwards, the collision recovery probability is calculated as:  $\alpha = (1 - PER)$ . Figure 4.5 shows the values of the capture probabilities versus the average signal to noise ratio per frame. In this thesis, the average capture probability is calculated from the corresponding average SNR at the current frame.

According to figure 4.5, the higher SNR at the receiver, the higher the collision recovery capability of the reader. Figure 4.5 shows two different receivers ZF and MMSE. The MMSE receiver gives better performance than the ZF receiver, and the performance increases when we increase the number of received antennas. According to the practical measurements, the practical SNR range for the successful slots is between 4 dB and 12 dB [79].

#### 4.2.4 Performance Analysis

In this section, the performance comparison between the proposed collision recovery aware number of tags estimation and the most common estimation algorithms in the state-of-the-art will be presented. We will again use the relative estimation error, as it is the most common comparison metric for estimation algorithms. Figure 4.6 displays the percentage of the relative estimation error for the proposed system compared to the literature versus the normalized number of tags  $n/L$ . According to figure 4.6, when the number of tags compared to the frame length increases, the relative estimation error increases. This is due to the increase of the number of collided slots per frame.

Figure 4.6a shows system which has no collision recovery capability ( $\alpha = 0$ ).

Figure 4.6: Relative estimation error  $\epsilon$  vs. normalized number of tags  $n/L$

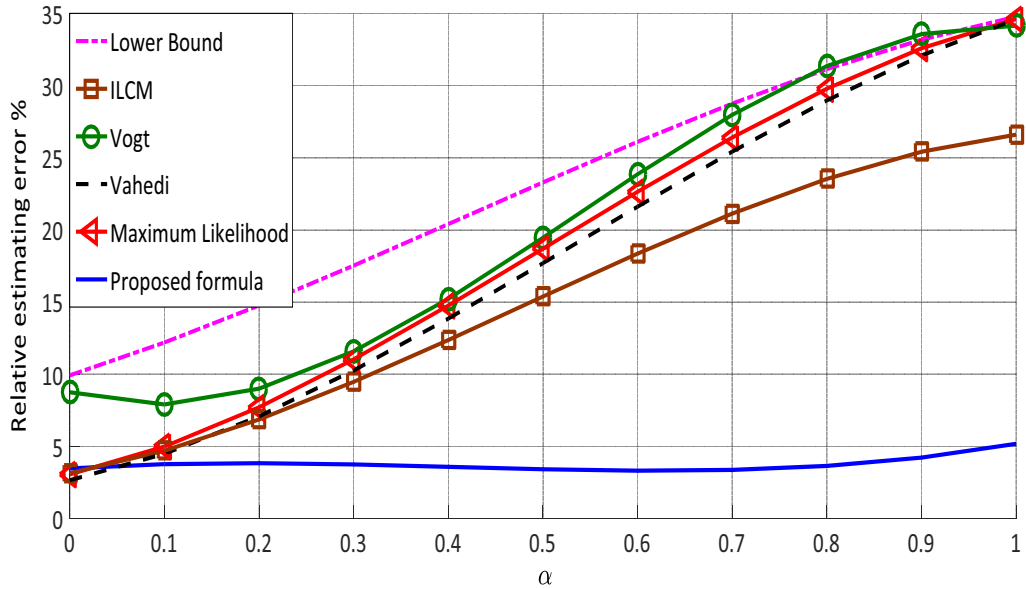


Figure 4.7: Relative estimation error vs. collision recovery probability  $\alpha$ , where  $L = n$

According to figure 4.6a, the proposed system gives identical relative estimation error compared to [73]. Moreover, the proposed system gives a closed form solution whereas the solution of [73] is based on numerical searching. This advantage decreases the complexity of the estimation algorithm. [74] which included the mutual independence of slot types has almost the same results compared to the proposed results. However, it includes a very complex searching algorithms compared to the proposed closed form solution. Figure 4.6b demonstrates the influence of the collision recovery capability on the proposed estimation protocol compared to other estimation protocols. In this simulations, the MMSE proposal in [82] is used with an average SNR=6 dB, which is a realistic assumption. According to figure 4.5, the corresponding value of the collision recovery probability can be set as  $\alpha = 0.7$ . According to figure 4.6b, the proposed solution has a more accurate estimation performance compared to the existing methods in the state-of-the-art.

Figure 4.7 shows the relative estimation error versus the full range of the collision recovery probability  $0 \leq \alpha \leq 1$ . In this simulation, the number of tags in the reading area is equal to the frame length i.e.  $n = L$ , which is the optimum case for the conventional FSA. Based on figure 4.7, when the value of

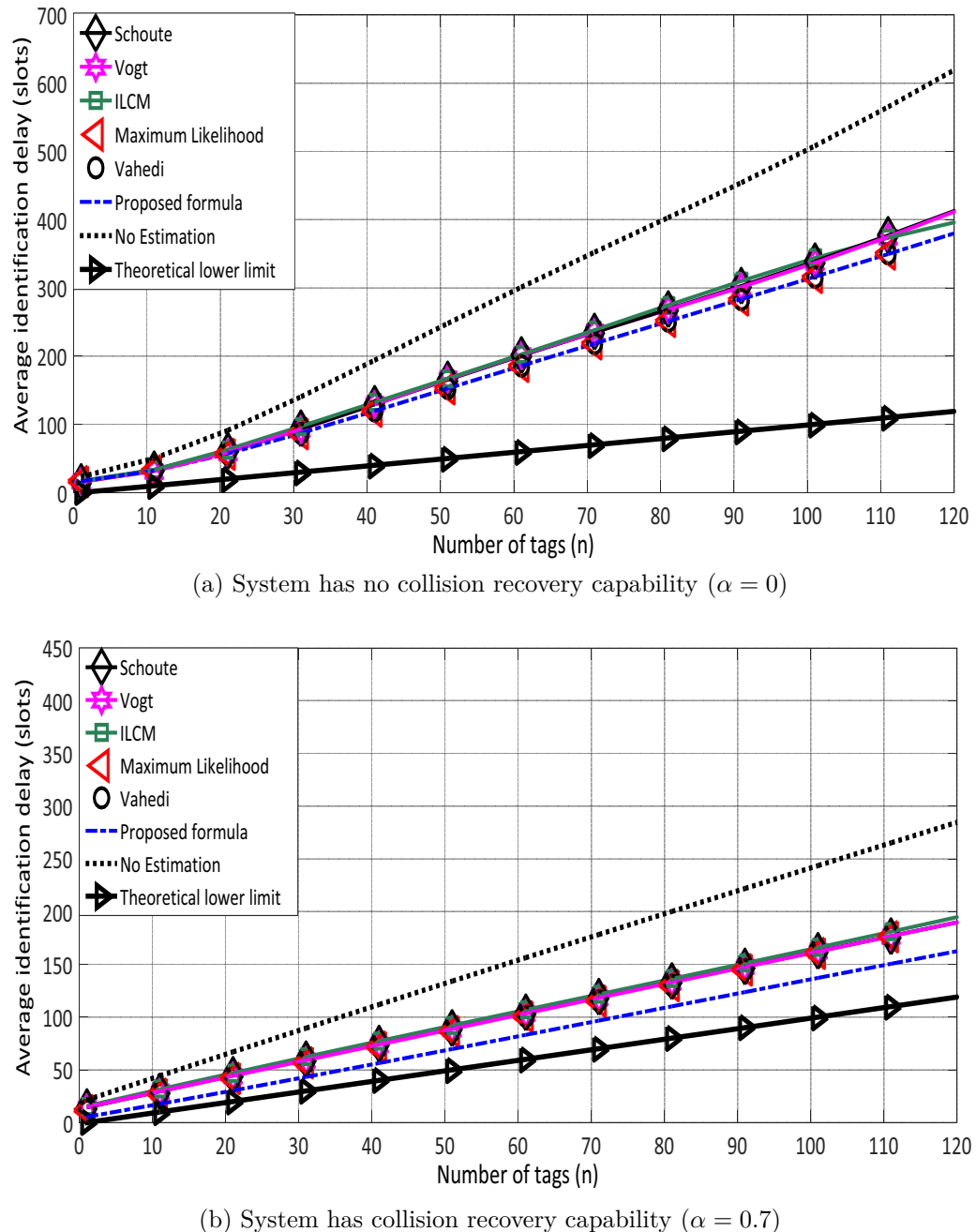


Figure 4.8: Average identification delay

the collision recovery probability increases, the relative estimation error of all estimation algorithms increases, except for the proposed estimation protocol that has almost constant performance, independent of the value of the collision recovery probability. The proposed method takes into account the collision recovery probability, which is produced by the PHY-layer. According to figure 4.7, the relative estimation error of the proposed algorithm is 4 %, which verifies the results of figure 4.6a at  $\frac{n}{L} = 1$  and verifies the simulation results of figure 4.6b at  $\frac{n}{L} = 1$ .

In dense RFID applications, the average identification delay (time) is the most important performance metric. Thus, figure 4.8 displays the average identification delay for a number of tags. In these simulations, an initial frame length of  $L_{ini} = 16$ , which is the conventional initial frame length used in EPCglobal standard [11] is used. Figure 4.8a shows the identification time for systems with no collision recovery capability ( $\alpha = 0$ ). According to EPCglobal C1 G2, the frame length can only have quantized values with  $2^Q$ , where  $Q$  is an integer between 0 and 15. Thus, the frame lengths in these simulations takes the nearest value  $2^Q$  for each frame length. According to 4.8a, the proposed system assigns identical results compared to [73] and [74], which are better than the other literature. Figure 4.8b shows the average identification delay for systems exhibiting a collision recovery probability  $\alpha = 0.7$ . According to figure 4.8b, the average identification delay has decreased for all the systems due to the collision recovery capability. However the proposed system saves the total identification time with almost 10 % compared to others due to the performance of estimation only.

According to EPCglobal C1 G2, the RFID reader cannot acknowledge more than single tag per slot. Therefore, the theoretical lower limit to identify  $n$  tags is  $n$  slots. According to figure 4.8, there is still room of improvement between the proposed algorithm and the theoretical lower limit. Therefore, in the following chapter, new proposals regarding the FSA frame length taking into consideration the PHY-layer properties will be presented.



# Chapter 5

## Frame Length Optimization

In FSA, there are two main factors controlling the reading efficiency, and hence the reading time in RFID systems. These two factors are: 1) The number of tags estimation which was discussed in chapter 4. 2) The optimal FSA frame length calculation which will be discussed in details in this chapter. Previous studies have focused on the frame length calculations using the conventional Dynamic Framed Slotted ALOHA algorithms [54]. In such systems, only the answer of a single tag is considered as a successful slot, and if multiple tags respond simultaneously, a collision occurs. Then all the replied tags in collided slot are discarded. In such systems the optimum frame length is equal to the number of tags in the reading area  $L = n$  [83]. However, as mentioned before, modern systems are capable of recovering this collision and converting the collided slot into a successful one [84]. In such a system, it is better to increase the number of collided slots compared to the number of empty slots by decreasing the optimum frame length. This is because these systems are able to gain more from the collided slots compared to the empty slots by converting the collided slots to successful slots. In addition, most of the previous studies assumed constant slot durations regardless the type of the slot. However, the duration of the slots in RFID systems depends on the slot type e.g. empty, successful, or collided. In these systems, the empty slots duration is smaller than than the collided slots duration and smaller than the successful slots duration. Therefore, it is better to increase the frame length, because the losses from the empty slots is less than the losses in the collided slots. In this chapter, the optimum frame length for DFSA will be calculated taking into consideration the collision recovery

capability and the difference effects in slots durations. These optimizations will be discussed in different scenarios depending on the RFID system.

This chapter is organized as follows: Section 1 discusses the effect of the different slot durations. For this, we will introduce the reading efficiency to have a new performance metric called time aware reading efficiency. Afterwards, a new closed form solution for the optimum frame length, which maximizes the reading efficiency, is proposed. In section 2, the effect of the collision recovery probability with constant coefficients in addition to the time differences in slot duration will be considered. Then, a novel closed form solution for the optimum frame length, which maximizes the system performance, will be presented. Section 3 illustrates the influence of using multiple collision recovery coefficients assuming constant slots duration, thus, eliciting a new reading efficiency called multiple collision recovery coefficients reading efficiency. Then, a novel closed form solution for the optimum frame length is also derived for this system. Finally, section 4 shows a new closed form solution for the optimum frame length for a system, taking into consideration the time difference in slot durations, in addition to the multiple collision recovery coefficients.

## 5.1 Time Aware System

In the recent years, some research groups have focused on optimizing the frame length in case of non-equal slot durations: In [85, 86], the authors proposed a numerical solution for the optimal frame length. These methods depend on searching for the optimal frame length which maximizes the reading efficiency. Moreover, they also depend on the tag-to-reader data rate, which make the searching process more complicated. In [87], the mean number of resolved tags in unit time is optimized. This is done by considering the different slot durations. However, this approach is based on a complex multidimensional table look-up, which may be time consuming. [88] suggested to search for the optimum frame length that minimizes the mean time needed to resolve a bunch of tags. However, the author reached a recursive Bellman-equation, which is difficult to be applied in systems with real-time restrictions.

In this section, we propose a novel closed form solution for the optimum frame length in FSA for RFID systems. The proposed solution gives a direct

and linear relation between the frame length  $L$ , and the number of tags  $n$  in the reading area. Furthermore, it includes a factor representing the different slot durations.

### 5.1.1 Closed Form Solution for Time Aware System

For calculating the proposed optimal time-aware frame size  $L_{TA}$ , which considers the different slot durations, it is important to define the time-aware reading efficiency  $\eta_{TA}$ . Let the time-aware reading efficiency be the ratio between the total successful time and the total frame time:

$$\eta_{TA} = \frac{t_s \cdot S}{t_e \cdot E + t_s \cdot S + t_c \cdot C}, \quad (5.1)$$

where  $t_s \cdot S$ ,  $t_e \cdot E$ , and  $t_c \cdot C$  are respectively the expected total successful, idle, and collided times. Furthermore,  $S$ ,  $E$ , and  $C$  are the expected numbers of successful, empty and collided slots.  $t_s$ ,  $t_e$ ,  $t_c$  are respectively the successful, idle, and collided slot durations.

The next step is to derive the new optimum frame length  $L_{TA}$  under the time-aware environment. According to EPCglobal C1 G2,  $L$  is always integer. Thus,  $L_{TA}$  can be optimized by finding the value of  $L$  which maximizes the time-aware reading efficiency. This is achieved by differentiating the reading efficiency in (5.1) with respect to the frame length  $L$  and equate the result to zero, where  $L$  can only has integer values:

$$\frac{\partial \eta_{TA}}{\partial L} = 0 \quad (5.2)$$

According to (3.1),  $E$ ,  $S$ , and  $C$  are a function of  $L$ . Taking into consideration that  $t_e$ ,  $t_s$ ,  $t_c$  are constants for a given system specification, we get:

$$\frac{(t_e E + t_s S + t_c C)t_s \frac{\partial}{\partial L}(S) - t_s S \frac{\partial}{\partial L}(t_e E + t_s S + t_c C)}{(t_e E + t_s S + t_c C)^2} = 0 \quad (5.3)$$

After multiplying both sides by the denominator and dividing by  $t_s$  (non-zero constant), the equation can be simplified to:

$$(t_e E + t_c C) \frac{\partial}{\partial L}(S) + t_s S \frac{\partial}{\partial L}(S) = S \frac{\partial}{\partial L}(t_e E + t_c C) + t_s S \frac{\partial}{\partial L} S \quad (5.4)$$

After subtracting the term which is multiplied by  $t_s$ , the equation finally results

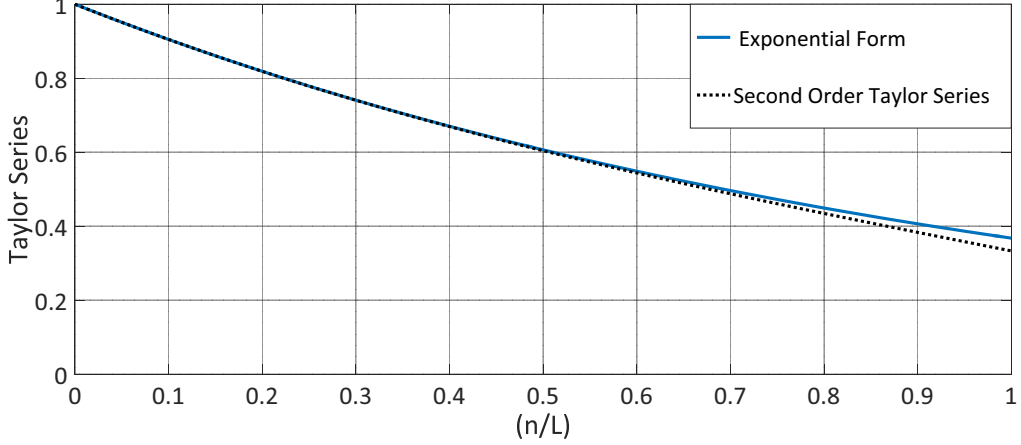


Figure 5.1: Second order Taylor series approximation for  $e^{-\frac{1}{\beta}}$ , where  $\beta = \frac{L}{n}$

in:

$$\{t_e E + t_c C\} \frac{\partial}{\partial L}(S) = S \frac{\partial}{\partial L} \{t_e E + t_c C\} \quad (5.5)$$

Then, substituting the values of  $E$ ,  $S$ , and  $C$  from (3.1) leads to:

$$\begin{aligned} & \left\{ t_e L \underbrace{\left(1 - \frac{1}{L}\right)^n}_{E} + t_c (L - \underbrace{\left(1 - \frac{1}{L}\right)^{n-1} (L - n - 1)}_{C}) \right\} \\ & \quad \times \underbrace{\frac{\partial}{\partial L} n \left(1 - \frac{1}{L}\right)^{n-1}}_{S} \\ & = n \underbrace{\left(1 - \frac{1}{L}\right)^{n-1}}_S \\ & \quad \times \frac{\partial}{\partial L} \left\{ t_e L \underbrace{\left(1 - \frac{1}{L}\right)^n}_{E} + t_c (L - \underbrace{\left(1 - \frac{1}{L}\right)^{n-1} (L - n - 1)}_{C}) \right\} \end{aligned} \quad (5.6)$$

By simplifying the result, the final exact equation for the proposed time-aware frame length is given by the implicit equation:

$$\left(1 - \frac{n}{L_{TA}}\right) = (1 - C_t) \left(1 - \frac{1}{L_{TA}}\right)^n, \quad (5.7)$$

where  $n$  is the number of tags, and  $C_t$  is the slot duration constant defined

as  $C_t = \frac{t_e}{t_c}$  with  $0 < C_t \leq 1$ , as  $t_e \leq t_c$  in practical applications. (5.7) shows the exact relation between the proposed time-aware frame length  $L_{TA}$  and the number of tags  $n$ , taking into consideration the time difference in the slot durations.

Unfortunately, (5.7) is an implicit equation. We will now derive an approximate, but explicit equation. (5.7) can be also expressed as:

$$\left(1 - \frac{1}{\beta}\right) = (1 - C_t) \left(1 - \frac{1}{\beta n}\right)^n, \quad (5.8)$$

where  $\beta = \frac{L_{TA}}{n}$ . As we are focusing on systems with many tags we can use the approximation

$$\lim_{n \rightarrow \infty} \left(1 - \frac{1}{\beta n}\right)^n = e^{-\frac{1}{\beta}}, \quad (5.9)$$

which simplifies (5.7) to:

$$\left(1 - \frac{1}{\beta}\right) = (1 - C_t) e^{-\frac{1}{\beta}}. \quad (5.10)$$

The analysis of (5.7) indicates that the relevant values for  $\beta = \frac{L_{TA}}{n}$  are in the region close to 1. Hence, a Taylor series for  $e^{-\frac{1}{\beta}}$  around one is developed which leads to:

$$e^{-\frac{1}{\beta}} \simeq 1 - \frac{1}{\beta} + \frac{1}{2\beta^2} \quad (5.11)$$

According to figure 5.1, this approximation is acceptable in the range of  $\frac{n}{L} \leq 1$  and has almost identical values when the number of tags is less than 0.7 the working frame length i.e.  $\frac{n}{L} \leq 0.7$ .

After substituting (5.10) and additional simplifications we get:

$$\beta^2 C_t - \beta C_t + 0.5(C_t - 1) = 0 \quad (5.12)$$

By solving (5.12), and rejecting the negative solution we finally obtain:

$$L_{TA} = \frac{n}{2} \left(1 + \sqrt{\frac{2}{C_t} - 1}\right) \quad (5.13)$$

The proposed equation gives a linear relation wrt. the number of tags  $n$ , and includes the slot duration constant  $C_t$ , which can be easily varied as a function of the transmission rate and the working standard.

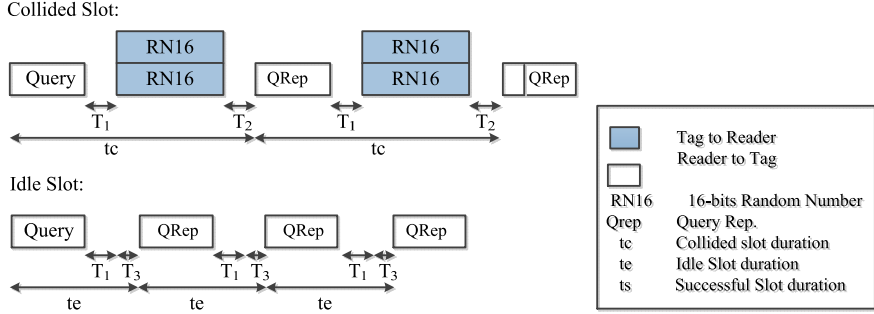


Figure 5.2: Slot durations during tag inventory rounds for the ISO 18000-6C standard

### 5.1.2 Slot Duration Constant Calculation For the EPC-global C1 G2

In this section, the calculation method of the slot duration constant  $C_t$  from the physical layer parameters will be discussed. Figure 5.2 shows the timings of collided and empty slots. Each slot contains different sequences of reader to tag commands and tag replies. Based on the EPCglobal C1 G2 standard [11], the slot duration constant is

$$C_t = \frac{t_e}{t_c}, \quad (5.14)$$

As shown in figure 5.2, the empty slot duration  $t_e$  is given by:

$$t_e = T_{QRep} + T_1 + T_3. \quad (5.15)$$

Here,  $T_{QRep}$  is the query repeat command time:

$$T_{QRep} = T_{FS} + T_{command}, \quad (5.16)$$

with,  $T_{FS} = 3.5 \cdot T_{ari}$ ,  $T_{command} = 6 \cdot T_{ari}$ , and  $T_{ari} = \frac{DR}{2.75} T_{pri}$ . By substituting in (5.16) we get

$$T_{QRep} = 3.5 \cdot DR \cdot T_{pri}, \quad (5.17)$$

where  $T_{ari}$  is reader symbol duration,  $T_{pri} = \frac{1}{BLF}$ ,  $BLF$  is the tag backscatter link frequency and  $DR$  is the so-called divide ratio constant that can take the two values  $DR = 8$  or  $\frac{64}{3}$ . Finally,  $M$  equals to 1, 2, 4, or 8, which represents

Table 5.1: Available slots duration constants  $C_t$  of the EPCglobal C1 G2 standards

Divide Ratio: $DR$	Modulation: $M$	Pilot Length: $n_p$	$C_t$
8	1	0	0.47
		12	0.41
	2	4	0.35
		16	0.28
	4	4	0.23
		16	0.18
	8	4	0.14
		16	0.1
	1	0	0.7
		12	0.65
	2	4	0.57
		16	0.5
64/3	4	4	0.43
		16	0.35
	8	4	0.3
		16	0.22

the modulation types FM0, Miller 2, 4, or 8, respectively.  $T_1$  is the time from the reader transmission to the tag response, which can be expressed as:

$$T_1 = \max \{DR \cdot T_{pri}, 10 \cdot T_{pri}\} \quad (5.18)$$

Next,  $T_3$  is the time that the reader waits after  $T_1$  before issuing another command. As it has no constraints, it can be assumed to be zero. After substituting (5.17) and (5.18) in (5.15),  $t_e$  can be expressed as:

$$t_e = T_{pri} \cdot (3.5 \cdot DR + \max \{DR, 10\}) . \quad (5.19)$$

Next, the collided slot duration  $t_c$  is given by:

$$t_c = T_{QRep} + T_1 + T_2 + T_{RN16}, \quad (5.20)$$

where  $T_2$  is the reader response time starting from the end of the tag response,  $T_2 = 6 \cdot T_{pri}$ , and  $T_{RN16}$  is the duration of 16 bits temporary data, 6 bits

preamble,  $n_p$  pilot tones, i.e.  $T_{RN16} = (22 + n_p) \cdot T_{pri}$ . Therefore,  $t_c$  can be expressed as:

$$t_c = T_{pri} \cdot (3.5 \cdot DR + \max \{DR, 10\} + 6 + 22 \cdot M + n_p \cdot M). \quad (5.21)$$

From (5.19) and (5.21), the final expression of  $C_t$  is:

$$C_t = \frac{3.5 \cdot DR + \max \{DR, 10\}}{3.5 \cdot DR + \max \{DR, 10\} + 6 + 22 \cdot M + n_p \cdot M}. \quad (5.22)$$

Table 5.1 shows the values of the slot duration constant of the EPCglobal C1 G2 standards. According to table 5.1, the slot duration constant  $C_t$  varies from 0.1 to 0.7, and this affects the optimum frame length directly.

### 5.1.3 Closed Form Solution vs. Numerical Solution

Figure 5.3a displays the behavior of the proposed frame length formula in (5.13) compared to the numerical solution in [88] for the complete range of the slot duration constant  $C_t$  for  $0 < C_t \leq 1$ . In the simulation, a fixed number of  $n = 100$  tags is used. According to figure 5.3, the proposed equation approaches the numerical solution proposed in [88] in the full range of  $C_t$  with very small bias coming from the Taylor series approximation in (5.11). According to the EPCglobal C1 G2 standard [11] the frame length is allowed to take only quantized values (power of 2). Thus, in figure 5.3b only the next quantized frame length is selected, which decreases the effect of the Taylor approximation. According to 5.3b, the proposed frame length fully match the numerical solution in the full range of  $C_t$ .

### 5.1.4 Mean Reading Time Reduction

In conventional FSA systems, the slots durations are considered as constant slots. Thus, the total identification time is calculated by counting the average total number of slots needed to identify the complete number of tags in the reading area. Then, according to literature, the mean reduction in number of slots is calculated according to the following equation:

$$\zeta \% = \left( \frac{\text{Slots}_{conv.} - \text{Slots}_{proposed}}{\text{Slots}_{conv.}} \right) \times 100 \quad (5.23)$$

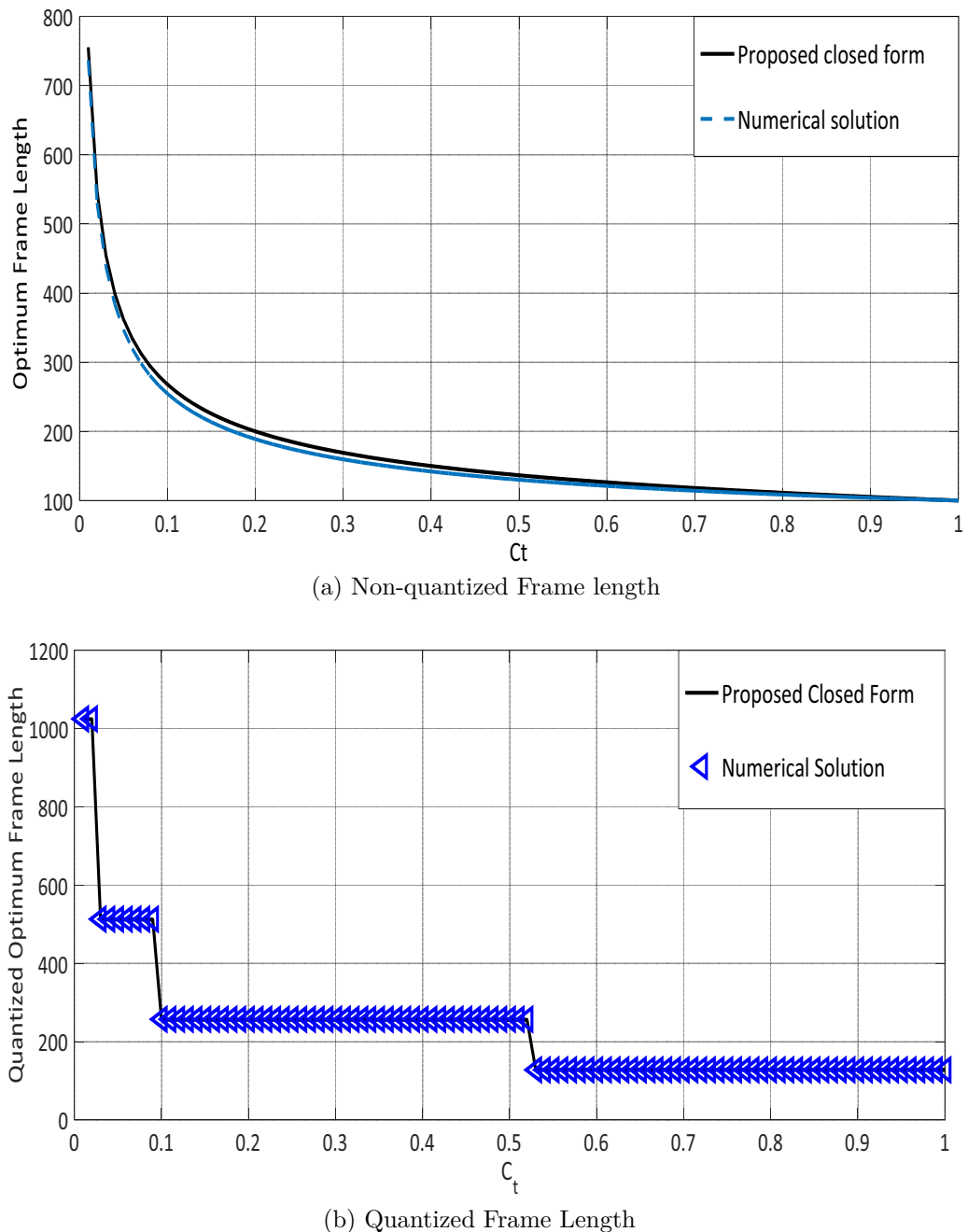


Figure 5.3: Optimum frame length  $L_{TA}$  as a function of the slot duration constant  $C_t$  ( $n = 100$  tags). The conventional case with identical slot durations corresponds to  $C_t = 1$ .

In time aware systems, the slots durations are variable. Therefore, the total identification time can only be calculated as time in seconds. Afterwards, the percentage of mean reading time reduction is calculated as follows:

$$\zeta_t \% = \left( \frac{T_{conv.} - T_{proposed}}{T_{conv.}} \right) \times 100 \quad (5.24)$$

Figure 5.4 shows simulation results for the reading time reduction of the proposed optimal time-aware frame length  $L_{TA}$  wrt. the classical optimal frame length  $L = n$  as a function of the slot duration constant  $C_t$ . These simulations assume a perfect knowledge of the number of tags  $n$ . According to the figure,  $C_t = 0$  means that the idle slot duration time  $t_e = 0$ . In this case, the optimum frame length  $L$  is theoretically infinite. According to the EPCglobal C1 G2 standard [11], the frame length is allowed to take only quantized values (power of 2). According to figure 5.3b, the number of tags in the reading area  $n = 100$  tags. Thus, the quantized optimum frame length is  $L = 1024$  slots. In this case, the proposed time-aware frame length can reduce the average reading time up to 12% compared to the conventional optimization criterion. With  $C_t = 1$ , which means that the slot durations are of identical length (the conventional FSA), the efficiency of the classical optimization, i.e.  $L = n$  is obtained.

In practice, the number of tags in the interrogation region is unknown. Hence, the anti-collision algorithms in real RFID systems consist of two stages: one estimates the number of tags in the interrogation area  $\hat{n}$  whereas the other calculates the optimal frame length  $L_{opt}$  based on  $\hat{n}$  for maximizing the reading efficiency. Figure 5.5 illustrates the mean reduction of the reading time using the proposed time-aware frame length for the proposed ML number of tags estimation and some well-known tag estimation algorithms using the value of the slot duration constant  $C_t = 0.2$ . The main purpose of these simulations is to show the practical effect on the reading time by working with the proposed frame length using different tag estimation algorithms. Each curve presents the mean reduction of the reading time between the proposed frame length and the conventional frame length  $L = n$  using the same estimation algorithm. When a simple tag estimation technique is used like Lower bound [54] or Schoute [52], we can reduce the reading time in the order of 10 to 12 %, thereby gaining around 9 % for better estimation algorithms like [89] and [90], and at last gaining 6 %

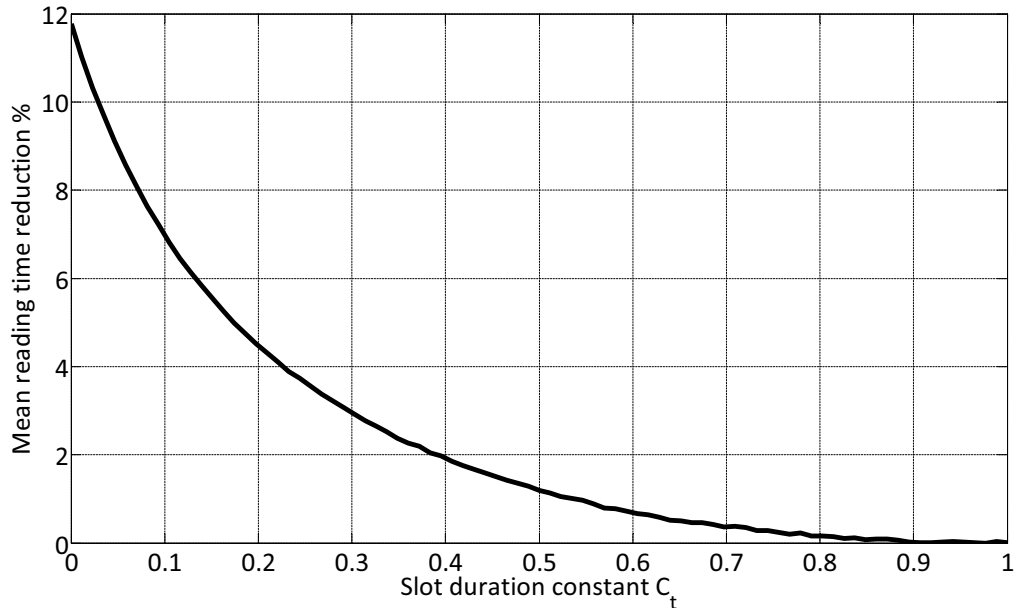


Figure 5.4: Percentages of saving time using the proposed TAFSA for an ideally known number of tags,  $C_t = 1$  is the conventional FSA

upon using the proposed ML estimation algorithm. According to figure 5.5, the better estimation algorithms, the less reading time reduction, because it decreases the number of iterations in FSA process. However, using a non-accurate number of tags estimation algorithms, FSA needs more iterations, with more FSA frame length adaptations. That gives more importance for the proposed formula compared to the classical frame length adaptations.

## 5.2 Time and Collision Recovery System

As mentioned in chapter 4, modern RFID readers are able to decode one of multiple collided tags, which is called the collision recovery capability  $\alpha$ . According to the literature we can divide the previous research, which considered the collision recovery capability in the frame length optimization, into three different groups: The first group considered only the average collision recovery probability for the frame length optimizations, such as [58]. The authors proposed a closed form equation for the optimum frame length maximizing the reading throughput per frame. The second group observed only the different

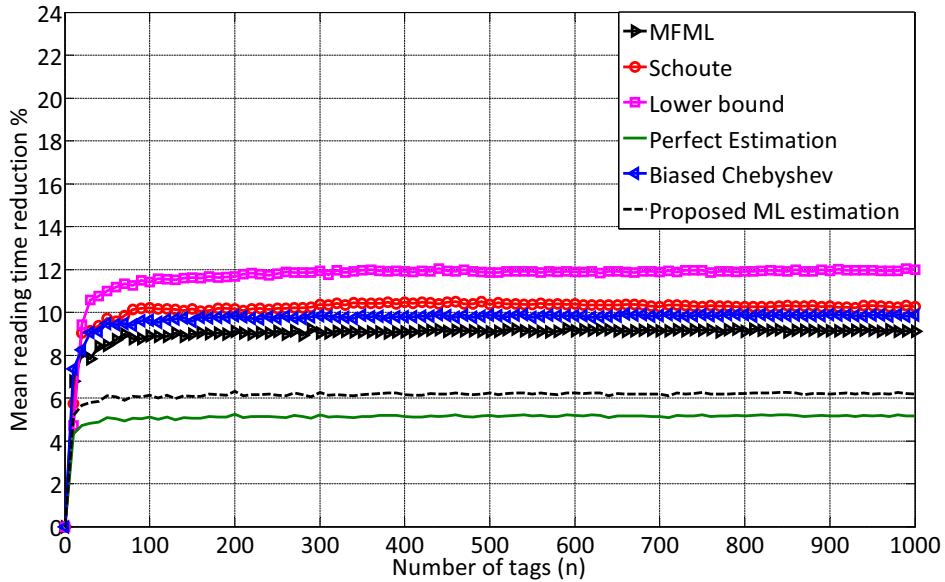


Figure 5.5: Percentages of saving time using the proposed TAFSA compared to the conventional frame length  $L = n$  for different anti-collision algorithms using  $C_t = 0.2$

slot durations, such as [88, 91] and as shown in the first proposal in the previous section. However, no closed form solution for the optimum frame length was derived. They calculated the optimum frame length numerically. The third group contemplated the different slot durations and the collision recovery probability, such as [86, 92, 93]. Both [86, 92] gave numerical solutions for the optimum frame length versus the collision recovery probability and the number of tags. The main problems of their numerical solutions are the multiple degrees of freedom. The solutions require a complex multidimensional look-up table that has to consider all possible degrees of freedom. [93] uses curve fitting to find a closed form solution for the optimum frame length at a specific collision recovery probability and timing. However, this solution can not be generalized for all values of slot's timing and collision recovery probabilities.

In this section, a closed form solution for the optimum frame length will be derived by optimizing the reading throughput per frame, which does not require any look-up table [86, 92]. In addition, we take into consideration the average collision recovery probability and the different slot durations. Moreover, the calculation method of the collision recovery probability based on the physical

layer will be clarified.

### 5.2.1 Closed Form Solution for Time and Collision Recovery System

Now, the proposed optimal time and collision recovery aware frame size  $L_{TCA}$  will be derived, which considers the different slot durations and the collision recovery probability. Thus, we will first introduce a new reading efficiency called Time and Collision Recovery Aware reading efficiency  $\eta_{TCA}$ . The main properties of this efficiency are the consideration of the different slot durations and the average collision recovery probability.

In this efficiency, we added the average collision recovery probability  $\alpha$  to the time aware efficiency in (5.1). Therefore the time and collision recovery probability aware efficiency can then be written as:

$$\eta_{TCA} = \frac{t_s \cdot S_c}{t_e \cdot E_c + t_s \cdot S_c + t_c \cdot C_c}. \quad (5.25)$$

where  $E_c$ ,  $S_c$  and  $C_c$  are respectively the expected number of empty, successful, and collided slots after adding the effect of the collision recovery probability  $\alpha$ . Their relation is given by:

$$E_c = E, S_c = S + \alpha \cdot C, C_c = (1 - \alpha) \cdot C. \quad (5.26)$$

The target is to find the optimum frame length  $L_{TCA}$  which maximizes the proposed reading efficiency in 5.25. This is achieved by differentiating the reading efficiency  $\eta_{TCA}$  of (5.25) with respect to the frame length  $L$  and equate the result to zero.

Clearly, the frame length  $L$  is an integer value. Therefore, differentiating the equation is not fully correct. However, we will later show that the resulting error is negligible. According to (5.26),  $E_c$ ,  $S_c$ , and  $C_c$  are a function of  $L$ . However,  $t_e$ ,  $t_s$ ,  $t_c$  are constants for a given system configuration. Thus, the equation can be simplified to

$$\frac{(t_e E_c + t_s S_c + t_c C_c) t_s \frac{d}{dL}(S_c) - t_s S_c \frac{d}{dL}(t_e E_c + t_s S_c + t_c C_c)}{(t_e E_c + t_s S_c + t_c C_c)^2} = 0 \quad (5.27)$$

After multiplying both sides by the denominator and dividing by  $t_s$  (non-zero

constant), and subtracting the term, which is multiplied by  $t_s$ , the equation results in:

$$(t_e E_c + t_c C_c) \frac{d}{dL} (S_c) = S_c \frac{d}{dL} (t_e E_c + t_c C_c). \quad (5.28)$$

Then, the substitution by the values of  $E_c$ ,  $S_c$ , and  $C_c$  from (5.26) leads to the final exact equation for the proposed time and collision recovery probability aware frame length:

$$\begin{aligned} (1 - \alpha) \cdot (1 - \frac{n}{L_{TCA}}) + \alpha \cdot C_t \cdot \left(1 - \frac{1}{L_{TCA}}\right) \\ + (C_t - 1) \cdot (1 - \alpha) \cdot \left(1 - \frac{1}{L_{TCA}}\right)^n = 0, \end{aligned} \quad (5.29)$$

where  $n$  is the number of tags, and  $C_t$  is the slot duration constant defined as  $C_t = \frac{t_e}{t_c}$ . Equation (5.29) shows the exact relation between the proposed collision recovery and time-aware optimum frame length  $L_{CTA}$  and the number of tags  $n$ . This equation takes into consideration the collision recovery probability and the different slot durations. However, this solution depends on a recursive equation. For reaching an explicit equation, (5.29) can be expressed as:

$$\begin{aligned} (1 - \alpha) \cdot (1 - \frac{1}{\beta}) + \alpha \cdot C_t \cdot \left(1 - \frac{1}{\beta n}\right) \\ + (C_t - 1) \cdot (1 - \alpha) \cdot \left(1 - \frac{1}{\beta n}\right)^n = 0, \end{aligned} \quad (5.30)$$

where  $\beta = \frac{L_{TCA}}{n}$ . As focusing on systems with a large number of tags  $n$ , again the following approximation can be used

$$\lim_{n \rightarrow \infty} \left(1 - \frac{1}{\beta n}\right)^n = e^{-\frac{1}{\beta}}, \quad (5.31)$$

which simplifies (5.30) to:

$$\begin{aligned} (1 - \alpha) \cdot \left(1 - \frac{1}{\beta}\right) + \alpha \cdot C_t \cdot \left(1 - \frac{1}{\beta n}\right) \\ + (1 - \alpha) \cdot (C_t - 1) e^{-\frac{1}{\beta}} = 0. \end{aligned} \quad (5.32)$$

The analysis of (5.29) indicates that the relevant values for  $\beta = \frac{L_{TCA}}{n}$  are in the

region close to one [86]. Hence, we can develop a Taylor series for  $e^{-\frac{1}{\beta}}$  around one which leads to:

$$e^{-\frac{1}{\beta}} \simeq 1 - \frac{1}{\beta} + \frac{1}{2\beta^2}. \quad (5.33)$$

After substituting (5.32) and some additional simplifications, we get:

$$\beta^2 C_t - \beta C_t \left(1 + \frac{\alpha}{n}\right) - 0.5 (1 - \alpha) \cdot (1 - C_t) = 0. \quad (5.34)$$

As  $\frac{\alpha}{n} \ll 1$ , (5.34) can be expressed as:

$$\beta^2 C_t - \beta C_t - 0.5 (1 - \alpha) \cdot (1 - C_t) = 0. \quad (5.35)$$

By solving (5.35) and rejecting the negative solution we finally reach the final solution:

$$L_{TCA} = \frac{n}{2} \left( (1 - \alpha) + \sqrt{(1 - \alpha)^2 + \frac{2}{C_t} (1 - \alpha) \cdot (1 - C_t)} \right). \quad (5.36)$$

As the optimization of (5.1) is a convex optimization problem, and there exists only one non-negative solution of (5.35), (5.36) leads to the global optimum. According to the literature, [92] is the only work which used the same performance metric  $\eta_{TCA}$  to get the optimum frame length. However, in this work the authors did not propose any closed form solution and they have to rely on multi-dimensional look-up tables.

As mentioned before, the value of  $\alpha$  strongly depends on the receiver type and the SNR. The value of collision recovery  $\alpha$  could be one of the values of figure 4.5, depending on the receiver type and the value of SNR.

### 5.2.2 Closed Form Solution vs. Numerical Solution

We will now compare the proposed closed form equation in (5.36) to the numerical results in [92]. Figure 5.6a shows both algorithms for the full range of the slot duration constant  $C_t$ . Assuming a fixed number of  $n = 100$  tags, figure 5.6a indicates that the proposed closed form approaches the numerical solution for different  $\alpha$  in the full range of  $C_t$ . Due to the Taylor series approximations in 5.33, there are slight differences between the proposed closed form and the

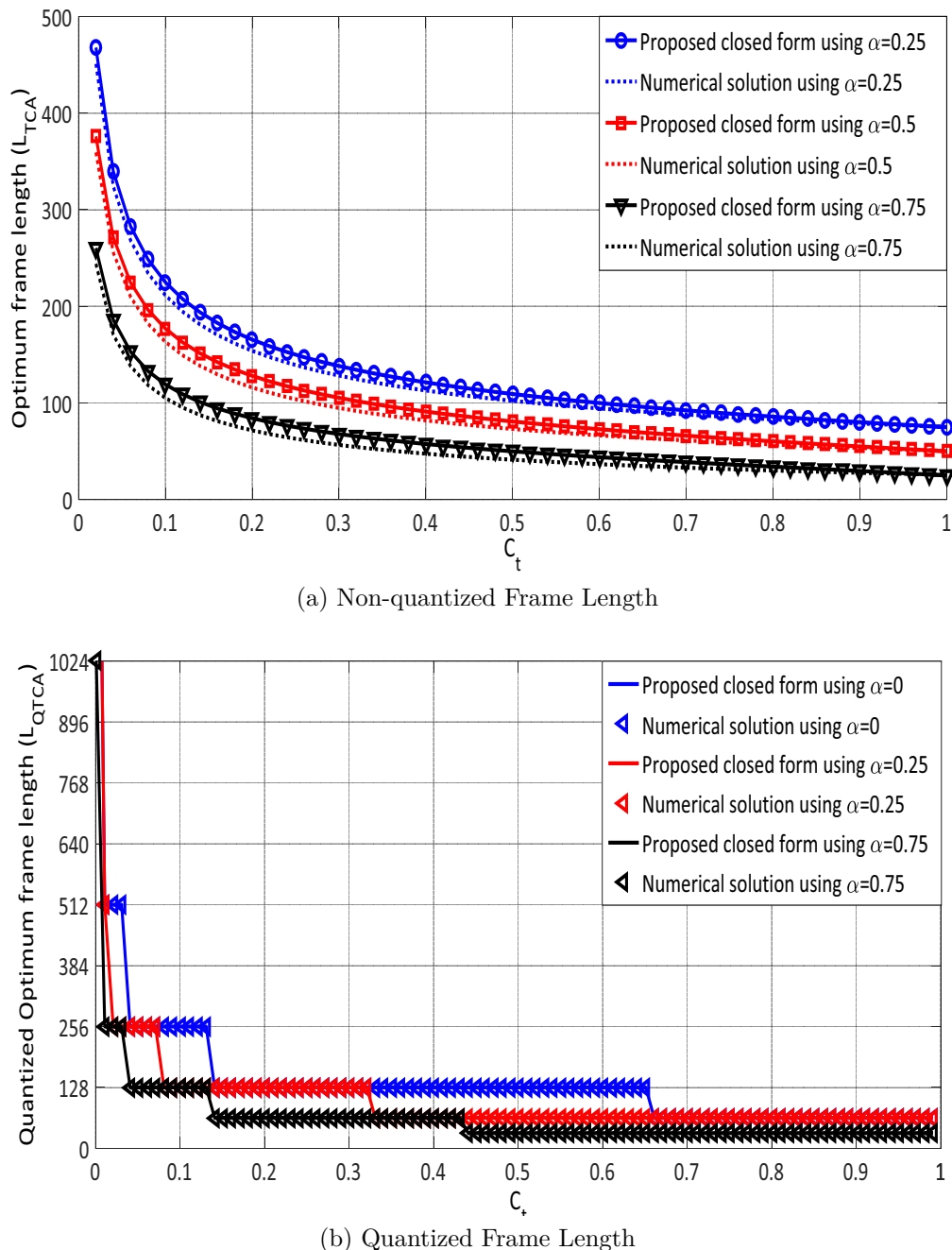


Figure 5.6: Optimum frame length  $L_{TCA}$  as a function of the slot duration constant  $C_t$  ( $n = 100$  tags) for the capture probabilities  $\alpha = 0.25, 0.5, 0.75$ .

numerical solution, where the numerical is the exact solution. As previously mentioned, the EPCglobal C1 G2 standard [11] frame length is allowed to take only quantized values (power of 2). Thus, the next quantized frame length is selected and this will eliminate the approximation error. Figure 5.6b shows that the proposed frame length fully match the numerical solution in the full range of  $C_t$ .

### 5.2.3 Mean Reduction of Reading Time

As mentioned previously, the most common performance metric of comparison is the mean reduction in reading time compared to the conventional frame length  $L = n$ . Figure 5.7 illustrates simulation results for the reading time reduction of the proposed optimal TCRA frame length  $L_{TCRA}$  wrt. the classical optimal frame length  $L = n$  for  $C_t = 0.2$  and different values of the collision recovery probability  $\alpha$ . These simulations assume a perfect knowledge of the number of tags  $n$ . According to figure 5.7, the mean reading time reduction increases when the value of  $\alpha$  increases, which gives more advantage to the proposed solution compared to the conventional one.

Figure 5.8 shows the mean reduction of the reading time using the proposed TCRA frame length compared to the conventional frame length  $L = n$  taking into consideration the effect of the number of tags estimation algorithms. According to figure 5.8, the minimum mean reading time reduction is obtained upon having perfect knowledge of the number of tags in the reading area, because it results in the minimum number of iterations for FSA process.

## 5.3 Multiple Collision Recovery System

To simplify the analysis, previous sections considered systems with equal collision recovery probability coefficients regardless the number of collided tags per slot. For example, the probability to resolve two collided tags is equal to the probability to resolve three or four collided tags per slot. However, in practice the probability to recover one tag from two collided tags is more than the probability to identify single tag from three collided tags. Therefore, in this section, the collision recovery probability will be considered as a variable coefficient  $\alpha_i$ ,

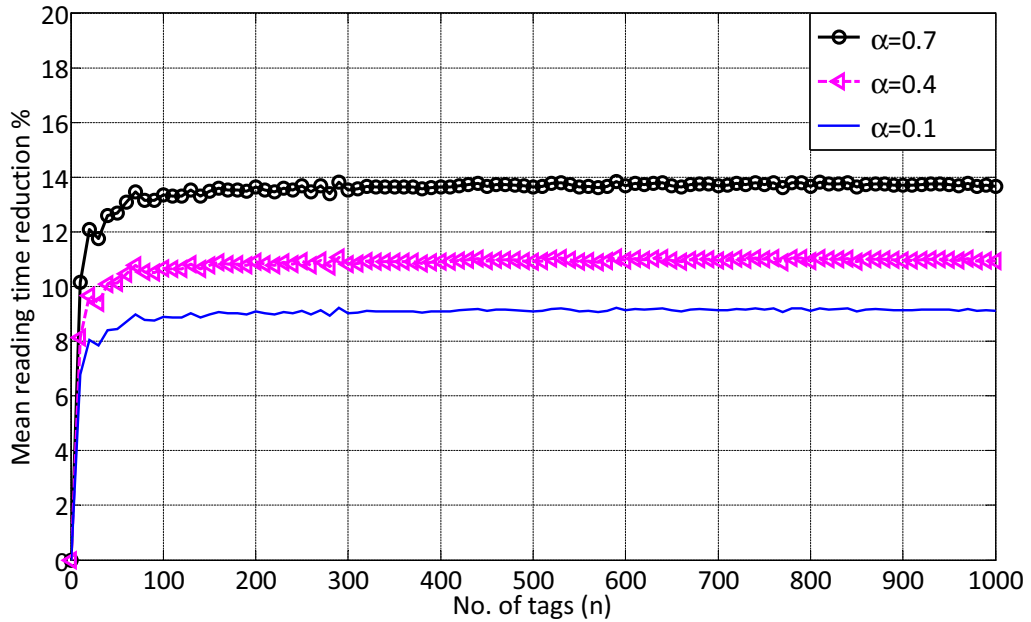


Figure 5.7: Reading time reduction using the proposed TCRA compared to the conventional frame length  $L = n$  for perfect number of tags estimation using  $C_t = 0.2$  and different values of  $\alpha$

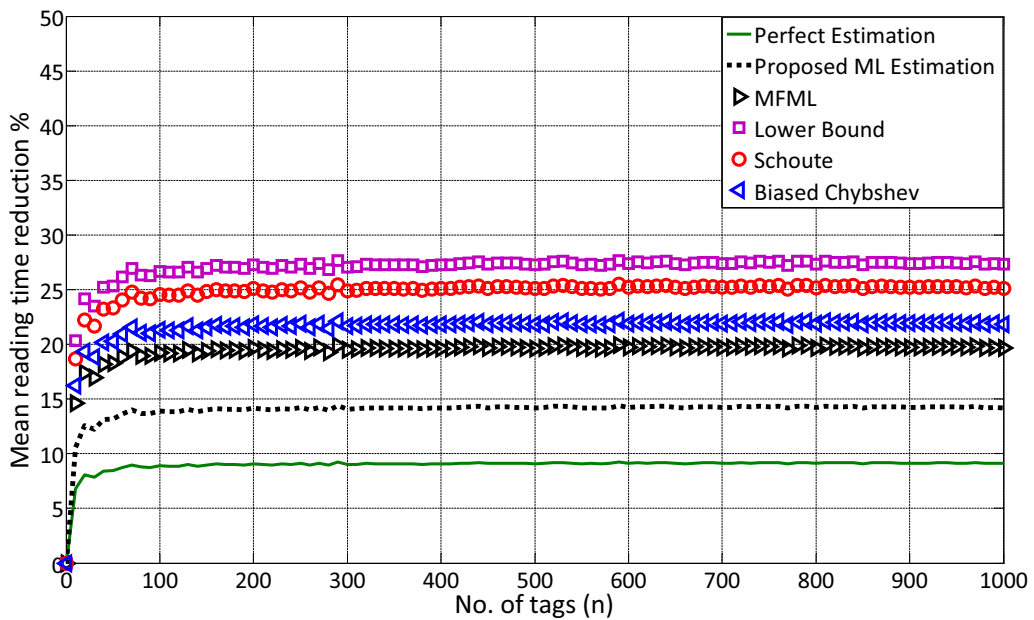


Figure 5.8: Percentages of saving time using the proposed TCRA compared to the conventional frame length  $L = n$  for different anti-collision algorithms using  $C_t = 0.2$  and  $\alpha = 0.1$

where  $i$  is the number of collided tags per slot.

In this section, a new reading efficiency metric called Multiple Collision Recovery Coefficients Reading Efficiency  $\eta_{MCRC}$  is proposed. The proposed efficiency includes a unique collision resolving coefficient for each number of collided tags. Hence, a novel closed form solution for the optimum FSA frame length is proposed which maximizes the proposed efficiency metric. Then, calculations of these coefficients based on a simple RFID reader model to show how the proposed system could be applied on real-life applications.

### 5.3.1 Closed Form Solution For Multiple Collision Recovery Aware System

This section will introduce a new FSA efficiency metric called Multiple Collision Recovery Coefficients Reading Efficiency  $\eta_{MCRC}$ . Afterwards, a closed form solution for the new optimum frame length  $L_{MCRC}$  under multiple collision recovery coefficients environment will be presented.

The main contribution of this efficiency is that it contains a specific collision recovery coefficient  $\alpha_i$  for each probability of collision  $P_{col.}(i)$ . These new coefficients indicate the ability of the reader to recover one tag from  $i$  collided tags. The proposed reading efficiency  $\eta_{MCRC}$  is expressed as:

$$\eta_{MCRC} = P(1) + \sum_{i=2}^n \alpha_i P_{col.}(i). \quad (5.37)$$

Figure 5.9 presents the distribution of the average collision probability in a frame of length  $0.5 \cdot n \leq L \leq 2 \cdot n$  uniformly. The simulations results are done using monte-carlo simulations for the FSA algorithm under condition of frame of length  $0.5 \cdot n \leq L \leq 2 \cdot n$  uniformly, which is the practical range of the frame length in RFID systems according to [86].

As shown in figure 5.9, the probability that the collided slot comes from two, three, or four collided tags is equal to  $P_{col.}(2) + P_{col.}(3) + P_{col.}(4) \simeq 96\%$ , and for the remaining tag collisions  $\sum_{i=5}^n P_{col.}(i) \simeq 4\%$ . Moreover, the values of the collision recovery coefficients  $\alpha_i$ ,  $i > 4$  are practically very small.

Therefore, the proposed  $\eta_{MCRC}$  for the practical RFID environment can be expressed as follows:

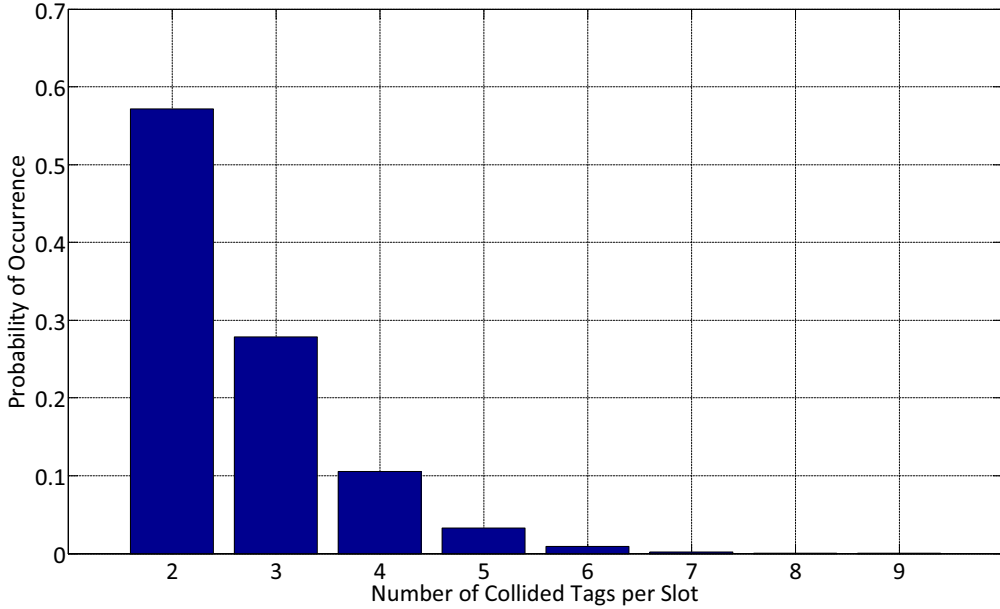


Figure 5.9: Distribution of collision probability for a collided slot in FSA, under condition of  $\frac{n}{2} \leq L \leq 2n$

$$\eta_{MCRC} = P(1) + \alpha_2 P_{col.}(2) + \alpha_3 P_{col.}(3) + \alpha_4 P_{col.}(4), \quad (5.38)$$

where  $\alpha_2$ ,  $\alpha_3$ , and  $\alpha_4$  are respectively the second, third, and fourth collision recovery coefficients.

The next step is to derive a closed form solution for the new optimum frame length  $L_{MCRC}$  under multiple collision recovery coefficients environment.  $L_{MCRC}$  can be optimized by finding the value of  $L$  which maximizes  $\eta_{MCRC}$ . According to [94], if  $L \gg 1$ , and  $n \gg i$ , we can assume a Poisson distribution:

$$P(i) \simeq \frac{1}{i!} \cdot \beta^{-i} \cdot e^{-\frac{1}{\beta}}, \quad (5.39)$$

where  $\beta = \frac{L}{n}$ . After substituting (5.39) in (5.38) we get:

$$\eta_{MCRC} = e^{-\frac{1}{\beta}} \cdot \left( \beta^{-1} + \frac{\alpha_2}{2} \beta^{-2} + \frac{\alpha_3}{6} \beta^{-3} + \frac{\alpha_4}{24} \beta^{-4} \right). \quad (5.40)$$

Now we have to find the value of  $\beta$  which maximizes  $\eta_{MCRC}$ . This is achieved by differentiating the reading efficiency in (5.40) with respect to  $\beta$  and equate

the result to zero. After differentiating, the equation can be simplified as:

$$-e^{-\frac{1}{\beta}} \cdot \left( \beta^{-2} + \beta^{-3}(\alpha_2 - 1) + \frac{\beta^{-4}}{2}(\alpha_3 - \alpha_2) + \frac{\beta^{-5}}{6}(\alpha_4 - \alpha_3) - \frac{\beta^{-6} \cdot \alpha_4}{24} \right) = 0. \quad (5.41)$$

Multiplying the equation by  $-e^{\frac{1}{\beta}} \cdot \beta^6$ , it finally results in:

$$\underbrace{1}_{a} \beta^4 + \underbrace{(\alpha_2 - 1)}_{b} \beta^3 + \underbrace{\frac{(\alpha_3 - \alpha_2)}{2}}_{c} \beta^2 + \underbrace{\frac{(\alpha_4 - \alpha_3)}{6}}_{d} \beta - \underbrace{\frac{\alpha_4}{24}}_{e} = 0. \quad (5.42)$$

Equation (5.42) has four roots [95]:

$$\begin{aligned} \beta_{1,2} &= -\frac{b}{4a} - S \pm 0.5 \sqrt{\underbrace{-4S^2 - 2P + \frac{q}{S}}_{X}} \\ \beta_{3,4} &= -\frac{b}{4a} + S \pm 0.5 \sqrt{\underbrace{-4S^2 - 2P - \frac{q}{S}}_{Y}}, \end{aligned} \quad (5.43)$$

where  $P = \frac{8ac - 3b^2}{8a^2}$ ,  $q = \frac{b^3 - 4abc + 8a^2d}{8a^3}$

$$\text{and, } S = 0.5 \sqrt{-\frac{2}{3}P + \frac{1}{3a} \left( Q + \frac{\Delta_0}{Q} \right)}, \quad Q = \sqrt[3]{\frac{\Delta_1 + \sqrt{\Delta_1^2 - 4\Delta_0^3}}{2}}.$$

$$\text{with, } \Delta_0 = c^2 - 3bd + 12ae, \quad \Delta_1 = 2c^3 - 9bcd + 27ad^2 - 72ace$$

Based on practical ranges for the collision recovery coefficients,  $\alpha_i$ ,  $0 \leq \alpha_i \leq 1$ , and  $\alpha_2 \geq \alpha_3 \geq \alpha_4$ . Therefore, we can proof that the signs of the polynomial coefficients are constant and not changing in all ranges of  $\alpha_i$  and can be presented as follows:  $a > 0$ ,  $b < 0$ ,  $c < 0$ ,  $d < 0$ , and  $e < 0$ .

According to Descartes' rules of sign [80], there is only one valid real positive solution for the equation. After analyzing (5.42) using Descartes' rules of sign [80], the proposed closed form optimum frame length  $L_{MCRC}$  under the multiple collision recovery coefficients environment is:

$$L_{MCRC} = \left( -\frac{b}{4a} + S + 0.5 \sqrt{-4S^2 - 2P - \frac{q}{S}} \right) \cdot n \quad (5.44)$$

According to (5.44), the proposed equation gives a linear relation wrt. the

number of tags  $n$ , and includes the effect of different collision recovery coefficients. In case that the RFID reader has no collision resolving capability, i.e.  $\alpha_2 = \alpha_3 = \alpha_4 = 0$ , the proposed formula gives  $L_{MCRC} = n$ , which is identical to the frame length in the conventional case. When the RFID reader has a full and equal collision resolving capability for the two, three, and four collided tags per slot, i.e.  $\alpha_2 = \alpha_3 = \alpha_4 = 1$ , the proposed formula gives  $L_{MCRC} = 0.452 \cdot n$ , which matches the results in [59].

### 5.3.2 Collision Recovery Coefficients Calculations

Now the calculation of the the collision recovery coefficients  $\alpha_2$ ,  $\alpha_3$  and  $\alpha_4$  will be clarified, which are the main optimization variables in our proposal. The values of these coefficients are strongly dependent on the receiver type. Calculations of the collision recovery coefficients are done based on an RFID reader model that utilizes the capture effect. The reader resolves the collision based on the strongest tag reply. Therefore, the collision can be resolved with a certain probability, if the strongest tag reply is stronger than the summation of the other collided tags at the same slot.

The main advantage of this reader is that it does not need any channel state information (CSI) to recover the strongest tag. According to EPCglobal C1G2 standard [11], collisions in RFID systems occur only within the 16 bits packet called *RN16*. If any single bit error occurs in this packet, the total packet has to be considered lost. Therefore, the meaning of the collision recovery probability coefficients  $\alpha_i$  is the probability that the RFID reader can identify a complete *RN16* packet from  $i$  collided tags. Therefore, the collision recovery coefficient can be expressed as  $\alpha_i = (1 - PER_i)$ , where  $PER_i$  is the Packet Error Rate for  $i$  collided tags. In this work, we measure the SNR for each slot, then we calculate the average SNR per frame as  $E\left\{\frac{|h|^2 \cdot x^2}{\sigma^2}\right\}$ , where  $\sigma$  is the standard deviation of the Additive White Gaussian Noise (AWGN) per slot, and at last, we used normalized signal power, i.e.  $E\{x^2\} = 1$ . Based on [81], we assumed that the equivalent channel coefficients  $h$  follow Rayleigh fading. The channel coefficients are independent zero mean circularly symmetric complex Gaussian random variables with normalized energy  $E\{|h|^2\} = 1$ , and all tags are statistically identical, which means all of them experience the same average

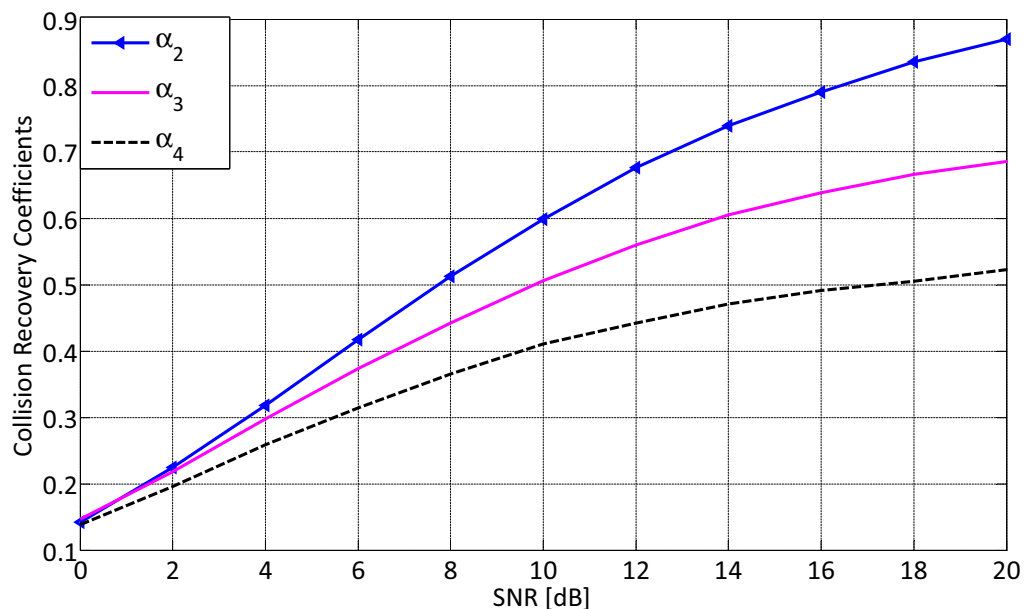


Figure 5.10: Simulation results for the average collision recovery coefficients versus SNR using the strongest tag reply receiver.  $\alpha_2$ ,  $\alpha_3$ , and  $\alpha_4$  are respectively the collision recovery probability or two, three, and four collided tags per slot.

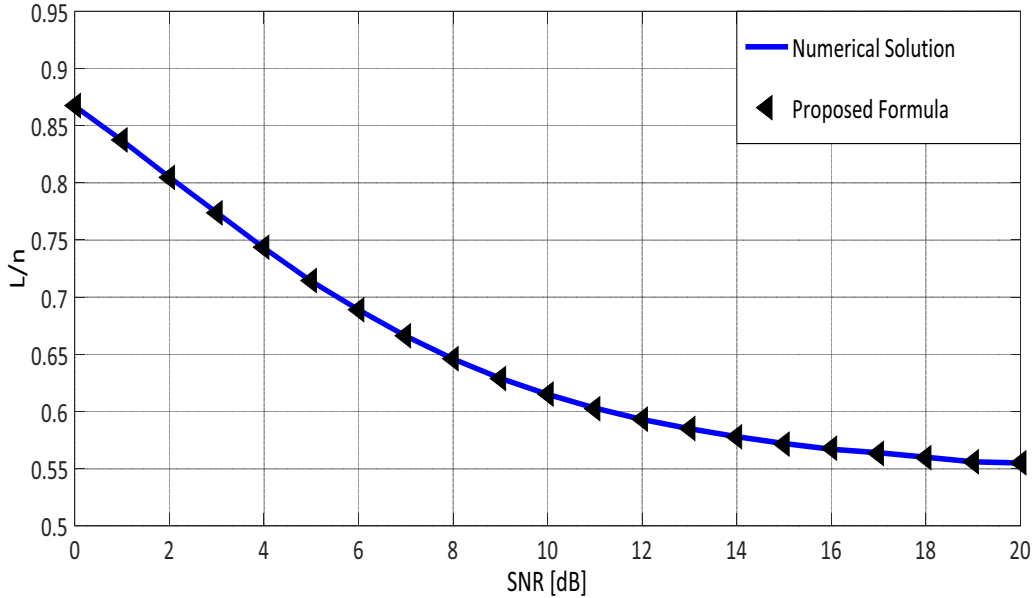


Figure 5.11: Frame length comparison between the proposed formula in (5.44) and the numerical solution for different SNR values.

path loss. Therefore, the average SNR per frame is  $E\left\{\frac{1}{\sigma^2}\right\}$ .

Figure 5.10 shows the values of the collision recovery coefficients versus the average SNR per frame using the strongest tag reply receiver. In these simulations, a sampling frequency of  $f_s = 8$  MHz is used, and the tags used FM0 as an encoding scheme. Finally, to clarify the worst case effect of the collision recovery coefficients, we used the highest symbol rate BLF = 640 kHz.

### 5.3.3 Closed Form Solution vs. Numerical Solution

For each RFID reader, each SNR leads to corresponding values for the collision recovery coefficients  $\alpha_2$ ,  $\alpha_3$  and  $\alpha_4$ . Figure 5.11 shows a comparison between the proposed formula (5.44) and the numerical solution which maximizes the reading efficiency in (5.40) versus the SNR. Both simulations used the same receiver model, which is the strongest tag reply receiver. According to figure 5.11, the proposed formula gives identical results compared to the numerical solution at the complete SNR range.

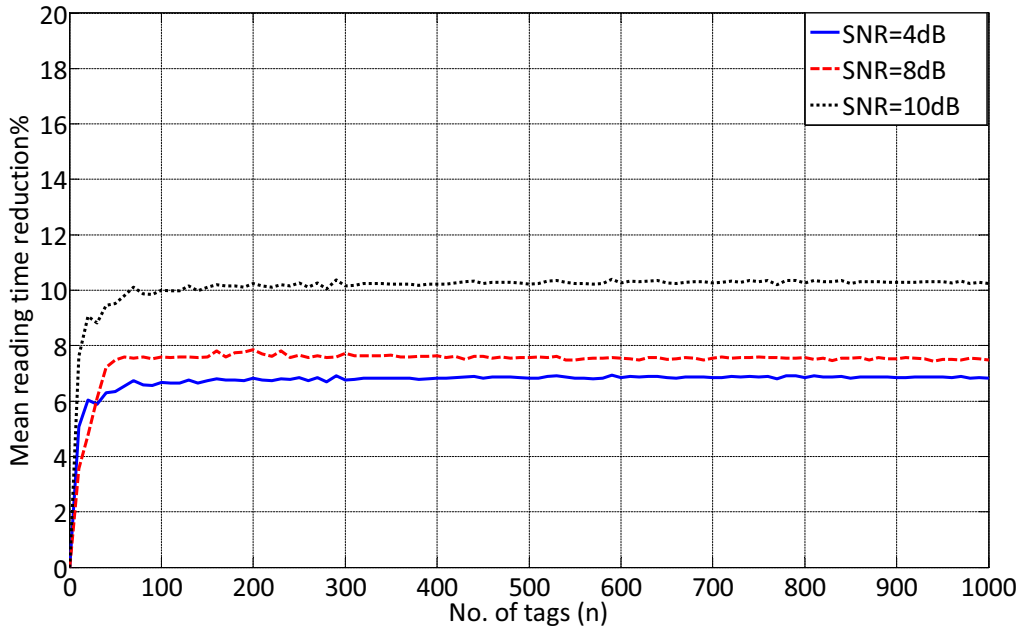


Figure 5.12: Mean reading time reduction using the proposed MCR compared to the conventional frame length  $L = n$  for perfect number of tags estimation using  $C_t = 0.2$  and different  $SNR$  values

### 5.3.4 Mean Reading Time Reduction

The total average number of slots needed to identify a complete bunch of tags is calculated using the strongest tag reply receiver in [57]. FSA with initial frame length  $L_{ini.} = 16$  is used as an anti-collision algorithm. Figure 5.12 illustrates a comparison between the percentages of saving time using the proposed MCR and the conventional frame length  $L = n$  assuming perfect number of tags estimation. The simulation uses  $C_t = 0.2$  and different  $SNR$  values. According to figure 5.12, when the value of the  $SNR$  increases, the collision recovery probability increases. Hence, the mean reading time reduction also increases.

Figure 5.13 shows the percentages of saving time with the proposed MCR compared to the conventional frame length  $L = n$  using different anti-collision algorithms with  $C_t = 0.2$  and  $SNR = 4$  dB.

In this section, the FSA reading efficiency is proposed for equal slot duration system with multiple collision recovery coefficients. However, practically, there are differences in the slot durations depending on the slot type. Therefore, in

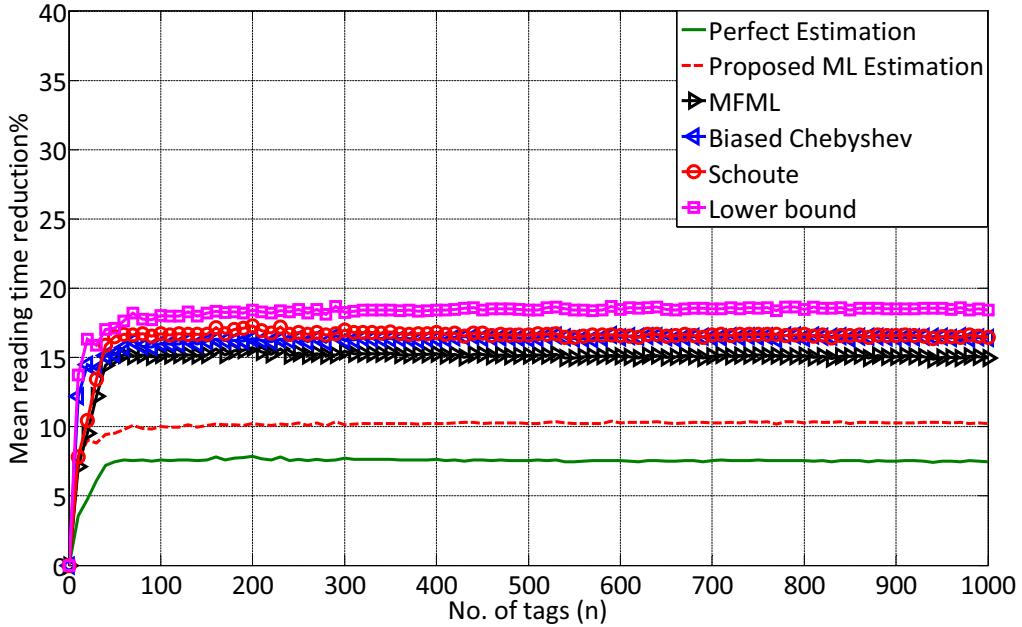


Figure 5.13: Mean reading time reduction using the proposed MCRA compared to the conventional frame length  $L = n$  using different anti-collision algorithms with  $C_t = 0.2$  and  $SNR = 4$  dB

the following section, the FSA reading efficiency will consider the differences in slot durations as well as the differences in the collision recovery coefficients.

## 5.4 Time and Multiple Collision Recovery System

In this section we present a new FSA reading efficiency metric called time aware multiple collision recovery coefficients reading efficiency  $\eta_{TAMCRC}$ . The main contribution in this new efficiency is that it contains a unique collision recovery coefficient  $\alpha_i$  for each probability of collision  $P(i)$ . These new coefficients indicate the ability of the reader to recover one tag from  $i$  collided tags, where this ability varies based on the number of collided tags. Moreover, it takes into consideration the different slot durations.

### 5.4.1 Closed Form Solution for Time Multiple Collision Recovery Aware System

According to figure 5.9, the probability that a collision results from two or three collided tags is approx. 85%. Moreover, the values of the collision recovery coefficient  $\alpha_i$  when  $i \geq 4$  (i.e. 4 or more collided tags) will be small. Therefore, only up to three collided tags will be considered. The next step is normalizing the slot duration  $t_k$  of successful and collided tags to unity. Furthermore, it will be assumed that empty slots are shorter than successful slots (i.e.  $t_0 \leq t_k$ ), which is the case for practical readers. Then, the proposed reading efficiency  $\eta_{TAMCRC}$  can be expressed as:

$$\eta_{TAMCRC} = \frac{P(1) + \alpha_2 P_{col.}(2) + \alpha_3 P_{col.}(3)}{1 + P(0) \cdot (C_t - 1)}, \quad (5.45)$$

where  $C_t = \frac{t_0}{t_k}$  represents the slots duration constant, and  $\alpha_2, \alpha_3$  are respectively the second, third collision recovery coefficients.

The next step is to derive a closed form for the new optimum frame length  $L_{TAMCRC}$  which maximizes  $\eta_{TAMCRC}$ . After substituting by (5.39) in (5.45) we obtain:

$$\eta_{TAMCRC} = \frac{e^{-\frac{1}{\beta}} \cdot (\beta^{-1} + \frac{\alpha_2}{2}\beta^{-2} + \frac{\alpha_3}{6}\beta^{-3})}{1 + e^{-\frac{1}{\beta}} \cdot (C_t - 1)} \quad (5.46)$$

where,  $\beta = \frac{L}{n}$ .

Now we have to find the value of  $\beta$  which maximizes  $\eta_{TAMCRC}$ . This is achieved by differentiating the reading efficiency in (5.46) with respect to  $\beta$  and equate the result to zero:

$$\frac{\partial \eta_{TAMCRC}}{\partial \beta} = 0 \quad (5.47)$$

After differentiating and simplifications, the final equation is a fourth order polynomial:

$$a \cdot \beta^4 + b \cdot \beta^3 + c \cdot \beta^2 + d \cdot \beta + e = 0, \quad (5.48)$$

where:  $a = \underbrace{-C_t}_{(<0)}$

$$\begin{aligned}
b &= \underbrace{C_t \cdot (1 - \alpha_2) - 1}_{(<0)} \\
c &= \underbrace{2 - C_t - \alpha_2}_{(>0)} + \underbrace{\frac{C_t}{2}(\alpha_2 - \alpha_3)}_{(>0)} \\
d &= \underbrace{\frac{1}{2}(\alpha_2 - \alpha_3) + \frac{1}{2}\alpha_2 \cdot (1 - C_t) + \frac{1}{6}C_t \cdot \alpha_3}_{(>0)} \\
e &= \underbrace{\frac{1}{6}\alpha_3 \cdot (2 - C_t)}_{(>0)}
\end{aligned}$$

As  $0 \leq \alpha_i \leq 1$ ,  $0 < C_t \leq 1$ , and  $\alpha_2 \geq \alpha_3$ , (5.48) has four roots [95]:

$$\begin{aligned}
\beta_{1,2} &= -\frac{b}{4a} - S \pm 0.5 \sqrt{\underbrace{-4S^2 - 2P + \frac{q}{S}}_X} \\
\beta_{3,4} &= -\frac{b}{4a} + S \pm 0.5 \sqrt{\underbrace{-4S^2 - 2P - \frac{q}{S}}_Y},
\end{aligned} \tag{5.49}$$

$$\text{with } P = \frac{8ac - 3b^2}{8a^2}, q = \frac{b^3 - 4abc + 8a^2d}{8a^3}$$

$$\text{and } S = 0.5 \sqrt{-\frac{2}{3}P + \frac{1}{3a} \left( Q + \frac{\Delta_0}{Q} \right)}, \quad Q = \sqrt[3]{\frac{\Delta_1 + \sqrt{\Delta_1^2 - 4\Delta_0^3}}{2}}$$

$$\text{with } \Delta_0 = c^2 - 3bd + 12ae, \quad \Delta_1 = 2c^3 - 9bcd + 27ad^2 - 72ace$$

According to the practical ranges of the collision recovery coefficients  $\alpha_i$  and  $C_t$ , it can be proved that the signs of the polynomial coefficients are constant and do not change in all ranges of  $\alpha_i$  and  $C_t$ . Thus their signs will be:

$$a < 0, b < 0, c > 0, d > 0, \text{ and } e > 0$$

According to Descartes' rules of sign [80], there is only one valid real positive solution for the equation. After analyzing (5.42) using Descartes' rules of sign [80], the proposed closed form optimum frame length  $L_{TAMCRC}$  under time and multiple collision recovery coefficients environment leads to:

$$L_{TAMCRC} = \left( -\frac{b}{4a} - S + 0.5 \sqrt{-4S^2 - 2P + \frac{q}{S}} \right) \cdot n \tag{5.50}$$

The proposed equation gives a linear relation wrt. the number of tags  $n$ , and

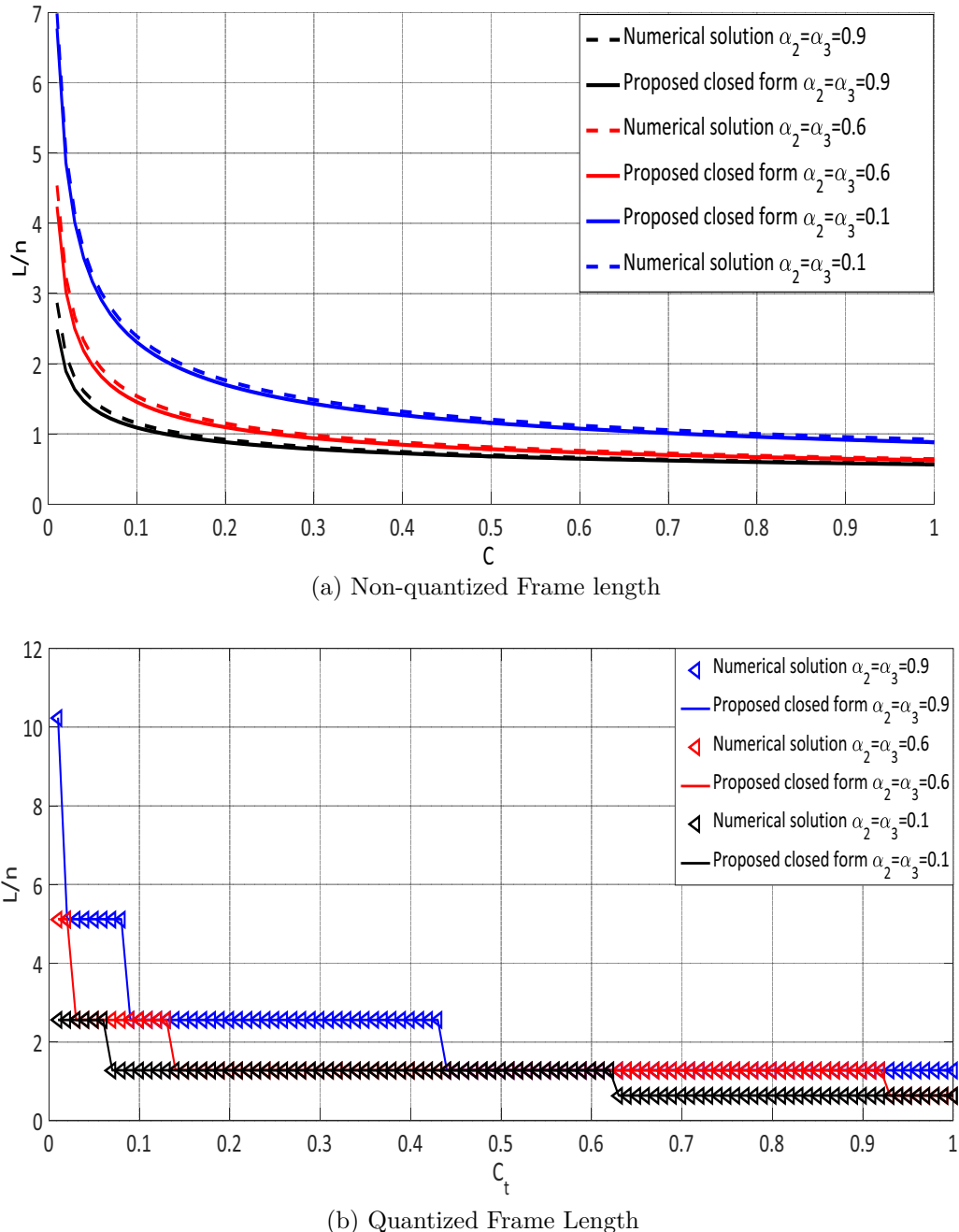


Figure 5.14: Frame length comparison between the proposed formula and the numerical solution versus the SNR using the strongest tag reply receiver.

includes the effect of different collision recovery coefficients and the slot duration constant. The values of these coefficients are set based on the RFID reader type as shown in [96]. The value of  $C_t$  can be calculated based on the transmission rate as shown in [79]. Based on (5.50), if the RFID reader has no collision resolving capability ( $\alpha_2 = \alpha_3 = 0$ ) and equal slots durations are used ( $C_t = 1$ ), we get  $L_{TAMCRC} = n$ . This is identical to the optimum frame length in the conventional case.

### 5.4.2 Closed Form Solution vs. Numerical Solution

In this section, the accuracy of the proposed closed form compared to the numerical solution will be discussed. Figure 5.14a illustrates a frame length comparison between the proposed formula in (5.50) and the numerical solution, which maximizes the reading efficiency in (5.45) versus full range of the slot duration constant  $C_t$  for different values of collision recovery coefficients  $\alpha_i$ . Both simulations used the same receiver model, which is the strongest tag reply receiver. According to figure 5.14, the proposed formula approaches the numerical solution within the full range of the complete range of  $C_t$ . As mentioned before, the EPCglobal C1 G2 standard [11] only allows taking quantized frame lengths (power of 2). Figure 5.14b shows that the proposed frame length fully match the numerical solution in the full range of  $C_t$ .

### 5.4.3 Mean Reading Time Reduction

Figure 5.15 presents the saved time using the proposed TMCRA compared to the conventional frame length  $L = n$  for perfect number of tags estimation. The simulation results are based on the slot duration constant  $C_t = 0.2$ , as it is considered as a practical value used in the EPCglobal class 1 gen 2 standards [11] and different values of  $SNR$ . According to figure 5.15, when the value of the  $SNR$  increases, the collision recovery probability increases. Hence, the mean reduction in reading time also increases.

Figure 5.16 shows the percentages of saving time using the proposed TM-CRA compared to the conventional frame length  $L = n$  using different anti-collision algorithms with  $C_t = 0.2$  and average  $SNR = 8$  dB.

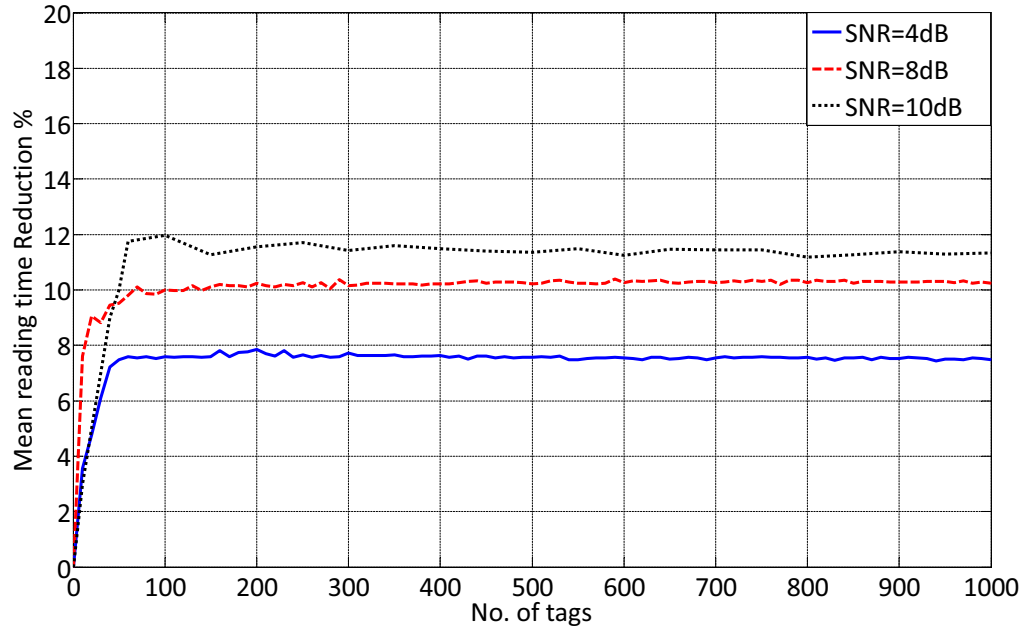


Figure 5.15: Mean reading time reduction using the proposed TMCRA compared to the conventional frame length  $L = n$  for perfect number of tags estimation using  $C_t = 0.2$

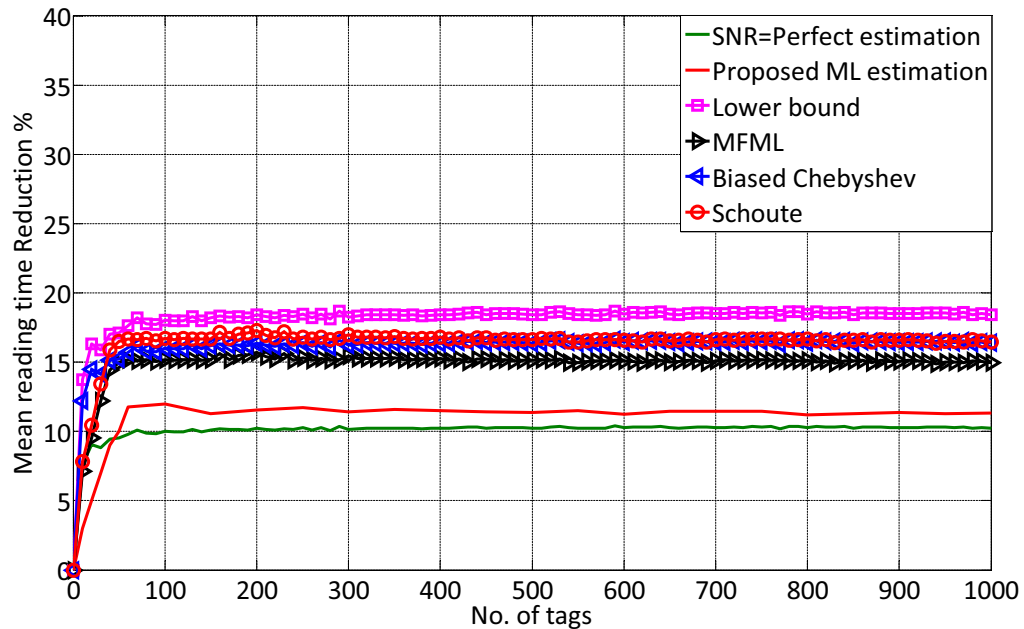


Figure 5.16: Mean reading time reduction using the proposed TMCRA compared to the conventional frame length  $L = n$  using different anti-collision algorithms with  $C_t = 0.2$  and  $SNR = 8$  dB

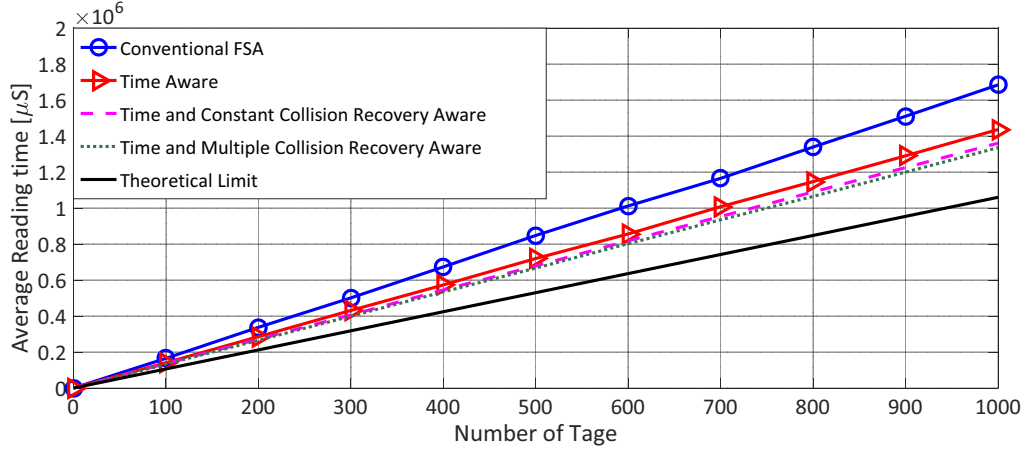


Figure 5.17: Average reading time of the proposed systems, conventional FSA and the theoretical limit without number of tags estimation

## 5.5 Comparison of the Proposed Algorithms

The most crucial performance metric in RFID systems is the average total reading time for a bunch of tags. This section will summarize the performance of the proposed systems. It compares between the total reading time of the proposed frame lengths and the conventional one which assumes that  $L_{opt} = n$ . Furthermore, it illustrates how far are the proposed systems compared to the theoretical lower limit of the EPCglobal C1 G2 standard [11], which gives the minimum identification time for UHF RFID system.

The following simulation results assume the following parameters: Slots duration constant  $C_t = 0.2$ , with  $te = 60 \mu\text{s}$ ,  $tc = 360 \mu\text{s}$ , and  $ts = 1060 \mu\text{s}$ , which are practical values from real measurements using a Universal Software Defined Radio Peripheral (USRP B210) [63]. We assume  $SNR = 10 \text{ dB}$ , with strongest tag reply receiver which leads to the following collision recovery coefficients,  $\alpha_2 = 0.6$ ,  $\alpha_3 = 0.5$ ,  $\alpha_4 = 0.4$ .

The following simulation results are divided into three case studies:

1. Average reading time without number of tags estimation: Figure 5.17 shows the simulation results for the average reading time of the proposed frame lengths compared to the conventional frame length  $L = n$  and the theoretical limit. No number of tags estimation algorithm is used in simulation results of figure 5.17. According to figure 5.17, the Time Aware

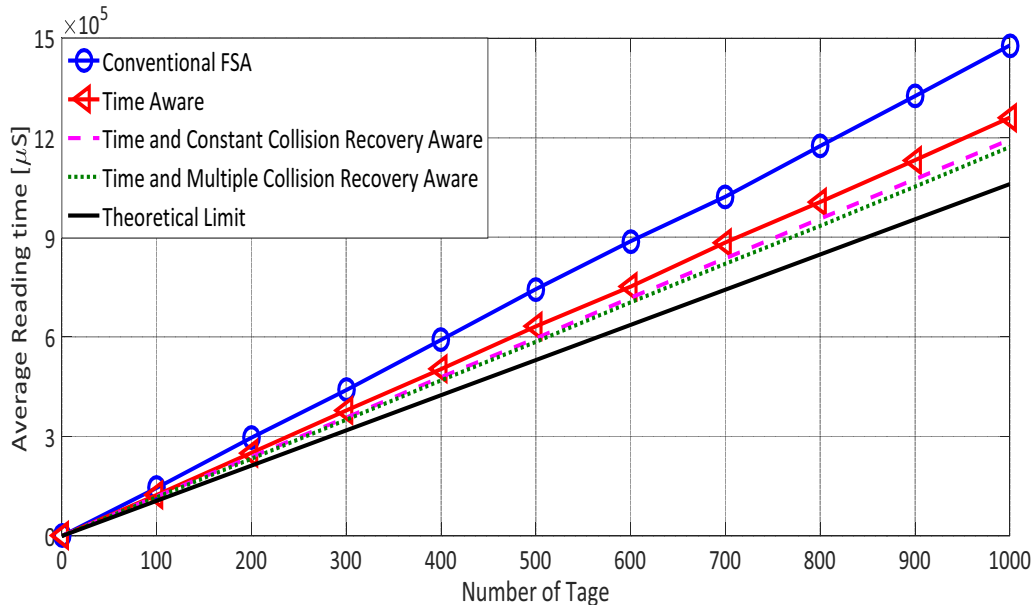


Figure 5.18: Average reading time of the proposed systems, conventional FSA and the theoretical limit using conventional ML number of tags estimation

frame length gives 15 % saving in the average total reading time compared to the conventional FSA. The Time and Constant Collision Recovery Aware frame length saves 5 % more than the Time Aware frame length, because of the new information about the collision recovery coefficient. In the Time and Constant Collision Recovery Aware the average collision recovery probability was assumed as  $\alpha = \alpha_2$ . In case of the time and multiple collision recovery frame length, we have 22 % average saving in the reading time. This is due to considering the different values of the collision recovery coefficients.

2. Average reading time with the conventional ML number of tags estimation: Figure 5.18 presents simulation results for the average reading time using conventional ML number of tags estimation [73], which neglect the collision recovery capability of the PHY layer. Due to the use of conventional ML number of tags estimation, the total average of reading time is decreased for all scenarios from 10 % to 15 % compared to the average reading time without number of tags estimation.
3. Average reading time with the collision recovery aware ML number of

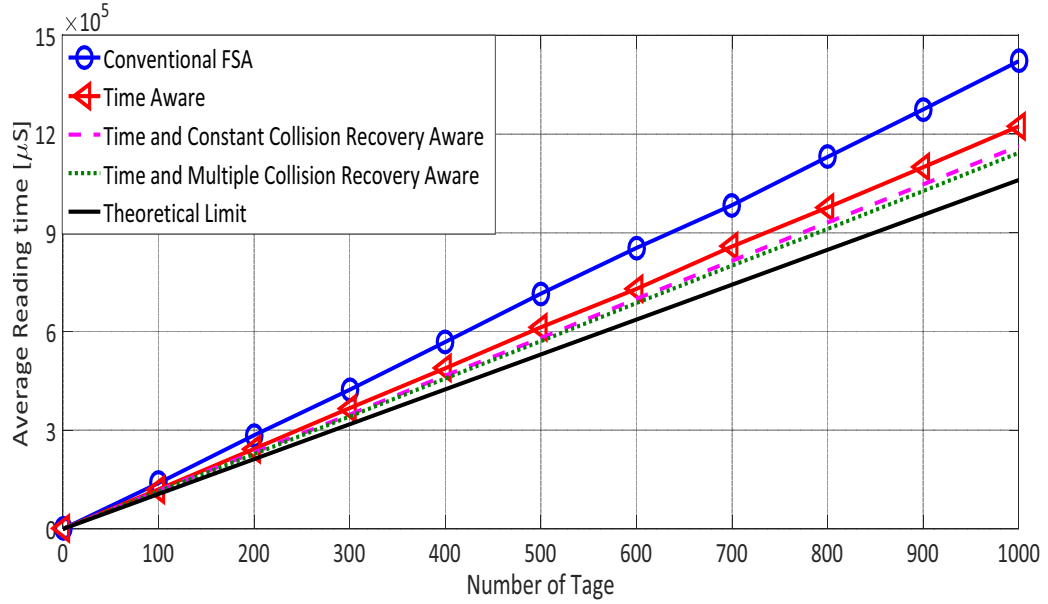


Figure 5.19: Average reading time of the proposed systems, conventional FSA and the theoretical limit with the proposed collision recovery aware ML number of tags estimation

tags estimation: Figure 5.19 shows the average reading time using the proposed Collision Recovery Aware ML number of tags estimation, which considers the collision recovery capability of the PHY layer. According to figure 5.19, the average total reading time using the Collision Recovery Aware number of tags estimation for the all proposed frame lengths and the conventional FSA are reduced with  $\approx 5\%$  compared to the case of using the conventional ML number of tags estimation [73].

According to the above results, there is still  $\approx 10\%$  lag of performance between the the proposed systems and the theoretical limit of the EPCglobal C1 G2 standard [11]. The main reason of this lagging in performance is that all the allowed optimization was only in the reader side. To follow the EPCglobal C1 G2 standard [11], the tags could not be modified. Thus in the next chapter, backwards compatible improvement of the EPCglobal Class 1 Gen 2 standard will be proposed. This proposed system is compatible with the EPCglobal C1 G2 standards, i.e. the proposed tags could be jointly operated with conventional tags and identified by conventional readers without affecting the performance. Additionally, conventional tags can also be operated together with the proposed

tags and can be identified by the proposed reader.



# Chapter 6

## Proposed Improvements of EPCglobal C1 G2

EPCglobal C1 G2 is the most renowned UHF RFID standard. It allows only for a single tag acknowledgment, even if the physical layer is able to identify multiple collided tags. This results in an overall reduced performance. Recent studies have focused on this problem e.g. [94] used the post-preamble proposed in [96] with a Multi Input Multi Output (MIMO) receiver to resolve collisions. The authors assumed that all the recovered tags can be acknowledged in parallel. However, this technique is not compatible with the EPCglobal C1 G2 standards [11], due to this post-preamble. Therefore, their proposal requires a new RFID standard. Furthermore, acknowledging more than one tag in parallel would cause a new problem called “tag collision” due to the simultaneous reception of multiple acknowledgment commands at the tag side. Moreover, this parallel acknowledgment will also cause Electronic Product Code (EPC) collisions at the reader side. The EPC packet is much longer than the RN16 packet, so it needs an advanced collision recovery algorithm, which will decrease the system performance.

To overcome these pitfalls, this chapter proposes a system that is capable to acknowledge multiple tags within a single slot, resulting in a significant increase in performance. The main advantage of this proposal is that, it is compatible with existing EPCglobal C1 G2 tags and readers. Hence, our improved tags can be read by conventional readers without affecting the performance. Furthermore, existing tags can be read simultaneously with our improved tags by



Figure 6.1: Conventional tag response

optimized readers.

This chapter is organized as follows: Section 1 presents a brief discussion about the conventional reading process using the EPCglobal C1 G2 standards. In section 2, we describe the proposed new system including the modifications of the tags and the reader. The performance of the proposed system will be analyzed in section 3. Finally, section 4 provides the practical measurements and the simulation results.

## 6.1 EPCglobal C1 G2 Reading Process

This section will describe, in brief, the conventional reading algorithm of the EPCglobal C1 G2 standards. The reader initially powers the tags in the reading area with a (CW). At this time, the powered tags are in the ready state waiting for the frame size information from the reader. Then, the reader broadcasts the frame size and notifies all tags of the beginning of a new frame with a Query command. As soon as the tags receive this command, each tag selects a slot from the frame by setting its slot counter, and enters the Arbitrate state. When the tag slot counter is equal to zero, the tag enters the Reply state and Backscatter its 16 bits random number (RN16) as a temporary ID in addition to a 18 bits pilot and preamble used for synchronization as shown in figure 6.1.

According to Frame Slotted ALOHA, there are three probabilities for each slot: 1) No tag reply: The reader considers this slot as an empty slot and transmits a Query-Rep command asking the tags to decrements their slot counters. 2) Only one tag responds (successful slot): The reader transmits an acknowledge command including the received RN16. Here the acknowledged tag enters the acknowledged state and replies with its EPC code. 3) Multiple tags reply (collided Slot): this case has two possibilities:

1. Systems that have no collision recovery capability as shown in figure 6.2

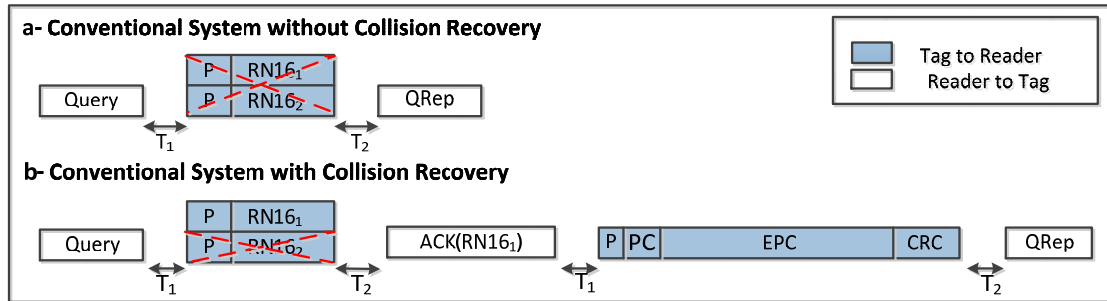


Figure 6.2: Two tags collided slot according to EPCglobal C1 G2 standards

(a): In such systems, the reader fails to identify any RN16, so it queries the next slot by sending another Query-Rep command. As soon as the collided tags receive the Query-Rep command, they enter the Arbitrate state waiting for the next frame. The maximum reading efficiency in such systems is 36%, if the working frame length is equal to the tag population size.

2. Systems that have collision recovery capability as shown in figure 6.2 (b): These systems have the ability to identify at least one RN16 from the responding tags. Then, the reader broadcasts an Acknowledge command including one of the identified RN16s. The tag which has the same RN16 replies its EPC code and mutes itself until the end of the reading process. However, the remaining tags forget their RN16s and enter the Arbitrate state waiting for the next frame. The main drawback of such systems is that the reader can only acknowledge one tag from the collided tags in a slot, even if it has the capability to identify all the responding RN16s. To overcome this drawback, backwards compatible extension are proposed in the following sections.

## 6.2 Proposed System Description

In this section, the detailed descriptions of the proposed tags and readers will be presented. Afterwards, the performance of the proposed system will be compared to conventional approaches.

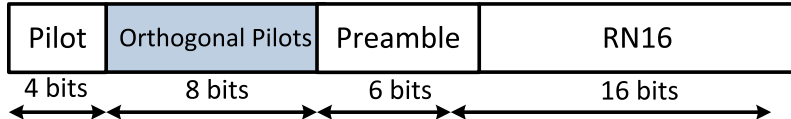


Figure 6.3: Tag response of the proposed tags including the new pilot sequences

### 6.2.1 Proposed Tag

The proposed tag has the ability to act like conventional UHF EPCglobal C1 G2 tags, which is the default mode. However, it loads extra properties when it is in the ready state and receives a new command called Switch command from the proposed reader. The following part presents the main modifications in the proposed tag:

According to the EPCglobal C1 G2 standards [11], conventional tags backscatter two possible preambles with the RN16 packet, either the short version (6 bits preamble) or the long version 18 bits (12 bits zeros as a pilot + 6 bits of the short version). For the proposed tag, the long version only is used, but with a new structure. As shown in figure 6.3, the new structure is 4 bits zeros used for synchronization and 8 bits orthogonal pilots used for channel estimation. Table 6.1 shows an example of the orthogonal pilots, which are similar to the orthogonal post-preamble used in [96]. In this thesis, the 12 pilot bits of the long version of the conventional tag response is divided to 4 zero bits and 8 orthogonal pilot bits. The 8 orthogonal pilot bits have to be orthogonal to the other pilot bits and also to the conventional pattern  $P_1$  (8 zero bits). This property gives our proposal the advantage to have the conventional long version tag reply as a valid tag response in the new system. This is in contrast to the proposal by [96], where the conventional tags are not compatible with their system.

In case of a resolved collision of multiple RN16s, we can apply our proposed pseudo parallel reading process. A tag receiving its valid RN16 replies with its EPC and goes to the acknowledged state. In contrast, a tag receiving an invalid RN16 (e.g. valid for another tag) goes to a new state called Wait state. In the latter state the tag memorizes its RN16 until one of the two possibilities occurs: a) receiving an acknowledgment command containing its RN16. In this case the tag replies with its EPC and goes to the acknowledged state, b) receiving

Table 6.1: Set of 8 orthogonal sequences [96]

Sequence	Orthogonal Pilots
$P_1$	1 -1 1 -1 1 -1 1 -1 1 -1 1 -1 1 -1 1 -1
$P_{18}$	1 -1 1 -1 1 -1 1 1 -1 1 -1 1 -1 1 -1 1 -1
$P_{69}$	1 -1 1 1 -1 1 -1 1 -1 1 -1 -1 1 -1 1 -1
$P_{86}$	1 -1 1 1 -1 1 -1 -1 1 -1 1 1 -1 1 1 -1 -1
$P_{171}$	1 1 -1 1 -1 -1 1 -1 1 1 -1 1 -1 1 -1 1 -1
$P_{188}$	1 1 -1 1 -1 -1 1 1 -1 -1 1 -1 1 1 -1 1 -1
$P_{239}$	1 1 -1 -1 1 1 -1 1 -1 -1 1 1 -1 -1 1 1 -1
$P_{256}$	1 1 -1 -1 1 1 -1 -1 1 1 -1 -1 1 1 -1 -1

Table 6.2: Proposed switch command

	Command
Number of bits	16
Description	1110001001100000

a command different from the acknowledged command, where the tag goes to the arbitrate state waiting for a new command.

When the proposed tag is in the Acknowledged state and receives a Query, Query-Adjust, or Acknowledgment command with a different RN16, it goes to the Ready state where it mutes itself until the end of the inventory process.

Figure 6.4 presents a state diagram with the required modifications of the tag state diagram given in [11] on page 47 figure 6.19.

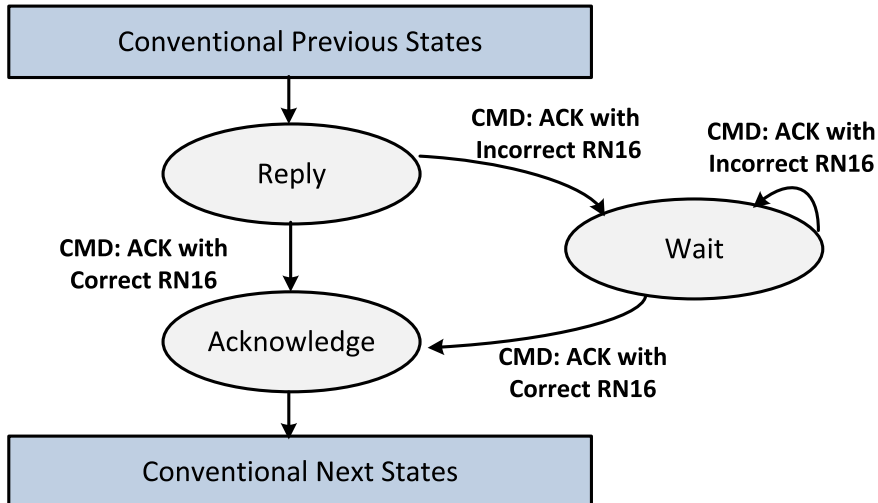


Figure 6.4: Modified part of tags state diagram

### 6.2.2 Proposed Reader

The proposed reader applies the normal FSA based on the conventional UHF EPCglobal C1 G2 standard, which means that it is able to operate normally with conventional tags. It starts its reading process with a new command called Switch command to check whether there are new tags in the reading area. It checks the tags replies. If there is any orthogonal pilot from table 6.1, it switches to the new mode. Whenever it receives only conventional tag replies, it works in the conventional mode.

The following part presents the main modifications of the proposed reader:

The Switch command should exist in the proposed reader. The main purpose of this command is to switch the new tags from the conventional mode to the new mode. It should be transmitted before the Query command. The conventional tags will consider this Switch command as an unknown command, but the proposed tags will recognize that they are working in the new system. Table 6.2 provides an example for the Switch command code, which is a16 bits command from the future use part of EPCglobal C1 G2 standards (*cf.* table 6.18 of [11]).

As discussed before, there are many problems in acknowledging more than one tag per slot in parallel, like the tag collisions, and the EPC collision at the reader side. On the other hand, the new system should benefit from the

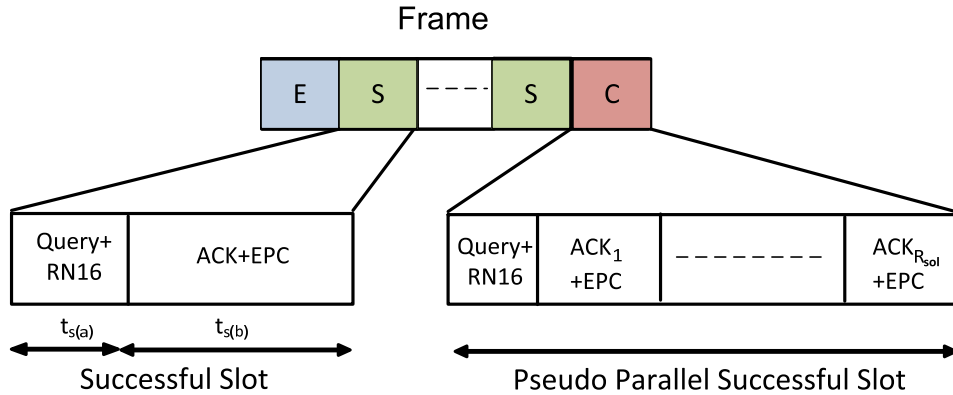


Figure 6.5: Example of the proposed pseudo parallel successful slot with parallel Query command and RN16 followed by successive Acknowledgment commands and EPcs

collision resolving capabilities of the modern readers. Therefore, the proposed reader has the capability of converting this collided slot into a pseudo parallel successful slot.

The reader starts each slot with a Query-Rep command asking for the RN16 of each tag. Then each tag back scatters its RN16 including one random orthogonal pilot from table 6.1 if it is one of the proposed tags or the conventional pilot ( $P_1$  from table 6.1) if it is a conventional tag. In case of a collided slot, the reader executes the following steps:

- Uses the orthogonal pilots to do channel estimation for the collided tags. Afterwards, it employs the channel information to recover the collided RN16s using a MIMO receiver, e.g. the receiver proposed in [94].
- Counts the number of recovered tags replies in the “Reply Counter”.
- Recognizes whether one of these replies is a conventional pilot or not by checking if one of the collided pilots is the conventional one,  $P_1$  in table 6.1. If yes, this is a conventional tag.

Using these information, the reader checks first if one of the replied tags is a conventional tag. In this case the reader only acknowledges this tag and waits for its EPC, ignoring the remaining new tags. Whenever all collided tags are new tags, the reader starts acknowledging them successively ordering them from the weakest to the strongest reply. The Reply Counter counts down with

Table 6.3: Example for unique pilot collision scenarios for up to eight colliding tags per slot [94]

Number of received tags $R$	Probability of unique scenario $P_{S_1}$
1	$P_{S_1} = 1$
2 1+1	$P_{S_1} = 0.875$
3 1+1+1	$P_{S_1} = 0.656$
4 1+1+1+1	$P_{S_1} = 0.41$
5 1+1+1+1+1	$P_{S_1} = 0.205$
6 1+1+1+1+1+1	$P_{S_1} = 0.077$
7 1+1+1+1+1+1+1	$P_{S_1} = 0.019$
8 1+1+1+1+1+1+1+1	$P_{S_1} = 0.002$

each received EPC from a tag and then sends the successive acknowledgment command until the Reply Counter reaches to zero. Figure 6.5 illustrates an example for the pseudo parallel successful slot.

### 6.3 Performance Analysis

Based on the new system, we propose a new reading efficiency formula considering the advantages of the new system:

$$\eta_{new} = \sum_{R=1}^M P(R) \cdot \left( \sum_{l=1}^R P_{S_l}(R) \cdot R_{sol} \cdot \varphi \right), \quad (6.1)$$

where  $P(R)$  is the probability that exactly  $R$  tags are active in one slot. It can be presented as:

$$P(R) = \binom{n}{i} \left( \frac{1}{L} \right)^i \left( 1 - \frac{1}{L} \right)^{n-i} \quad (6.2)$$

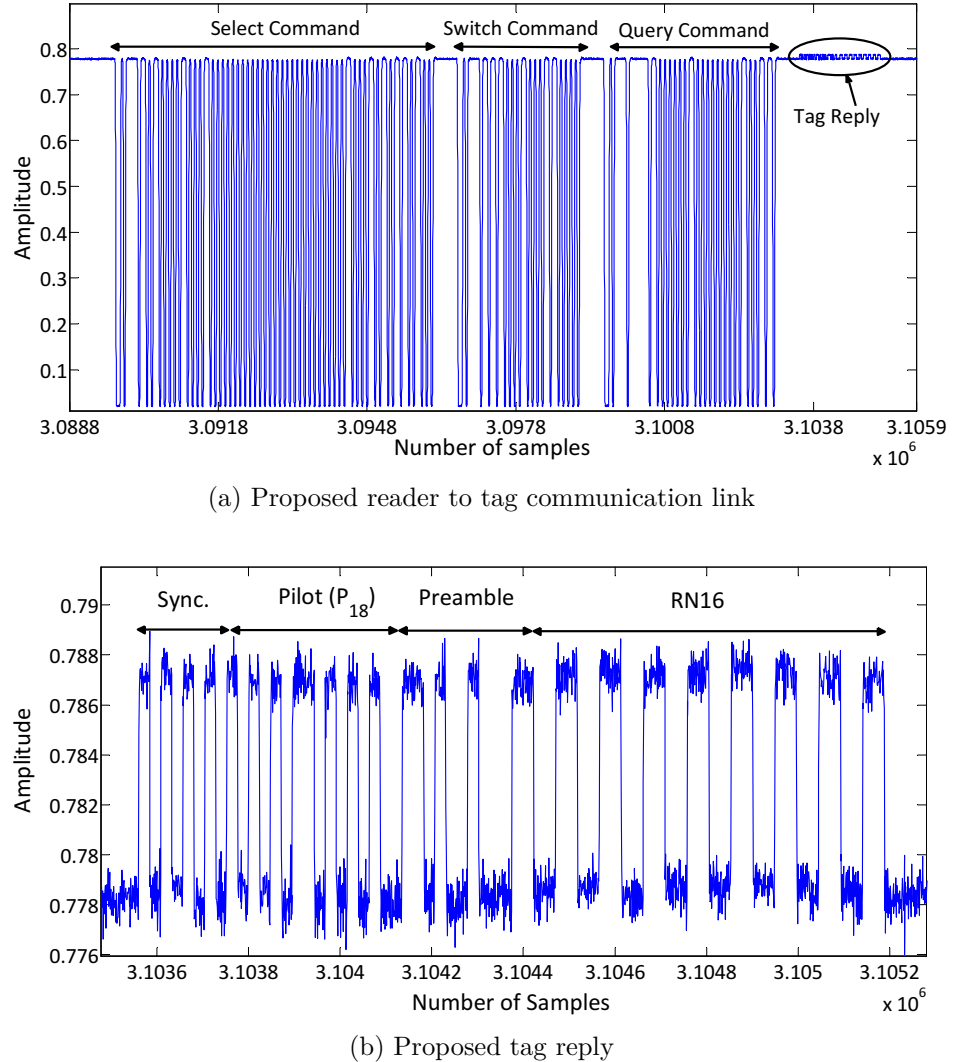


Figure 6.6: Communication link measurement

$M$  presents the maximum number of tags that can be resolved. For the proposed case,  $M$  is the number of orthogonal codes, i.e.  $M = 8$ , and  $R_{sol}$  is the number of recovered tags.

Since the colliding tags have randomly distributed pilots, several collision scenarios are possible as shown in [94].  $P_{S_l}(R)$  represents the probability that scenario  $S_l$  happens. It can be calculated from the binomial distribution as explained in [94]. For the proposed case, we consider only the unique scenarios  $(1 + 1 + \dots + 1)$ , i.e. if more than one tag has the same pilot, the reader will not be able to resolve this collision. Therefore, we have limited number of scenarios.

Table 6.4: System Parameters of EPCglobal C1 G2 standards [11]

Parameters	Values
$T_{Q-Rep}$	$78 T_{pri}$
$T_1$	$10 T_{pri}$
$T_2$	$20 T_{pri}$
$T_{RN16}$	$34 T_{pri}$
$T_{ACK}$	$236 T_{pri}$
$T_{EPC}$	$102 T_{pri}$

Table 6.3 shows all values of the unique scenarios  $P_{S_l}(R)$ .

According to figure 6.5, the conventional successful slot  $t_s$  is divided in to two parts: The first part presents time of the Query-Rep command and the RN16 tag reply  $t_{s(a)}$ , whereas the second part is the time of the Acknowledgment command and the EPC tag reply  $t_{s(b)}$ . Thus, the successful slot time is:

$$t_s = t_{s(a)} + t_{s(b)}, \quad (6.3)$$

where  $t_{s(a)}$  and  $t_{s(b)}$  can be expressed as:

$$\begin{aligned} t_{s(a)} &= T_{qRep} + T_1 + T_2 + T_{RN16} \\ t_{s(b)} &= T_{ACK} + T_1 + T_2 + T_{EPC} \end{aligned} \quad (6.4)$$

Table 6.4 shows numerical values from the EPCglobal C1 G2 standards [11] as a function of the link pulse-repetition interval  $T_{pri}$ . According to these values, the time of the Query-Rep command and receiving the RN16s presents 30% of the conventional successful slot duration. The time of the acknowledgment command and the EPC tag reply represents 70% of the conventional successful slot duration.

For comparability, the proposed reader does not acknowledge more than one tag in parallel. However, we propose a pseudo parallel successful slots. The reader sends a Query command in parallel to all the tags, then receives the RN16s in parallel. Next, the reader sends Acknowledgment commands successively to the resolved tags. Therefore, the duration of the proposed pseudo parallel slot is:

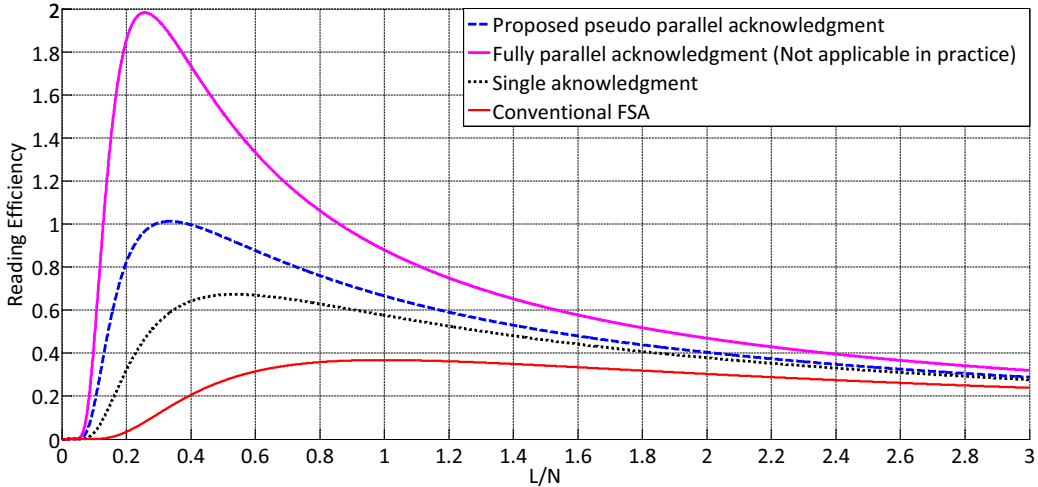


Figure 6.7: Reading efficiency for the conventional FSA and different acknowledgment scenarios using 8-orthogonal pilots

$$t_{pseudo} = t_{s(a)} + R_{sol} \cdot t_{s(b)}, \quad (6.5)$$

where  $R_{sol}$  is the number of recovered tags. These tags are acknowledged successively. Therefore, the proposed efficiency should include a factor representing the effect of the pseudo parallel spreading in time. This factor is called the pseudo parallel factor  $\varphi$ . According to the numerical values in table 6.4, it can be expressed as:

$$\varphi = \left( \frac{1}{0.3 + 0.7 \cdot R_{sol}} \right) \quad (6.6)$$

## 6.4 Measurement and Simulation Results

We have implemented our proposed tag modifications on the Wireless Identification Sensing Platform (WISP 5.0) [97], and the proposed reader on the Universal Software Radio Peripheral (USRP B210) [63]. A real example of the communication link between the proposed reader and the proposed tags is monitored using the USRP. Figure 6.6a provides a real measurement of the reader to tag communication link. According to the figure, the link starts with a normal Select command to set some conventional tag parameters. Then the reader broadcasts a Switch command asking the proposed tags to switch to the

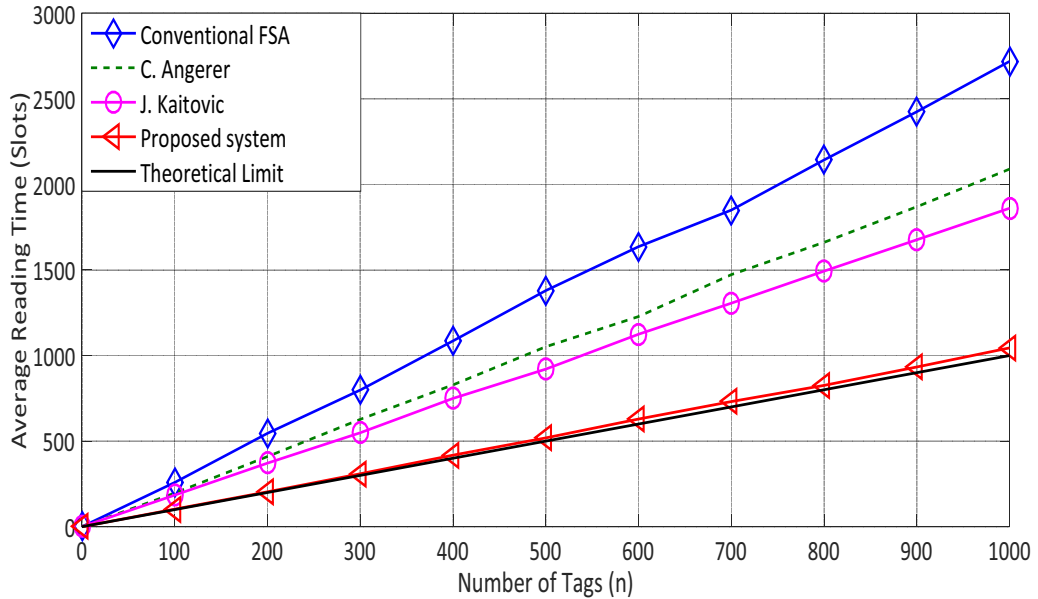


Figure 6.8: Comparison between the average reading time for different systems

new mode. The conventional tags will not recognize this command, so they will simply ignore it. Afterwards, the reader sends a Query command asking the tags to reply with their RN16. Figure 6.6b presents a focused simulations of the tag reply of figure 6.6a. As shown in figure 6.6b, the proposed tag reply starts with 4 bits zeros used for synchronization followed by 8 bits (one of the orthogonal pilots in table 6.1). In this example the tag replied with  $P_{18}$ . It is followed by a 6 bits preamble. Finally, the tag backscatters its RN16. The system is tested in a mixed network between the conventional and the proposed tags. The RN16 of the conventional and proposed tags were identified successfully.

The performance analysis is achieved through Monte Carlo simulations. Figure 6.7 shows a comparison between the reading efficiency of the conventional FSA and different acknowledgment scenarios use the 8 orthogonal pilot sequences. The first scenario is the system proposed by [94]. This system assumes fully parallel acknowledgment for all recovered tags. However, it is not compatible with the EPCglobal C1 G2 standard and can not be applied in practice. The second scenario deduces that it can acknowledge a single tag and neglect the other replies. This system does not benefit from the strong collision recov-

ery capability of the reader. The third one is the proposed pseudo successful slot. This system compromises between the single tag acknowledgment and the fully parallel acknowledgment with almost 100% maximum efficiency .

Figure 6.8 shows the average reading time of the proposed system compared to the conventional FSA and other recent EPCglobal C1 G2 compatible systems using collision recovery techniques. According to figure 6.8, the average reading time of our proposed system is decreased compared to the conventional FSA by 60%. In [81] the authors proposed a collision recovery system that is able to recover up to two collided tags. However, in our simulations it is assumed that the authors are able to recover all collided tags. Accordingly, the average reading time of our proposal is lower than the reading time of [81] and [98] by 50% and 35%, respectively, using single acknowledgment. Finally, the proposed system approaches the theoretical limit of the EPCglobal C1 G2 standards [11]. This gain is only attainable using the modified compatible tags. However, the proposed maximum performance using the conventional tags was presented in the results of chapter 5.



# **Chapter 7**

## **Conclusions and Future Work**

Nowadays, there has been a great interest in RFID due to the vast array of applications used in this field. RFID systems provide low cost and low power object identification and tracking mechanisms, being the key requirement for anticipated ultra dense applications, e.g., logistics. In such applications, dense number of tags are expected and fast identification is required. In this thesis, different proposals aimed to minimize the total identification time by optimizing the FSA anti-collision algorithm.

This chapter will summarize the main outcomes of this thesis, as well as the possible issues that may be addressed in future work.

### **7.1 Conclusions**

The advanced RFID readers proposed in this thesis improve performances and shorten the read out time. They incorporate different PHY layer parameters in order to efficiently optimize the MAC anti-collision protocols. They merged the collision recovery coefficients and the differences in slot durations. Thus, in order to benefit from the collision recovery expertise, changes in the number of tags estimations should be applied. Besides, the higher collision recovery capability of the system, the shorter optimum frame length is recommended. According to the differences in slot duration results, the smaller the duration of the empty slot compared to that of the collided slot, the longer optimum FSA frame length is required. Additionally, the evaluation of the complete read out process is performed and the obtained results prove that the proposed ad-

vanced RFID readers significantly decrease the identification time. Due to the simple tags implementation in EPCglobal C1 G2, improvements in the standards would be recommended to approach the theoretical limit of the reading time.

## **7.2 Open Issues and Future Work**

Despite the effort invested in this dissertation, there are still some remaining issues left that require further investigations. To mention but some examples, the influence of the initial frame length of the proposed system is neglected. The influence of the initial frame length should be analyzed. In addition, the MAC layer knowledge of the current SNR should send a feedback signal to the PHY layer. In this signal, the MAC layer decide to start resolving the current collided slot either to a successful or unsuccessful slot, depending on the current value of the SNR. Thereby, if the current SNR value is below a certain threshold, it might be better to leave this slot to a normal collided slot. On the other hand, when the current value of the SNR is above this threshold, it would be better to resolve this collided slot to a successful slot. Finally, practical assessment of the proposed work through measurements would be beneficial for a more comprehensive evaluation.





# List of Abbreviations

ACK	Acknowledgment
CDMA	Code Division Multiple Access
CW	continuous wave
DFSA	Dynamic Frame Slotted ALOHA
EPC	Electronic Product Code
FDMA	Frequency Division Multiple Access
FSA	Framed Slotted ALOHA
FSA	Framed Slotted ALOHA
HF	High Frequency
LF	Low Frequency
MAC	Medium Access Control
ML	Maximum Likelihood
MMSE	Minimum Mean-Square Error
PER	Packet Error Rate
RN16	Random Number 16
SA	Slotted ALOHA
SCS	Slot Count Selection

SDMA	Space Division Multiple Access
SNR	Signal to Noise Ratio
TDMA	Time Division Multiple Access
UHF	Ultra High Frequency
USRP	Universal Software Defined Radio Peripheral
ZF	Zero Forcing
RFID	Radio Frequency Identification

111

aaa

112

aaa

aaa

114

aaa

# List of Own Publications

1. H. A. Ahmed; H. Salah; J. Robert; A. Heuberger, "A Closed-Form Solution for ALOHA Frame Length Optimizing Multiple Collision Recovery Coefficients' Reading Efficiency," in IEEE Systems Journal , vol.PP, no.99, pp.1-4
2. H. Salah, H. A. Ahmed, J. Robert and A. Heuberger, "A Time and Capture Probability Aware Closed Form Frame Slotted ALOHA Frame Length Optimization," in IEEE Communications Letters, vol. 19, no. 11, pp. 2009-2012, Nov. 2015.
3. Hamed Salah, Hazem A. Ahmed, Joerg Ropert, and Albert Heuberger, "Performance Evaluation of Rate Estimation for UHF RFID Systems" International Journal of RF Technologies, vol. 7, no. 2-3, pp. 87-104, 2016
4. H. A. Ahmed, H. Salah, J. Robert and A. Heuberger, "Time aware closed form frame slotted ALOHA frame length optimization," 2016 IEEE Wireless Communications and Networking Conference, Doha, 2016, pp. 1-5.
5. H. A. Ahmed, H. Salah, J. Robert and A. Heuberger, "A closed form solution for frame slotted ALOHA utilizing time and multiple collision recovery coefficients," 2016 IEEE Topical Conference on Wireless Sensors and Sensor Networks (WiSNet), Austin, TX, 2016, pp. 11-14.
6. H. A. Ahmed, H. Salah, J. Robert and A. Heuberger, "An Efficient RFID Tag Estimation Method Using Biased Chebyshev Inequality for Dynamic Frame Slotted ALOHA," Smart SysTech 2014; European Conference on Smart Objects, Systems and Technologies, Dortmund, Germany, 2014, pp. 1-4.

7. H. Salah, H. A. Ahmed, J. Robert and A. Heuberger, "A Study of Software Defined Radio Receivers for Passive RFID Systems," Smart SysTech 2014; European Conference on Smart Objects, Systems and Technologies, Dortmund, Germany, 2014, pp. 1-5.
8. H. A. Ahmed, H. Salah, J. Robert and A. Heuberger, "A New Optimization Criteria For Frame Slotted ALOHA Utilizing Time And The Collision Recovery Coefficients," Smart SysTech 2015; European Conference on Smart Objects, Systems and Technologies, Aachen, Germany, 2015, pp. 1-4.
9. H. Salah, H. A. Ahmed, J. Robert and A. Heuberger, "FFT Based Rate Estimation for UHF RFID Systems," Smart SysTech 2015; European Conference on Smart Objects, Systems and Technologies, Aachen, Germany, 2015, pp. 1-5.
10. H. A. Ahmed, H. Salah, J. Robert and A. Heuberger, "Backwards compatible improvement of the EPCglobal class 1 gen 2 standard," 2015 IEEE International Conference on RFID Technology and Applications (RFID-TA), Tokyo, 2015, pp. 114-119.
11. H. A. Ahmed, H. Salah, J. Robert and A. Heuberger, "A closed form solution for frame slotted ALOHA utilizing time and multiple collision recovery coefficients," 2016 IEEE Topical Conference on Wireless Sensors and Sensor Networks (WiSNet), Austin, TX, 2016, pp. 11-14.
12. H. Salah, H. A. Ahmed, J. Robert and A. Heuberger, "Maximum Likelihood decoding for non-synchronized UHF RFID tags," 2016 IEEE Topical Conference on Wireless Sensors and Sensor Networks (WiSNet), Austin, TX, 2016, pp. 89-92.
13. H. A. Ahmed, H. Salah, J. Robert and A. Heuberger "A Closed Form Solution For Collision Recovery Aware Number of Tags Estimation", IEEE Sensor Letter. (Submitted).
14. H. Salah, H. A. Ahmed, J. Robert and A. Heuberger "Multiple Antennas Collision Recovery Receiver Based on Stimulating The Rate Tolerance for UHF RFID Systems" IEEE Systems Journal. (Submitted)

# Bibliography

- [1] R. Want, “An introduction to rfid technology,” *IEEE Pervasive Computing*, vol. 5, pp. 25–33, Jan 2006.
- [2] N. C. Karmakar, *RFID ReadersReview and Design*, pp. 83–121. Wiley-IEEE Press, 2010.
- [3] N. Raza, V. Bradshaw, and M. Hague, “Applications of rfid technology,” in *IEE Colloquium on RFID Technology*, pp. 1–5, 1999.
- [4] S. Piramuthu and Y.-J. Tu, “Improving accuracy of rfid tag identification,” in *2007 IET-UK International Conference on Information and Communication Technology in Electrical Sciences*, pp. 692–696, Dec 2007.
- [5] H. E. Matbouly, K. Zannas, Y. Duroc, and S. Tedjini, “Analysis and assessments of time delay constrains for passive rfid tag-sensor communication link: Application for rotation speed sensing,” *IEEE Sensors Journal*, vol. 17, pp. 2174–2181, Apr 2017.
- [6] A. Habib, M. A. Afzal, H. Sadia, Y. Amin, and H. Tenhunen, “Chipless rfid tag for iot applications,” in *2016 IEEE 59th International Midwest Symposium on Circuits and Systems*, pp. 1–4, Oct 2016.
- [7] H. Ma, Y. Wang, K. Wang, and Z. Ma, “The optimization for hyperbolic positioning of uhf passive rfid tags,” *IEEE Transactions on Automation Science and Engineering*, vol. PP, no. 99, pp. 1–11, 2017.
- [8] N. Ayer and D. W. Engels, “Evaluation of iso 18000-6c artifacts,” in *2009 IEEE International Conference on RFID*, pp. 123–130, Apr 2009.

- [9] S. R. Aroor and D. D. Deavours, “Evaluation of the state of passive uhf rfid: An experimental approach,” *IEEE Systems Journal*, vol. 1, pp. 168–176, Dec 2007.
- [10] X. Yang, L. Meng, F. Yu, L. Yang, Q. Wu, J. Su, J. Lu, and G. Li, “Design and test of a rfid uhf tag,” in *2009 Pacific-Asia Conference on Circuits, Communications and Systems*, pp. 346–349, May 2009.
- [11] “EPC radio-frequency protocols class-1 generation-2 UHF RFID protocol for communications at 860 MHz 960 MHz version 1.1.0 2006.”
- [12] S. q. Geng, D. m. Gao, C. Zhu, M. He, and W. c. Wu, “An improved dynamic framed slotted aloha algorithm for rfid anti-collision,” in *2008 9th International Conference on Signal Processing*, pp. 2934–2937, Oct 2008.
- [13] S.-R. Lee, S.-D. Joo, and C.-W. Lee, “An enhanced dynamic framed slotted aloha algorithm for rfid tag identification,” in *The Second Annual International Conference on Mobile and Ubiquitous Systems: Networking and Services*, pp. 166–172, Jul 2005.
- [14] F. Ricciato and P. Castiglione, “Pseudo-random aloha for enhanced collision-recovery in rfid,” *IEEE Communications Letters*, vol. 17, pp. 608–611, Mar 2013.
- [15] L. Fu, L. Liu, M. Li, and J. Wang, “Collision recovery receiver for epc gen2 rfid systems,” in *2012 3rd IEEE International Conference on the Internet of Things*, pp. 114–118, Oct 2012.
- [16] D. D. Donno, V. Lakafosis, L. Tarricone, and M. M. Tentzeris, “Increasing performance of sdr-based collision-free rfid systems,” in *IEEE International Microwave Symposium Digest*, pp. 1–3, Jun 2012.
- [17] H. Mahdavifar and A. Vardy, “Coding for tag collision recovery,” in *2015 IEEE International Conference on RFID (RFID)*, pp. 9–16, Apr 2015.
- [18] D. Harris, “Radio transmission system with modulatable passive responder,” *US. Patent*, 2927321, 1960.

- [19] W. Charles, “Portable radio frequency emitting identifier,” *US. Patent 4384288*, 1973.
- [20] F. Vernon, “Applications of the microwave homodyne,” *Journal of Transactions of the IRE Professional Group on Antennas and Propagation*, vol. 4, pp. 110–116., 1952.
- [21] K. V. S. Rao, “An overview of backscattered radio frequency identification system (rfid),” in *Microwave Conference, Asia Pacific*, vol. 3, pp. 746–749 vol.3, 1999.
- [22] D. Friedman, H. Heinrich, and D. W. Duan, “A low-power cmos integrated circuit for field-powered radio frequency identification tags,” in *1997 IEEE International Solids-State Circuits Conference. Digest of Technical Papers*, pp. 294–295, Feb 1997.
- [23] A. Cerino and W. P. Walsh, “Research and application of radio frequency identification (rfid) technology to enhance aviation security,” in *Proceedings of the IEEE 2000 National Aerospace and Electronics Conference. NAECON 2000. Engineering Tomorrow*, pp. 127–135, 2000.
- [24] M. Kossel, H. Benedickter, and W. Baechtold, “An active tagging system using circular polarization modulation,” in *1999 IEEE MTT-S International Microwave Symposium Digest (Cat. No.99CH36282)*, vol. 4, pp. 1595–1598 vol.4, Jun 1999.
- [25] W. Che, Y. Yang, C. Xu, N. Yan, X. Tan, Q. Li, H. Min, and J. Tan, “Analysis, design and implementation of semi-passive gen2 tag,” in *2009 IEEE International Conference on RFID*, pp. 15–19, Apr 2009.
- [26] A. Janek, C. Steger, R. Weiss, J. Preishuber-Pfluegl, and M. Pistauer, “Lifetime extension of semi-passive uhf rfid tags using special power management techniques and energy harvesting devices,” in *AFRICON 2007*, pp. 1–7, Sept 2007.
- [27] J. Garcia, A. Arriola, F. Casado, X. Chen, J. I. Sancho, and D. Valderas, “Coverage and read range comparison of linearly and circularly polarised

- radio frequency identification ultra-high frequency tag antennas," *IET Microwaves, Antennas Propagation*, vol. 6, pp. 1070–1078, Jun 2012.
- [28] M. A. Islam and N. Karmakar, "A linearly polarized (lp) reader antenna for lp and orientation insensitive (oi) chipless rfid tags," in *2016 9th International Conference on Electrical and Computer Engineering (ICECE)*, pp. 431–434, Dec 2016.
  - [29] L. Shafai and K. Antoszkiewicz, "Circular polarized antennas employing linearly polarized radiators," in *1988 Symposium on Antenna Technology and Applied Electromagnetics*, pp. 1–4, Aug 1988.
  - [30] N. Usami and A. Hirose, "Proposal of wideband reconfigurable circular-polarized single-port antenna," in *2014 Asia-Pacific Microwave Conference*, pp. 34–36, Nov 2014.
  - [31] T. Jiayin, H. Yan, and M. Hao, "A novel baseband-processor for lf rfid tag," in *2007 7th International Conference on ASIC*, pp. 870–873, Oct 2007.
  - [32] M.-W. Seo, Y.-C. Choi, Y.-H. Kim, and H.-J. Yoo, "A 13.56mhz receiver soc for multi-standard rfid reader," in *2008 IEEE International Conference on Electron Devices and Solid-State Circuits*, pp. 1–4, Dec 2008.
  - [33] M. Hirvonen, N. Pesonen, O. Vermesan, C. Rusu, and P. Enoksson, "Multi-system, multi-band rfid antenna: Bridging the gap between hf- and uhf-based rfid applications," in *2008 European Conference on Wireless Technology*, pp. 346–349, Oct 2008.
  - [34] D. W. Engels and S. E. Sarma, "The reader collision problem," in *IEEE International Conference on Systems, Man and Cybernetics*, vol. 3, pp. 6 pp. vol.3–, Oct 2002.
  - [35] J. Waldrop, D. W. Engels, and S. E. Sarma, "Colorwave: an anticollision algorithm for the reader collision problem," in *Communications, 2003. ICC '03. IEEE International Conference on*, vol. 2, pp. 1206–1210 vol.2, May 2003.

- [36] D. Wang, J. Wang, and Y. Zhao, “A novel solution to the reader collision problem in rfid system,” in *2006 International Conference on Wireless Communications, Networking and Mobile Computing*, pp. 1–4, Sept 2006.
- [37] J. Ho, D. W. Engels, and S. E. Sarma, “Hiq: a hierarchical q-learning algorithm to solve the reader collision problem,” in *International Symposium on Applications and the Internet Workshops (SAINTW’06)*, pp. 4 pp.–, Jan 2006.
- [38] N. Li, X. Duan, Y. Wu, S. Hua, and B. Jiao, “An anti-collision algorithm for active rfid,” in *2006 International Conference on Wireless Communications, Networking and Mobile Computing*, pp. 1–4, Sept 2006.
- [39] V. Pillai, R. Martinez, J. Bleichner, K. Elliot, S. Ramamurthy, and K. V. S. Rao, “A technique for simultaneous multiple tag identification,” in *Fourth IEEE Workshop on Automatic Identification Advanced Technologies (AutoID’05)*, pp. 35–38, Oct 2005.
- [40] L. C. Wang and H. C. Liu, “A novel anti-collision algorithm for epc gen2 rfid systems,” in *2006 3rd International Symposium on Wireless Communication Systems*, pp. 761–765, Sept 2006.
- [41] L. Liu and S. Lai, “Aloha-based anti-collision algorithms used in rfid system,” in *2006 International Conference on Wireless Communications, Networking and Mobile Computing*, pp. 1–4, Sept 2006.
- [42] H. C. Liu and J.-P. Ciou, “Performance analysis of multi-carrier rfid systems,” in *International Symposium on Performance Evaluation of Computer Telecommunication Systems*, vol. 41, pp. 112–116, Jul 2009.
- [43] J. Yu, K. Liu, and G. Yan, “A novel rfid anti-collision algorithm based on sdma,” in *2008 4th International Conference on Wireless Communications, Networking and Mobile Computing*, pp. 1–4, Oct 2008.
- [44] L. C. Wuu, Y. J. Chen, C. H. Hung, and W. C. Kuo, “Zero-collision rfid tags identification based on cdma,” in *2009 Fifth International Conference on Information Assurance and Security*, vol. 1, pp. 513–516, Aug 2009.

- [45] C. Zhai, Z. Zou, Q. Chen, L. Zheng, and H. Tenhunen, “Optimization on guard time and synchronization cycle for tdma-based deterministic rfid system,” in *2015 IEEE International Conference on RFID Technology and Applications (RFID-TA)*, pp. 71–75, Sept 2015.
- [46] J. Myung, W. Lee, J. Srivastava, and T. Shih, “Tag-Splitting: Adaptive Collision Arbitration Protocols for RFID Tag Identification,” *IEEE Transactions on Parallel and Distributed Systems*, vol. 18, no. 6, pp. 763–775, 2007.
- [47] R. Hush and C. Wood, “Analysis of tree algorithms for rfid arbitration,” in *In IEEE International Symposium on Information Theory*, p. 107, IEEE, 1998.
- [48] A. E. M.Jacomet and U. Gehrig, “Contactless identification device with anticollision algorithm,” in *in: IEEE Computer Society, Conference on Circuits, Systems, Computers and Communications*, 1999.
- [49] J. Park, M. Y. Chung, and T.-J. Lee, “Identification of RFID Tags in Framed-Slotted ALOHA with Tag Estimation and Binary Splitting,” in *First International Conference on Communications and Electronics, 2006. ICCE '06.*, pp. 368–372, 2006.
- [50] A. Leon-Garcia and I. Widjaja, *Communication Networks: Fundamental Concepts and Key Architectures*. McGraw-Hill Press, Boston, 1996.
- [51] J. E. Wieselthier, A. Ephremides, and L. A. Michaels, “An exact analysis and performance evaluation of framed aloha with capture,” *IEEE Transactions on Communications*, vol. 37, pp. 125–137, Feb 1989.
- [52] F. Schoute, “Dynamic Frame Length ALOHA,” *IEEE Transactions on Communications*, vol. 31, no. 4, pp. 565–568, 1983.
- [53] A. Zanella, “Estimating collision set size in framed slotted aloha wireless networks and rfid systems,” *Communications Letters, IEEE*, vol. 16, pp. 300–303, Mar 2012.
- [54] H. Vogt, “Efficient object identification with passive RFID rags,” in *International Conference on Pervasive Computing, Zürich*, Aug. 2002.

- [55] L. Zhu and T. Yum, "Optimal framed aloha based anti-collision algorithms for rfid systems," *IEEE Transactions on Communications*,, vol. 58, pp. 3583–3592, December 2010.
- [56] H. Vogt, "Multiple object identification with passive rfid tags," in *Systems, Man and Cybernetics, 2002 IEEE International Conference on*, vol. 3, pp. 6 pp. vol.3–, Oct 2002.
- [57] X. Yang, H. Wu, Y. Zeng, and F. Gao, "Capture-aware estimation for the number of rfid tags with lower complexity," *IEEE Communications Letters*, vol. 17, pp. 1873–1876, Oct 2013.
- [58] B. Li and J. Wang, "Efficient anti-collision algorithm utilizing the capture effect for iso 18000-6c rfid protocol," *Communications Letters, IEEE*, vol. 15, pp. 352–354, Mar 2011.
- [59] D. Donno, L. Tarricone, L. Catarinucci, V. Lakafosis, and M. Tentzeris, "Performance enhancement of the rfid epc gen2 protocol by exploiting collision recovery," *Progress In Electromagnetics Research B*,, vol. 43, 53–72, 2012.
- [60] A. Bui, C. Nguyen, T. Hoang and A. Pham, "Tweaked query tree algorithm to cope with capture effect and detection error in rfid systems," in *2015 International Conference on Communications, Management and Telecommunications (ComManTel)*, pp. 46–51, Dec 2015.
- [61] M. Nemati, H. Takshi, and V. Shah-Mansouri, "Tag estimation in rfid systems with capture effect," in *2015 23rd Iranian Conference on Electrical Engineering*, pp. 368–373, May 2015.
- [62] S. Choi, J. Choi, and J. Yoo, "An efficient anti-collision protocol for tag identification in rfid systems with capture effect," in *2012 Fourth International Conference on Ubiquitous and Future Networks (ICUFN)*, pp. 482–483, Jul 2012.
- [63] Ettus Research, "USRP B210." <http://www.ettus.com/product/details/UB210-KIT>, 2015.

- [64] D. Lee, K. Kim, and W. Lee, "*Q+-Algorithm: An Enhanced RFID Tag Collision Arbitration Algorithm*", pp. 23–32. Berlin, Heidelberg: Springer Berlin Heidelberg, 2007.
- [65] I. Joe and J. Lee, "A novel anti-collision algorithm with optimal frame size for rfid system," in *Software Engineering Research, Management Applications, 2007. SERA 2007. 5th ACIS International Conference on*, pp. 424–428, Aug 2007.
- [66] M. Daneshmand, C. Wang, and K. Sohraby, "A new slot-count selection algorithm for rfid protocol," in *Communications and Networking in China, 2007. CHINACOM '07. Second International Conference on*, pp. 926–930, Aug 2007.
- [67] M. U. Farooq, M. Asif, S. W. Nabi, and M. A. Qureshi, "Optimal adjustment parameters for epc global rfid anti-collision q-algorithm in different traffic scenarios," in *2012 10th International Conference on Frontiers of Information Technology*, pp. 302–305, Dec 2012.
- [68] I. Uysal and N. Khanna, "Q-frame-collision-counter: A novel and dynamic approach to rfid gen 2's q algorithm," in *2015 IEEE International Conference on RFID Technology and Applications (RFID-TA)*, pp. 120–125, Sept 2015.
- [69] C. Floerkemeier, "Transmission control scheme for RFID object identification," in *Pervasive Wireless Networking Workshop (IEE PERCOM)*, 2006.
- [70] J.-R. Cha and J.-H. Kim, "Novel anti-collision algorithms for fast object identification in rfid system," in *11th International Conference on Parallel and Distributed Systems (ICPADS'05)*, vol. 2, pp. 63–67, Jul 2005.
- [71] J.-R. Cha and J.-H. Kim, "Dynamic framed slotted aloha algorithms using fast tag estimation method for rfid system," in *Consumer Communications and Networking Conference*, vol. 772, 2006.
- [72] B. S. Wang, Q. S. Zhang, D. K. Yang, and J. S. Di, "Transmission control solutions using interval estimation method for epc c1g2 rfid tag identifi-

- cation,” in *2007 International Conference on Wireless Communications, Networking and Mobile Computing*, pp. 2105–2108, Sept 2007.
- [73] W.-T. Chen, “An accurate tag estimate method for improving the performance of an rfid anticollision algorithm based on dynamic frame length aloha,” *Automation Science and Engineering, IEEE Transactions on*, vol. 6, pp. 9–15, Jan 2009.
- [74] E. Vahedi, V. Wong, I. Blake, and R. Ward, “Probabilistic analysis and correction of chen’s tag estimate method,” *Automation Science and Engineering, IEEE Transactions on*, vol. 8, pp. 659–663, Jul 2011.
- [75] M. Kodialam and T. Nandagopal, “Fast and reliable estimation schemes in rfid systems,” in *Proceedings of the 12th annual international conference on Mobile computing and networking*, pp. 322–333, ACM, 2006.
- [76] P. Solic, J. Radic, and N. Rozic, “Linearized combinatorial model for optimal frame selection in gen2 rfid system,” in *RFID , 2012 IEEE International Conference on*, pp. 89–94, Apr 2012.
- [77] P. Harremoes, “Binomial and poisson distributions as maximum entropy distributions,” *IEEE Transactions on Information Theory*, vol. 47, pp. 2039–2041, Jul 2001.
- [78] G. V. Weinberg, “Bit error rate approximations using poisson and negative binomial sampling distributions,” *Electronics Letters*, vol. 44, pp. 217–219, Jan 2008.
- [79] H. Salah, H. Ahmed, J. Robert, and A. Heuberger, “A time and capture probability aware closed form frame slotted aloha frame length optimization,” *Communications Letters, IEEE*, vol. 19, pp. 2009–2012, Nov 2015.
- [80] D. Struik, *A Source Book in Mathematics 1200-1800*. Princeton University Press, 1986.
- [81] C. Angerer, R. Langwieser, and M. Rupp, “Rfid reader receivers for physical layer collision recovery,” *Communications, IEEE Transactions on*, vol. 58, pp. 3526–3537, Dec 2010.

- [82] T. Sansanayuth, P. Suksompong, C. Chareonlarpnopparut, and A. Taparugssanagorn, “Rfid 2d-localization improvement using modified landmarc with linear mmse estimation,” in *2013 13th International Symposium on Communications and Information Technologies (ISCIT)*, pp. 133–137, Sept 2013.
- [83] H. Wu and Y. Zeng, “Bayesian tag estimate and optimal frame length for anti-collision aloha rfid system,” *Automation Science and Engineering, IEEE Transactions on*, vol. 7, pp. 963–969, Oct 2010.
- [84] W. J. Shin and J. G. Kim, “A capture-aware access control method for enhanced rfid anti-collision performance,” *IEEE Communications Letters*, vol. 13, pp. 354–356, May 2009.
- [85] X. Xu, L. Gu, J. Wang, G. Xing, and S.-C. Cheung, “Read more with less: An adaptive approach to energy-efficient rfid systems,” *Selected Areas in Communications, IEEE Journal on*, vol. 29, pp. 1684–1697, Sept 2011.
- [86] J. Alcaraz, J. Vales-Alonso, E. Egea-Lopez, and J. Garcia-Haro, “A stochastic shortest path model to minimize the reading time in dfsa-based rfid systems,” *IEEE Communications Letters*, vol. 17, pp. 341–344, Feb 2013.
- [87] G. Khandelwal, A. Yener, K. Lee, and S. Serbetli, “Asap : A mac protocol for dense and time constrained rfid systems,” in *IEEE International Conference on Communications, 2006. ICC '06.*, vol. 9, pp. 4028–4033, June 2006.
- [88] A. Zanella, “Adaptive batch resolution algorithm with deferred feedback for wireless systems,” *IEEE Transactions on Wireless Communications*, vol. 11, pp. 3528–3539, October 2012.
- [89] J. Vales-Alonso, V. Bueno-Delgado, E. Egea-Lopez, F. Gonzalez-Castano, and J. Alcaraz, “Multiframe maximum-likelihood tag estimation for rfid anticollision protocols,” *Industrial Informatics, IEEE Transactions on*, vol. 7, pp. 487–496, Aug 2011.

- [90] H. A. Ahmed, H. Salah, J. Robert, and A. Heuberger, “An Efficient RFID Tag Estimation Method Using Biased Chebyshev Inequality for Dynamic Frame Slotted ALOHA,” *Smart Systech*, 2014.
- [91] D. Liu, Z. Wang, J. Tan, H. Min, and J. Wang, “Aloha algorithm considering the slot duration difference in rfid system,” in *RFID, 2009 IEEE International Conference on*, pp. 56–63, April 2009.
- [92] H. Wu and Y. Zeng, “Passive rfid tag anticollision algorithm for capture effect,” *IEEE Sensors Journal*, vol. 15, pp. 218–226, Jan 2015.
- [93] A. Mokhtari, mehregan mahdavi, R. E. Atani, and M. Maghsoodi, “Using capture effect in dfsa anti-collision protocol in rfid systems according to iso18000-6c standard,” *Majlesi Journal of Mechatronic Systems*, vol. 1, no. 3, 2012.
- [94] J. Kaitovic, R. Langwieser, and M. Rupp, “A smart collision recovery receiver for rfids,” *EURASIP Journal on Embedded Systems*, no. 1, 2013.
- [95] M. Abramowitz and I. A. Stegun, *Solutions of Quartic Equations*. New York: Dover, 1972.
- [96] J. Kaitovic, M. Simko, R. Langwieser, and M. Rupp, “Channel estimation in tag collision scenarios,” in *RFID, 2012 IEEE International Conference on*, pp. 74–80, Apr 2012.
- [97] Sensor Systems Laboratory. <http://sensor.cs.washington.edu/WISP.html>, 2011.
- [98] M. Nabeel, A. Najam, Y. Duroc, and F. Rasool, “Multi-tone carrier technique for signal recovery from collisions in uhf rfid with multiple acknowledgments in a slot,” in *Emerging Technologies (ICET), 2013 IEEE 9th International Conference on*, pp. 1–5, Dec 2013.